



Mechanical and Physical Risk Prevention

Studies and Research Projects



REPORT R-785



Development of a Method of Measuring Nanoparticle Penetration through Protective Glove Materials under Conditions Simulating Workplace Use

*Patricia Dolez
Ludwig Vinches
Gérald Perron
Toan Vu-Khanh
Philippe Plamondon*

*Gilles L'Espérance
Kevin Wilkinson
Yves Cloutier
Chantal Dion
Ginette Truchon*





The Institut de recherche Robert-Sauvé en santé et en sécurité du travail (IRSST), established in Québec since 1980, is a scientific research organization well-known for the quality of its work and the expertise of its personnel.

OUR RESEARCH is *working* for you !

Mission

To contribute, through research, to the prevention of industrial accidents and occupational diseases and to the rehabilitation of affected workers;

To disseminate knowledge and serve as a scientific reference centre and expert;

To provide the laboratory services and expertise required to support the public occupational health and safety network.

Funded by the Commission de la santé et de la sécurité du travail, the IRSST has a board of directors made up of an equal number of employer and worker representatives.

To find out more

Visit our Web site for complete up-to-date information about the IRSST. All our publications can be downloaded at no charge.

www.irsst.qc.ca

To obtain the latest information on the research carried out or funded by the IRSST, subscribe to *Prévention au travail*, the free magazine published jointly by the IRSST and the CSST.

Subscription: www.csst.qc.ca/AbonnementPAT

Legal Deposit

Bibliothèque et Archives nationales du Québec
2013

ISBN: 978-2-89631-680-9 (PDF)

ISSN: 0820-8395

IRSST – Communications and Knowledge

Transfer Division

505 De Maisonneuve Blvd. West

Montréal, Québec

H3A 3C2

Phone: 514 288-1551

Fax: 514 288-7636

publications@irsst.qc.ca

www.irsst.qc.ca

© Institut de recherche Robert-Sauvé

en santé et en sécurité du travail,

June 2013



Mechanical and Physical Risk Prevention

Studies and Research Projects



REPORT R-785

Development of a Method of Measuring Nanoparticle Penetration through Protective Glove Materials under Conditions Simulating Workplace Use

Disclaimer

The IRSST makes no guarantee as to the accuracy, reliability or completeness of the information in this document. Under no circumstances may the IRSST be held liable for any physical or psychological injury or material damage resulting from the use of this information.

Document content is protected by Canadian intellectual property legislation.

*Patricia Dolez, Ludwig Vinches, Gérald Perron, Toan Vu-Khanh
École de technologie supérieure*

*Philippe Plamondon, Gilles L'Espérance
École polytechnique de Montréal*

*Kevin Wilkinson
Université de Montréal*


*Yves Cloutier, Chantal Dion, Ginette Truchon
Prévention des risques chimiques et biologiques, IRSST*

Clic Research
www.irsst.qc.ca



A PDF version of this publication
is available on the IRSST Web site.

This study was funded in the framework of an agreement between the IRSST and NanoQuébec.
The conclusions and recommendations are solely those of the authors.
This publication is a translation of the French original; only the original version (R-734) is authoritative.



In compliance with IRSST policy, the research results published in this document have been peer-reviewed.

ACKNOWLEDGMENTS

The authors wish to thank the following people for their enthusiastic contributions to this research project: Swann Mahé, Alice Jambou, Félicien Deltombe and Nicolas Testori, trainees at École de technologie supérieure (ÉTS); Mehdi Ben Salah, Abdelhakim Djebara, Rachid El Aidani and Carlos Arrieta, doctoral students at ÉTS; Riad Khettabi, postdoctoral fellow at ÉTS; Rute Domingos and Mohammad Abdul Kader Khan, postdoctoral fellows at the Université de Montréal; Florent Bridier, researcher at ÉTS; Philippe Bocher and Stéphane Hallé, professors at ÉTS; Petros Koutrakis, professor at Harvard University; Alexandre Vigneault and Michel Drouin, engineers at ÉTS; Radu Romanica, Patrick Sheridan and Jean-Guy Gagnon, technicians at ÉTS; Brigitte Blanchette, laboratory technician at IRSST; and Hélène Lalande, coordinator of the environmental chemistry laboratory at McGill University.

ABSTRACT

With the exponential growth in industrial applications of nanotechnologies and the corresponding increased risk of occupational exposure to nanomaterials, adoption of the precautionary principle is advisable. To apply this principle, personal protective equipment against nanoparticles must be made available, even though it should be regarded only as a last line of defence in an overall risk control strategy. In an effort to address the current lack of tools and knowledge in this area, a method was developed to measure the penetration of nanoparticles through protective glove materials under conditions simulating workplace use.

The method consists of an experimental setup for exposing glove samples to nanoparticles in powder form and in colloidal solution, while subjecting them simultaneously to static or dynamic mechanical loading as well as conditions simulating the microclimate inside the gloves. The setup is connected to a data acquisition and control system. To complete the method, a sampling protocol was developed and a series of nanoparticle detection techniques was selected.

Preliminary tests were performed using this method to measure the resistance of four models of protective gloves of different thicknesses made of nitrile, latex, neoprene and butyl rubber to the penetration of commercial TiO₂ nanoparticles in powder form or colloidal solution. The results appear to indicate that nanoparticles may penetrate through some types of gloves, particularly when the gloves are subjected to repeated mechanical deformations and the nanoparticles are in colloidal solution form. Further work is required to confirm these results, and consideration should be given to determining the parameter configurations and values that best simulate different possible workplace situations. Nevertheless, there are already good grounds for recommending that gloves should be changed regularly, especially when they are thinner models and especially when they have been exposed to nanoparticles in colloidal solution.

These findings underscore the relevance and importance of pursuing research in this field. Future work will benefit from the willingness of other teams interested in protective equipment against nanoparticles to collaborate and share their expertise.

CONTENTS

ACKNOWLEDGMENTS	I
ABSTRACT	III
1. INTRODUCTION	1
1.1 Importance of Subject and Origin of Occupational Health and Safety Issue	1
1.2 Scientific and Technical Importance of Subject of Study	1
1.3 Goal of Project and Specific Objectives	4
2. EXPERIMENTAL METHODS.....	7
2.1 Materials	7
2.1.1 Gloves	7
2.1.2 Nanoparticles	7
2.2 Nanoparticle Detection and Fine Structure Characterization Techniques	8
2.2.1 Transmission Electron Microscopy	8
2.2.2 Scanning Electron Microscopy with Field Emission Gun	8
2.2.3 Atomic Force Microscopy	9
2.2.4 Scanning Mobility Particle Sizer	9
2.2.5 Fluorescence Correlation Spectroscopy.....	9
2.2.6 Nanoparticle Tracking Analysis	10
2.2.7 Inductively Coupled Plasma Mass Spectroscopy	10
2.2.8 X-Ray Diffraction	10
2.3 Glove Material and Colloidal Solution Characterization Techniques	10
2.3.1 Measurement of Elongation and Weight Gain to Determine Swelling	11
2.3.2 Measurement of Mechanical Properties.....	11
2.3.3 Complementary Analyses	12
3. DESIGN OF MEASUREMENT METHOD	15
3.1 Measurement Method Specifications	15
3.2 Experimental Setup.....	16
3.3 System Control, Data Acquisition and Handling Protocol	18
3.4 Analysis Techniques and Sampling Protocol.....	20
4. RESULTS.....	25
4.1 Characterization of Nanoparticles.....	25

4.1.1	TiO ₂ Powder Nanoparticles	25
4.1.2	TiO ₂ Nanoparticles in Colloidal Solution	28
4.2	Characterization of Glove Materials	31
4.2.1	Chemical Analysis	31
4.2.2	State of Surface	32
4.2.3	Mechanical Behaviour	34
4.3	Characterization of Impact of Deformations on Glove Materials and Nanoparticles	36
4.3.1	Impact on Mechanical Behaviour of Glove Materials	36
4.3.2	Impact on Nanoparticle Agglomeration State	37
4.4	Characterization of Impact of Nanoparticle Carrier Fluids in Colloidal Solution on Glove Materials	38
4.4.1	Swelling	38
4.4.2	Impact on Dynamic Mechanical Behaviour	49
4.5	Characterization of Impact of Deformations and Nanoparticle Carrier Fluids on State of Glove Surfaces	50
4.6	Characterization of Impact of Environmental Stresses on Glove Materials	53
4.6.1	Impact of Temperature on Mechanical Behaviour of Glove Materials	54
4.6.2	Swelling of Glove Materials in Physiological Solutions	54
4.7	Measurement of Penetration of Nanoparticles through Glove Materials	55
4.7.1	Results for TiO ₂ Powder	56
4.7.2	Results for Colloidal Solutions of TiO ₂	60
5.	DISCUSSION	63
5.1	Method Chosen to Measure Penetration of Nanoparticles through Glove Materials	63
5.2	Penetration of Nanoparticles in Powder through Glove Materials	66
5.3	Penetration of Nanoparticles in Colloidal Solution through Glove Materials	67
5.4	Applicability of Method to Other Types of Research	67
6.	CONCLUSIONS, PROSPECTS AND RECOMMENDATIONS	69
	BIBLIOGRAPHY	71
	APPENDIX A: DRAWINGS OF EXPERIMENTAL SETUP	79
	APPENDIX B: USER MANUAL	95

TABLES

Table 1 – Characteristics of protective gloves selected for study.....	7
Table 2 – Mass fraction of TiO ₂ measured by TGA, for three colloidal solutions (water, EG, PG)	30
Table 3 – Mass concentration of titanium in gloves (outer surface, inner surface and cross-section)	32
Table 4 – Results of lengthwise and crosswise tensile testing of nitrile, latex, neoprene and butyl rubber gloves	35
Table 5 – Elongation and force at rupture for nitrile, latex, neoprene and butyl rubber gloves when subjected to biaxial strain	36
Table 6 – Maximum rate of weight gain for four glove materials (nitrile, latex, neoprene and butyl rubber) in three colloidal solutions of TiO ₂ (in water, EG and PG).....	44
Table 7 – Mean coefficients of diffusion in nitrile, latex and neoprene, for three colloidal solutions of TiO ₂ (in water, EG and PG).....	45
Table 8 – Change in weight in relation to initial weight, for samples of nitrile, latex and neoprene immersed for 40 days in three colloidal solutions of TiO ₂ (in water, EG and PG) then dried under a hood.....	46
Table 9 – Comparison of values of secant modulus at 100% for nitrile, latex, neoprene and butyl rubber, measured at 25°C and 40°C	54
Table 10 – NP concentrations measured by NTA in blank and in sampling solution, for latex, neoprene and butyl rubber exposed simultaneously to TiO ₂ powder and to biaxial dynamic loading for 7 hours (results for series 1, with defective seal).....	58
Table 11 – Titanium concentrations measured by ICP-MS in sampling solution, for nitrile, latex, neoprene and butyl rubber exposed to TiO ₂ powder for 7 hours, without deformation of the sample.....	60
Table 12 – Titanium concentrations measured by ICP-MS in sampling solution, for nitrile, latex, neoprene and butyl rubber exposed to colloidal solution of TiO ₂ in water for 7 hours, without deformation of the sample	61

FIGURES

Figure 1 – Diagram of probe with conical-spherical tip applying biaxial deformation.....	12
Figure 2 – Diagram of experimental setup	16
Figure 3 – Schematic representation of change in sample deformation over time as dynamic mechanical stress is applied.....	17
Figure 4 – Tip geometries for deformation probe.....	17
Figure 6 – “Conduct experiment” interface of system control and data acquisition program.....	19
Figure 7 – Photograph of SMPS pipe intake after attempt to detect TiO ₂ powder NPs.....	20
Figure 8 – Images of TiO ₂ powder (a) by FEG-SEM on surface of nitrile glove and (b) by AFM on surface of latex glove.....	21
Figure 9 – FEG-SEM images of TiO ₂ powder on surface of nitrile glove: (a) secondary electron imaging and (b) backscattered electron imaging	21
Figure 10 – Diagram of setup, with sampling solution.....	22
Figure 11 – Comparison of results of sampling solution analyses by ICP-MS done on November 3, 2010, and January 28, 2011	23
Figure 12 – TEM images of TiO ₂ powder: (a) agglomerated NPs, (b) individual NP	25
Figure 13 – X-ray diffraction spectrum of TiO ₂ powder	26
Figure 14 – EDS spectrum of TiO ₂ powder	27
Figure 15 – Particle size distribution of TiO ₂ powder based on circular diameter measured from TEM images, with smoothing line by inverse Gaussian distribution.....	27
Figure 16 – Relative weight loss as a function of temperature, according to TGA of colloidal solution of TiO ₂ NPs in PG and of technical and ultrapure PG	29
Figure 17 – Comparison of FT-IR spectra of colloidal solution of TiO ₂ in water and of ultrapure water.....	30
Figure 18 – Example of EDS spectrum of outer surface of nitrile glove	31
Figure 19 – SEM images of outer surface of gloves: (a) nitrile, (b) latex, (c) neoprene and (d) butyl rubber.....	33
Figure 20 – SEM images of (a) inner surface of neoprene glove and (b) cross-section.....	33
Figure 21 – Stress-strain curves for nitrile, latex, neoprene and butyl rubber when subjected to uniaxial tension (crosswise)	34
Figure 22 – Force-displacement curves for nitrile, latex, neoprene and butyl rubber when subjected to biaxial strain	35
Figure 23 – Relative change in work corresponding to a 50% biaxial deformation of samples of butyl rubber and nitrile, as a function of the duration of exposure to biaxial mechanical loading (one deformation every 5 minutes)	37

Figure 24 – FEG-SEM images of surface of neoprene samples exposed to TiO ₂ powder in conjunction with biaxial dynamic loading of 50% for durations of (a) 1.5 h and (b) 7 h.....	38
Figure 25 – Weight gain as a function of immersion time of nitrile in colloidal solution of TiO ₂ in water, with four repeats	39
Figure 26 – Weight gain as a function of immersion time of nitrile in colloidal solution of TiO ₂ in water and in ultrapure water	40
Figure 27 – Weight gain as a function of immersion time of nitrile and of nitrile WRF in ultrapure water.....	41
Figure 28 – Weight gain as a function of immersion time of nitrile in colloidal solutions of TiO ₂ in water, EG and PG	42
Figure 29 – Weight gain of nitrile, latex, neoprene and butyl rubber as a function of immersion time in colloidal solution of TiO ₂ in water.....	43
Figure 30 – Weight gain of nitrile, latex and neoprene for long immersion times in colloidal solution of TiO ₂ in water	43
Figure 31 – Weight gain of latex as a function of immersion time (days) in colloidal solutions of TiO ₂ in water, EG and PG	46
Figure 32 – Relative length change of nitrile (crosswise) as a function of immersion time in colloidal solutions of TiO ₂ in water and in PG.....	47
Figure 33 – FT-IR spectrum for residue from swelling of neoprene in EG for 7 days	48
Figure 34 – EDS spectrum of analysis of residue from swelling of neoprene in EG for 7 days.....	49
Figure 35 – Relative change in work required for a 50% biaxial deformation of samples of nitrile as a function of the duration of exposure to biaxial mechanical loading (one deformation every 5 minutes) in conjunction or not with exposure to colloidal solution of TiO ₂ in water	50
Figure 36 – SEM images of outer surface of nitrile gloves: (a) when new, (b) after 7 hours of biaxial deformations.....	51
Figure 37 – Change in area of imperfections in nitrile and neoprene (outer surface) as a function of duration of biaxial dynamic loading	51
Figure 38 – Impact of 7 hours of exposure to PG, biaxial dynamic loading and the combination of the two on the area of imperfections of nitrile, butyl rubber, neoprene and latex gloves (outer surface)	52
Figure 39 – Impact of 7 hours of exposure to PG, biaxial dynamic loading and the combination of the two on the area of imperfections of nitrile, butyl rubber, neoprene and latex gloves (inner surface)	53
Figure 40 – Relative length change of nitrile as a function of immersion time in physiological solutions of pH 4 and pH 6 and in ultrapure water	55

Figure 41 – ICP-MS measurements of titanium in sampling solution as a function of experiment duration, for nitrile and butyl rubber exposed simultaneously to TiO ₂ powder and biaxial dynamic loading: comparison of two series of tests	57
Figure 42 – ICP-MS measurements of titanium in sampling solution as a function of experiment duration, for nitrile and butyl rubber exposed or not to TiO ₂ powder in addition to biaxial dynamic loading	57
Figure 43 – AFM image (scale of 3 μm) of a sampling solution in pure water centrifuged on a mica substrate from a nitrile sample subjected for 7 hours to biaxial dynamic loading (50%) and to TiO ₂ powder	59
Figure 44 – AFM image (scale of 500 nm) of a sampling solution in pure water centrifuged on a mica substrate from a nitrile sample subjected for 7 hours to biaxial dynamic loading (50%) and to TiO ₂ powder.....	60
Figure 45 – ICP-MS measurements of titanium in sampling solution as a function of experiment duration, for nitrile and butyl rubber exposed or not to colloidal solution of TiO ₂ in water in addition to biaxial dynamic loading	61

1. INTRODUCTION

1.1 Importance of Subject and Origin of Occupational Health and Safety Issue

Nanotechnology is a booming field. The risks of workplace exposure to nanoparticles (NPs) are real and could increase exponentially (Maynard, 2005). With the growth in commercial applications of nanomaterials and their potential toxicity, a number of people have spoken out about the need to give careful consideration to the risks of handling and using them and to the measures to take to prevent possible occupational health problems (CEST, 2006; ICTA, 2007; Schulte et al., 2007). This realization has prompted health and safety organizations around the world to recommend adoption of the precautionary principle until the issue of nanomaterial toxicity has been dealt with satisfactorily (Ostiguy et al., 2009; Afsset, 2010; OECD, 2010).

Given this context, considerable effort has been made in recent years to address existing shortcomings in regulations (Hansen, 2009; Jackson et al., 2009; Kaluza et al., 2009; OECD, 2010; PCAST, 2010, NTRC, 2010). This includes development of standards (BSI, 2007; Dalla Via, 2008; Bard et al., 2009), best practices guidelines (Ostiguy et al., 2008a; ISO, 2008; Ricaud, 2009; Hallock et al., 2009; Amoabediny, 2009) and risk assessment and control methods (Paik et al., 2008; Giacobbe, 2009; Ellenbecker, 2010; van Niftrik et al., 2010). While personal protective equipment should be regarded only as a last line of defence in the traditional approach to occupational health and safety, such equipment against NPs needs to be made available immediately (Schulte et al., 2008). This need has been identified as a priority by a number of agencies in Quebec (Ostiguy et al., 2008b), the United States (NIOSH, 2005; NNI, 2006), France (Afsset, 2006; Bloch, 2006) and other jurisdictions. However, knowledge, data and measurement methods are very limited in this field, at a time when questions are being raised about the effectiveness of existing protection equipment against nanoparticles (Dolez et al., 2010a).

In the workplace, the main pathway to NP exposure is inhalation (Ostiguy et al., 2008a). Exposure by the cutaneous route has not been studied much, partly because of the widely held belief that skin offers an impermeable barrier to NPs (Truchon et al., 2008). Yet a growing number of studies have pointed to the possible percutaneous absorption of NPs, such as in the case of skin damaged by abrasion (Zhang et al., 2008), repeated flexion (Rouse et al., 2007) or even through intact skin (Ryman-Rasmussen et al., 2006). Pores, hair follicles and sweat glands may also play a role in facilitating absorption of NPs through the skin (Hervé-Bazin, 2007). The nanoparticles are then carried throughout the body by the lymphatic circulatory system (Papp et al., 2008). Induced direct toxic effects have also been reported for epidermal keratinocyte cells exposed to carbon nanotubes and other types of NPs (Shvedova, 2003).

1.2 Scientific and Technical Importance of Subject of Study

Only a relatively small number of research teams are working in the field of NP-specific cutaneous protection equipment. On account of the lack of standard test methods for NP-specific protective clothing, researchers have developed their own measurement systems. For air-permeable materials like fabrics used in protective clothing, the test setups used are generally

similar to the test methods for respiratory protective equipment (Dolez et al., 2010a). The sample is subjected to an aerosol spray of NPs, and the NP concentration upstream and downstream of the sample is measured using standard NP counting techniques (Hanley, 2006; Hofacre, 2006; Huang et al., 2007; Golanski et al., 2009b). An alternative technique was devised for the European NanoSafe 2 project: it uses a permeation-diffusion cell so that NPs can be applied without any air flow (Golanski et al., 2008a; 2008b; 2009a; 2009b). This no-air-flow technique was used with both air-permeable membranes and non-porous materials such as protective polymer gloves. Work is now under way to apply the technique to nanohydrosols (Golanski et al., 2010). Other researchers experimenting with protective textile and elastomer gloves have used scanning electron microscopy to observe how NPs behave on the surface of samples following static or dynamic contact (Ahn et al., 2006). Lastly, a more comprehensive approach, involving the complete protective ensemble, is currently under development at the National Personal Protective Technology Laboratory of the U.S. National Institute of Occupational Safety and Health (NIOSH, 2006; NRC, 2007).

With these test methods, results have been generated for various air-permeable textiles used in protective clothing. Testing was done with a variety of NPs, oleic acid, potassium chloride, sodium chloride, graphite, titanium dioxide (TiO_2) and platinum, in the form of aerosols as small as 10 nm (Hanley, 2006; Hofacre, 2006; Huang et al., 2007; Golanski et al., 2008a; 2008b; 2009a; 2009b). For textiles, NP penetration rates as high as 80% have been reported (Afsset, 2008). A thin membrane of high-density, non-woven polyethylene has been found to be much more effective against NPs than other types of even thicker textiles (Golanski et al., 2008a; 2008b; 2009a; 2009b). Moreover, based on the decrease in filtration efficacy measured with a reduction in particle size and air flow, researchers have concluded that the interaction between NPs and these air-permeable textiles is consistent with the general theory of filtration (Hofacre, 2006; Huang et al., 2007; Golanski et al., 2009b; Afsset, 2008). It should be noted, however, that some results do seem to indicate a different behaviour, such as the existence of a plateau in the rate of penetration of graphite NPs through cotton fabric for particle sizes larger than 50 nm (Golanski et al., 2009b) and higher penetration rates at 30 nm than at 80 nm for graphite NPs through a textile identified as “paper (Best Body)” (Golanski et al., 2008a).

For non-porous membranes like those used in protective gloves, the amount of data available is much more limited, and some of it is even contradictory. Non-null values for the diffusion coefficient have been reported for five commercial gloves made of nitrile, latex, neoprene and vinyl exposed to an aerosol of 30 and 80 nm graphite NPs in a system with no air flow, prompting the authors to suggest double-gloving (Golanski et al., 2008a). Yet the same team, for the same models of gloves and the same system of measurement, subsequently reported no penetration for 40 nm graphite NPs (Golanski et al., 2009b) or for 10 nm TiO_2 and platinum NPs (Golanski et al., 2009a). However, a porosity rate of between 0.3% and 1% has been measured for these gloves using a helium permeation method (Golanski et al., 2009b). Significant work therefore remains to be done before there can be any certainty about the effectiveness of protective gloves against NPs.

All these results and the measurement methods used to produce them concern NPs applied in aerosol form. Workplace exposure to NPs also involves powders and colloidal solutions, with the latter being used to reduce the risks of aerosolization. This exposure is particularly relevant for protective gloves and could turn out to be a source of new problems. Scanning electron

microscopy observations of the surface of latex and nitrile gloves after static or dynamic contact with clay or alumina powder NPs show that the particles tend to build up in the micrometric pores at the glove surface (Ahn et al., 2006). In the case of NPs in colloidal solution, worries have been expressed about greater risks related to the presence of a carrier fluid (Nanotechnology Workgroup, 2007). Polymers, which are the base material in protective clothing, can be sensitive to the action of solvents (Rodot, 2006). Even aqueous solvents can cause significant swelling of some rubbers, leading to changes in their physical and mechanical properties (Wang et al., 1999; Park et al., 2001; Singh, 2003). Another possible consequence of the presence of solvents as NP carriers is a phenomenon of entrainment in the diffusion process. Diffusion of water through vinyl, nitrile and latex gloves was recently reported (Golanski et al., 2010). It is also possible that the natural migration of low molecular weight species (LMWS), observed, for instance, with rubbers (Volynskii et al., 1988), may act as a vehicle for NPs. The adjuvants used in the formulation of polymers may also potentially play this role and even coat the NPs in passing. The effectiveness of protective clothing, especially gloves, must therefore be measured when exposed to NPs in powder and in colloidal solution.

Another parameter to consider is the fact that when protective clothing is worn as part of an occupational activity, the materials in the clothing are subjected to a large number of stresses—physical, chemical, thermal and mechanical, among others. In addition to the impact of the different types of aggressors, including NPs, that they must protect against, protective clothes also undergo the effects of normal wear and tear, especially mechanical and environmental effects.

With respect to mechanical factors, a number of different modes of stress must be considered. First of all, the protective clothing material, especially in gloves, can be subjected to a compressive force when pressure is exerted on or by an external object. For instance, grip forces of up to 500 N have been measured for adult hands (Nicolay et al., 2005; Edgren et al., 2004; Meyer et al., 2001). In a situation where NPs are caught between the protective clothing and the surface of an object, this compressive force can exert pressure on the particles and contribute to their penetration into the material. For rubber membranes, permeability with respect to gases, with which NPs may be associated on account of their small size (Balazy et al., 2004; Schneider, 2007), increases as the pressure of the gases rises (Prabhakar et al., 2005).

A second form of mechanical stress is material extension. Some parts of protective clothing, especially at joints, can be subjected to significant stretching forces. In the case of protective gloves, the materials used are generally highly extensible in order to allow this stretching and not limit flexibility and restrict movements. But barrier properties, especially when it comes to NPs, can be different in a deformed state than in a non-deformed state. For instance, a significant decrease in breakthrough time and an increase in diffusion coefficient have been measured for natural rubber, bromobutyl and nitrile in contact with various organic solvents and subjected to low elongation rates (up to 20%) (Li et al., 1999). It is therefore conceivable that a similar effect could occur in the case of NP penetration and that the deformed material may be more permeable to NPs.

A last type of mechanical stress caused by the normal use of protective clothing concerns repeated flexing motions. Cyclical deformation of the material can lead to a deterioration of its mechanical properties, similarly to fatigue. In addition, periodic variation in the physical

configuration of the material/particle system at the microscopic level can also be the direct cause of easier penetration, for example, if the walls of the pores of the material in which the particle agglomerates accumulate end up bursting as a result of compression failure or shearing. Testing of pig skin has shown that repeated flexing increases the penetration of 3.5 nm fullerene-based peptide NPs, in terms of both diffusion speed and quantity (Rouse et al., 2007). It is therefore important to examine the impact of repeated deformation of glove materials, especially elastomers, on their resistance to NP penetration.

Besides mechanical stresses, protective clothing is also subjected to a variety of stresses related to the physical environment in which it is worn. For instance, some working environments are characterized by extreme temperature and humidity. In addition, there is a microclimate inside protective clothing that has temperature and humidity conditions different from those of the ambient environment (Sullivan et al., 1992). For instance, skin surface temperatures of around 35°C have been recorded inside soccer gloves during laboratory exercises representative of the efforts made by goalkeepers (Purvis et al., 2000). The properties of materials in general, and of polymers in particular, are sensitive to temperature (Burllett, 2004). Barrier characteristics, such as resistance to permeation (De Kee, 2000) and swelling from solvents (Sombatsompop, 1998), are likewise affected by temperature. As for pH, its mean value is between 5.4 and 5.9 at the surface of the skin (Schmid-Wendtner et al., 2006), with slightly lower values (4.3) having been reported for the palm of the hands (Kurabayashi et al., 2002), given that the more humid interdigital areas generally have a slightly higher pH (Schmid-Wendtner et al., 2006) and that a pH of between 6 and 6.5 was measured for sweat during effort (Hayden et al., 2004). Furthermore, water in the form of humidity or perspiration can also act as a swelling agent on glove materials and affect their properties (Singh, 2003). The characteristics of the liquid inside gloves, its composition and its pH, for instance, may influence the effects. Finally, NPs, and particularly their agglomeration state, can also be sensitive to environmental conditions, including temperature and humidity, which can change the way they interact with a given material.

1.3 Goal of Project and Specific Objectives

The general objective of this project was to develop a method for characterizing the effectiveness of protective glove materials against NPs by simulating the conditions under which they are used in the workplace: the form in which the nanoparticles are applied (powder or colloidal solution), the mechanical stresses on the gloves and the microclimate inside them. In addition, a few preliminary results were obtained for the main materials used to make protective gloves and for one of the major NPs for Quebec, TiO₂. The ultimate goal of the research is to ensure that the protective gloves worn in occupational activities involving potential contact with NPs provide a level of impermeability that meets the requirements of the precautionary principle that now applies to NPs.

To achieve this goal, six main specific objectives were pursued:

1. Devise a flexible, versatile, experimental setup for applying NPs as a powder or colloidal solution to the sample, while at the same time subjecting the sample to mechanical and environmental stresses.

2. Identify measurement techniques and an analytical procedure that meet study requirements, both for detection of the penetration of NPs through the sample and for characterization of their fine structure on either side of the membrane.
3. Assess the significance of the impact of mechanical and environmental stresses and of the conditions of application of NPs on their penetration through polymer membranes.
4. Propose a method for measuring penetration of NPs through glove materials that includes mechanical and environmental stresses relevant to required workplace protection and measurement techniques identified as being optimal and the most easily available for detecting the penetration of NPs through glove material samples.
5. Produce preliminary results on the protectiveness of certain glove materials—butyl rubber, neoprene, nitrile and latex—that could provide a basis for preliminary recommendations regarding the best choice of glove for protection against the risks of NP exposure.
6. Acquire some basic knowledge about the mechanisms governing the interaction between NPs and polymer membranes.

Another aim of the project was to test a number of hypotheses, including evaluating the effectiveness of commercially available protective gloves against NPs. In addition, tests were conducted to determine whether the mechanical and environmental stresses on glove materials, as well as the carrier fluids of colloidal solutions, have an effect on NP penetration.

2. EXPERIMENTAL METHODS

This section describes the materials, gloves and NPs used in the study. It also outlines the various techniques used to detect and characterize the fine structure of the NPs, as well as those used to perform a complementary analysis of the glove materials and colloidal solutions. The experimental setup devised for the study is described in Section 3 Design of Measurement Method.

2.1 Materials

2.1.1 Gloves

Four models of gloves, made of four different elastomer materials — nitrile rubber, latex, butyl rubber and neoprene — were selected. Some of their characteristics are given in Table 1. The materials have different properties for resisting chemical aggressors (Perron et al., 2002; Mellström et al., 2005; Dolez et al., 2010b). Nitrile offers high resistance to oils, fuels and certain organic solvents. Latex is resistant to alcohols, bases and oxidizing acids, but is sensitive to hydrocarbons and organic solvents. Neoprene provides moderate resistance to chemicals, particularly oils and petroleum. Lastly, butyl rubber is very resistant to polar chemicals in liquid, gas and aerosol form, which makes it a preferred material for protection against chemical hazards (Jin et al., 2005). It is sensitive to hydrocarbons, however.

Table 1 – Characteristics of protective gloves selected for study

Model	Material	Thickness	Type of glove
Best Nitri-Care 3005-PFL	nitrile	0.10 mm	disposable
Ansell Conform [®] XT 69-318	latex	0.10 mm	disposable
Ansell Neoprene [™] 29-865	neoprene	0.45 mm	unsupported
Best Butyl 878	butyl rubber	0.70 mm	unsupported

A few comparison tests for swelling were also conducted on Ansell Touch-N-Tuff 92-500 disposable nitrile gloves, which, according to the manufacturer, do not contain any fillers, silicones or plasticizers. In this report they are identified as nitrile WRF (without reinforcing fillers).

2.1.2 Nanoparticles

Nanoparticles of TiO₂ were used to develop the method. They are one of the most common manufactured nanomaterials (Robichaud et al., 2009). TiO₂ powder was obtained from Nanostructured & Amorphous Materials, Inc. (Houston, TX). According to the manufacturer, it consists of 99.7% anatase (spherical allotropic form) with a particle diameter of 15 nm. Three commercial colloidal solutions of TiO₂ in different carrier fluids were also used. TiO₂ solutions, 15wt% in water and 20wt% in ethylene glycol (EG), were purchased from Nanostructured & Amorphous Materials, while a 20wt% solution in propylene glycol (PG) was obtained from M K

Impex (Mississauga, ON). All three solutions contain 15 nm anatase particles, according to the manufacturers' specifications.

Some of the measurements presented in this report were also taken using solvents corresponding to the carrier fluids of the colloidal solutions. For each of the three carrier fluids (water, EG, PG), two purity levels were used: technical and ultrapure. Note that PG (or propane-1, 2-diol) is considered to be non-toxic and used as a food additive. EG (or ethane-1, 2-diol), on the other hand, is recognized as being toxic when ingested (Health Canada).

2.2 Nanoparticle Detection and Fine Structure Characterization Techniques

One of the challenges of this research project was to identify NP detection and fine structure characterization techniques that met the needs of the research method being developed. For this purpose, a series of techniques were tested and evaluated to determine their applicability to the method. Some of them were also used to test manufacturers' specifications regarding the characteristics of the supplied NPs.

2.2.1 Transmission Electron Microscopy

Transmission electron microscopy (TEM) has found many applications in the observation of NPs (Beaupré et al., 2004; Muller et al., 2008). The device used for this study was a JEOL JEM-2100F equipped with a 200 kV field emission gun. It is part of the materials characterization equipment at the centre for microscopic characterization of materials ((CM)²) of Montreal's École Polytechnique. The microscope's maximum resolution is approximately 1.9 ångström. It is equipped with an X-ray detector (EDS) and an electron energy loss spectrometer (EELS). It is also capable of Z-contrast imaging in which areas with higher mean atomic number elements appear brighter.

2.2.2 Scanning Electron Microscopy with Field Emission Gun

Scanning electron microscopy (SEM) has often been used to observe NPs (Beaupré et al., 2004), enabling analysis in terms of size and particle shape. The standard technique requires use of a conducting substrate, such as a metal surface or a conducting strip. For a non-conducting sample, the surface must be covered with a thin (around 15 nm) deposit of gold. Samples can also be made conductive by depositing carbon on them by evaporation. Since carbon is amorphous and has a low atomic number, it is far more transparent to electrons than a gold deposit and enables high-magnification observations while preserving good spatial resolution.

Combining field emission gun technology with scanning electron microscopy (FEG-SEM) has significantly increased the potential of this technique for studying nanomaterials (Goldstein et al., 2003). The resolution limit of FEG-SEM can reach 1 nm. Moreover, the combination of the two technologies makes it possible to work at very low voltages (3 kV or less), which means that

non-conducting samples can be observed directly without any need for a conducting deposit. The FEG-SEM images presented in this report were taken with a JEOL JSM-7600F at École Polytechnique's (CM)² laboratory.

To determine the agglomeration state of NPs on deformed gloves, carbon was deposited on the samples to make them conductive. As a result, an acceleration voltage of 2 kV could be used, which made it possible to take backscattered electron images and so obtain a chemical contrast. The chemical contrast is essential for detecting the TiO₂ NPs that could be hidden in the glove's surface relief. Without a conducting deposit, the maximum possible acceleration voltage was 0.5 kV, which is insufficient for backscattered electron imaging.

2.2.3 Atomic Force Microscopy

Atomic force microscopy (AFM) broadens the possibilities for analysing the surface of materials in general and has found many applications in the study of NPs (West et al., 2006). One major advantage of this technique is that it does not require any sample surface preparation, it can be used for both conducting and insulating materials and it can operate in many different types of environments (air, vacuum, liquid, etc.). It is also possible to submit colloidal samples to centrifugation on a mica substrate, for instance, to enable dry process analysis (Wilkinson et al., 1999). The AFM device used for this study was a Veeco Nanoscope IIIa (mechanical engineering department, ÉTS). The measurements were taken in tapping mode.

2.2.4 Scanning Mobility Particle Sizer

The aerosol concentration in the air can be measured continuously using a scanning mobility particle sizer (SMPS). This is one of the most common techniques for characterizing ultrafine particles and NPs (Witschger et al., 2005a). The SMPS used for this study was the TSI model. It is part of the materials characterization equipment in the mechanical engineering department at ÉTS. With its two columns, it provides coverage of the 1–125 nm and 10–1000 nm detection ranges.

2.2.5 Fluorescence Correlation Spectroscopy

Fluorescence correlation spectroscopy (FCS) is a technique for analysing the diffusion times of molecules and NPs on the basis of fluctuations in fluorescence intensity. It is used to determine molecular dynamics in solution (Domingos et al., 2009; 2010). Diffusion coefficients can be used to determine not only the size of fluorescent NPs, but also their aggregation kinetics and the structure of the resulting aggregates. Owing to the nature of the signal, this technique is far less biased toward large NPs than dynamic light scattering is. The laboratory of Professor K. Wilkinson at the Université de Montréal is equipped with a confocal microscope (Leica TCS SP5) having an argon ion laser and an avalanche photodiode detector (Leica) for taking measurements by FCS and analysing fluctuations in fluorescence. TiO₂ NPs are marked by fluorophores such as rhodamine.

2.2.6 Nanoparticle Tracking Analysis

Nanoparticle tracking analysis (NTA) can be used to measure the size, distribution and concentration of NPs in a liquid medium (Carr, 2007). The advantage of this kind of NP analysis over dynamic light scattering (DLS) technology lies in the fact that it is based on automatic detection of individual particles, which takes into account the polydispersity of the sample, while still providing satisfactory statistical sampling data. Moreover, since it tracks the trajectories of individual particles, size measurements are not skewed by a given size category, which makes it possible to obtain mean size distributions by number of particles. A NanoSight LM20, recently acquired by Professor Wilkinson's lab at the Université de Montréal, was used. It has an analysis range of 20 to 1,000 nm and operates with a green laser (532 nm).

2.2.7 Inductively Coupled Plasma Mass Spectroscopy

Inductively coupled plasma mass spectroscopy (ICP-MS) is an elementary quantification technique based on mass spectrometry analysis of ions generated by inductively coupled plasma. It is an extremely sensitive detection technique, of the order of ng/L to µg/L. The results presented here were obtained with a Varian 820 ICP-MS. The collision reaction interface (CRI) technology used in the device limits polyatomic interferences and helps to reduce its resolution limits, for instance, from 3 to 1.3 ng/L for titanium ions (Wang et al., 2010). The measurements were conducted at McGill University's environmental chemistry laboratory.

2.2.8 X-Ray Diffraction

X-ray diffraction analyses were conducted with a Philips X'Pert diffractometer (at École Polytechnique's (CM)² laboratory). The powder was placed on a sample holder (approximately 10 x 10 x 1 mm³) designed for powder analysis. To identify the phases present, a scan was performed over a range of angles of diffraction (2θ), from 15° to 90°. To determine the size of the crystals, the analysis was done only over a few degrees around the highest peak of the anatase-structured TiO₂ (plan (101) at 25.32°). A standard TiO₂ having particles larger than 100 nm was used in order to have the full width at mid-height of a diffraction peak corresponding to a particle size larger than the limit measurable with this technique.

2.3 Glove Material and Colloidal Solution Characterization Techniques

A number of techniques have been used to characterize the nature and behaviour of glove materials when exposed to mechanical stresses and to the carrier fluids of NPs in colloidal solution. Analyses of the formulation of colloidal solutions have also been conducted.

2.3.1 Measurement of Elongation and Weight Gain to Determine Swelling

In the case of NPs in colloidal solution, the carrier fluids may cause the glove material elastomers to swell. The solvent can be absorbed into the membrane by diffusion. If the contact time is long enough in relation to the diffusion time for the liquid to come through the opposite side, an NP transport effect is conceivable. This process can therefore potentially affect the penetration of NPs in colloidal solution, with respect to both the mechanisms involved and the transport kinetics. To examine this phenomenon, length change and weight gain measurements were taken. These techniques can be used to quantify the level of interaction between the solvent and the polymer (Perron et al., 2002). A significant increase in length indicates a large solubility of the solvent in the polymer. From the results of the weight gain and length change measurements, a mean diffusion coefficient of the solvent in the polymer can be calculated (Perron et al., 2002).

The measurements were carried out by immersing rectangular samples of the gloves, taken from the palm, in three TiO₂ colloidal solutions and in technical and ultrapure solvents corresponding to the carrier fluids of these solutions. At regular intervals, each sample was removed from the fluid, its surface gently wiped and then measured. Weight was measured using an analytical balance (0.1 mg), while change in length was measured with a vernier. Two sample sizes were used: 4 x 50 mm for the length change measurements, and 10 x 50 mm for the weight gain measurements. For the length change measurements, the samples were cut in two directions: lengthwise (L, parallel to the fingers) and crosswise (T). For each condition, from 2 to 5 repeats were measured.

Swelling tests were also carried out with physiological solutions of different pHs simulating sweat, formulated according to standard EN 1811 (CEN, 1998). The basic solution consisted of deionized water containing 0.5% sodium chloride, 0.1% lactic acid and 0.1% urea. Its pH was adjusted by adding ammonia. Length change measurements were taken on samples of the four materials immersed in physiological solutions with pH of 4 and 6, as well as in ultrapure water.

2.3.2 Measurement of Mechanical Properties

Given the possible impact of mechanical stressors on NP penetration through protective gloves, the mechanical behaviour of the glove materials was characterized.

The first tests concerned mechanical behaviour under uniaxial deformation. Measurements were taken in accordance with standard method ASTM D-412 (ASTM, 2002). Tensile test pieces were cut lengthwise and crosswise from the palms of the gloves and subjected to deformation at a velocity of 500 mm/min until sample failure, in a universal testing machine (MTS Alliance RF/200). The measurements were repeated five times for each condition. Characteristics in terms of modulus of elasticity, tensile strength and elongation at break were calculated from the data.

Some measurements of mechanical behaviour under uniaxial tension were taken on samples raised to 40°C by putting an oven inside the testing machine. A dwell time of 3 minutes after introducing the test piece was needed for the system to reach temperature equilibrium.

The reaction of the glove materials to biaxial mechanical loading was also analysed, given that that type of deformation is relevant to the conditions of use of the gloves (Larivière et al., 2010). Two test setups were used. In both cases, a probe with a conical-spherical tip applied a biaxial deformation to the sample held in position above a circular opening (see Figure 1). For measurements involving elongation at break, the flexibility-testing setup corresponding to the fixed double curvature technique (Harrabi et al., 2008) was used in combination with a universal testing machine (Instron 1137, mechanical engineering department, ÉTS) equipped with a 150 N load cell. The measurements were taken at a probe travel speed of 500 mm/min. The diameter of the opening of the setup's sample holder was slightly larger (57 mm) than the internal diameter (54 mm) of the exposure chamber of the experimental design developed for the study. The ratio between the probe diameter and the opening diameter (0.63) was also slightly larger than that corresponding to the project's experimental design (0.48). For each condition, the measurements were repeated five times.

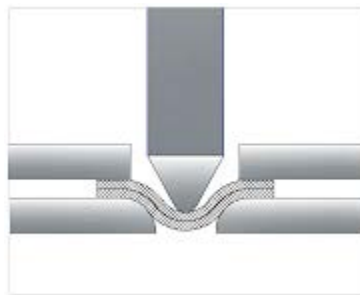


Figure 1 – Diagram of probe with conical-spherical tip applying biaxial deformation

The materials were also tested under dynamic loading, with each downward and upward cycle of the probe being separated from the following one by a 5-minute pause. The setup used for this type of measurement was the experimental design developed for the project and described in the following section (see Figure 2). Probe travel speed was around 500 mm/min. This setup also made it possible to study the joint impact of biaxial dynamic loading and contact with solvents corresponding to the carrier fluids of the NP colloidal solutions. For this purpose, a certain amount of fluid was kept in contact with the outer surface of the sample throughout the experiment. The data resulting from these measurements were analysed by calculating the work corresponding to a glove deformation of between 0 and 30 mm caused by the conical-spherical probe.

2.3.3 Complementary Analyses

The states of the inner and outer surfaces of the glove materials were analysed by SEM (Hitachi S3600N, mechanical engineering department, ÉTS). These observations were likewise made after the samples had been subjected to various dynamic deformation treatments and/or contact with solvents corresponding to the NP carrier fluids. The EDS module associated with the SEM also made it possible to analyse the composition of the glove materials (inner and outer surfaces and cross-section).

Thermogravimetric analyses (Perkin Elmer Diamond TGA/DTA, mechanical engineering department, ÉTS) and Fourier transform infrared spectroscopy analyses (Nicolet FT-IR 6700, mechanical engineering department, ÉTS) were conducted on the TiO₂ colloidal solutions in an effort to characterize the composition of the carrier fluids and identify any possible additives. The TGA measurements were taken between 20°C and 250°C at a speed of 5°C/min. The FT-IR analyses were performed in ATR mode between 500 and 4,000 cm⁻¹.

Lastly, the FT-IR was also used to characterize the composition of the glove material swelling residue in the solvents corresponding to the carrier fluids of the NP colloidal solutions. The study was completed by an X-ray analysis using the EDS module of the FEG-SEM (Hitachi SU-70, mechanical engineering department, ÉTS).

3. DESIGN OF MEASUREMENT METHOD

One of the main objectives of this project was to develop a method for measuring NP penetration through glove materials that could simulate workplace glove use. The conditions that had to be considered were the mode of exposure to the NPs (in powder and as a colloidal solution), the application of mechanical stress to the samples and the microclimate found inside the gloves. The measurement method included an experimental setup that met the requirements of the specifications, as well as one or more analysis techniques for detecting NP penetration. An experimental setup control and data acquisition system was also devised.

3.1 Measurement Method Specifications

Specifications for the measurement method were defined on the basis of the project objectives. The specification requirements can be divided into four categories:

- NP application conditions
- Stresses reflecting real workplace glove use
- Sampling system
- Operational safety

The setup had to be able to handle NPs in powdered form and in colloidal solution. These conditions governing NP application, particularly relevant in the case of protective gloves, are necessarily a factor in the choice of materials for the experimental setup because NPs can be sensitive to electrostatic forces in the air (Hervé-Bazin, 2007) and are subject to adsorption processes in a liquid medium (Meiling et al., 2010).

Of the stresses that reflect the conditions under which the gloves are used, those chosen for this study were the mechanical deformations undergone by the gloves and the microclimate found inside them. Two types of mechanical deformations are relevant to protective gloves: biaxial stretching, at the joints, for example, with maximum deformation values of as much as 80% on the back of the hand (Vu-Khanh et al., 2011), and compression corresponding to prehension actions, for instance, with prehensive forces of up to 500 N (Meyer et al., 2001). Both types of stress can be exerted statically or dynamically. Simulating the microclimate found inside the glove requires temperatures of at least 35°C (Purvis et al., 2000), humidity of up to 98% (Sullivan et al., 1992) and contact with a physiological solution having a pH between 4.3 and 6.5 (Kurabayashi et al., 2002; Hayden et al., 2004).

The sampling system had to be able to accommodate the various techniques investigated for detecting and characterizing the fine structure of NPs. Note that the sampling medium for the NPs can be gas (air), or liquid in the case of a physiological solution in contact with the glove sample. Given the difficulty of handling NPs, the sampling system had to be designed so as to reduce the risks of contamination and thereby limit the occurrence of false positives.

Finally, to ensure operator safety, all the handling associated with the setup, chiefly its assembly, operation, dismantling and cleaning, had to be done inside a glove box. This also included placing the sample membrane in position, introducing the NPs and sampling them.

3.2 Experimental Setup

The experimental setup designed and made for this project is shown in Figure 2. It includes an exposure chamber and a sampling chamber, which also serves as a physiological chamber. The two chambers, having an internal diameter of 54 mm and heights of 38 and 50 mm, respectively (see Appendix A), are separated by a circular sample of glove material. Rubber seals ensure airtightness. Each chamber has a series of ports equipped with connectors and stopcocks for sampling and decontamination operations. All the components of the setup that come into contact with NPs are made of ultra-high molecular weight polyethylene (UHMWPE) in order to limit the adsorption effect of NPs in colloidal solution observed by FCS in the case of other types of materials, such as anodized aluminum (Mahé, 2009).

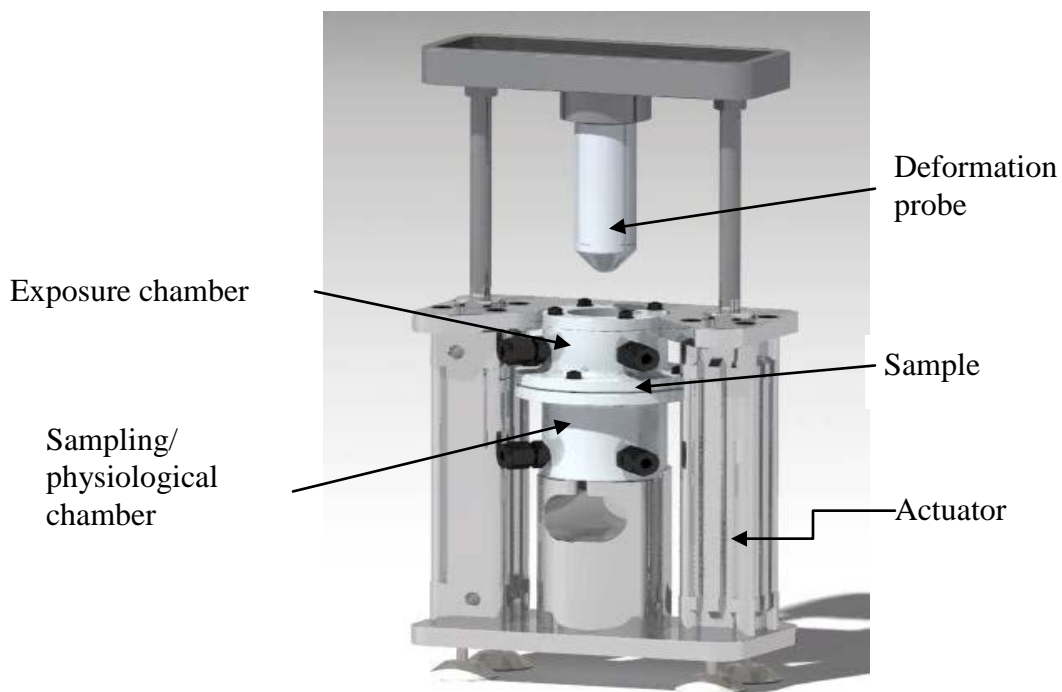


Figure 2 – Diagram of experimental setup

The NPs were introduced into the exposure chamber, where they came into contact with the outer surface of the glove. For NPs in powder, a second thin, circular, nitrile membrane was placed on top of the sample to keep the NPs in contact with the sample surface and prevent them from dispersing inside the exposure chamber, especially when the deformation stress was applied to the sample. The sampling chamber serves a dual purpose: detecting NPs that have passed through the sample and simulating the microclimate inside the gloves. The role of physiological chamber requires temperature and humidity conditions that reflect levels reported in the

literature, as well as contact of the sample with a physiological solution simulating sweat, formulated according to standard EN 1811 (CEN, 1998).

Deformations were applied to the samples by means of two pneumatic actuators controlled by an electrovalve and a cylindrical probe with an interchangeable tip. A 900 N load cell and a position detector allowed computer control of the deformation force and displacement over time, as well as acquisition of the relevant data. The system was designed so that the deformations could be applied statically or dynamically. Figure 3 shows the change in deformation of the sample over time as dynamic mechanical stress was applied. The time between two successive deformations could be adjusted, and the deformations could be applied when the glove sample was exposed to NPs.

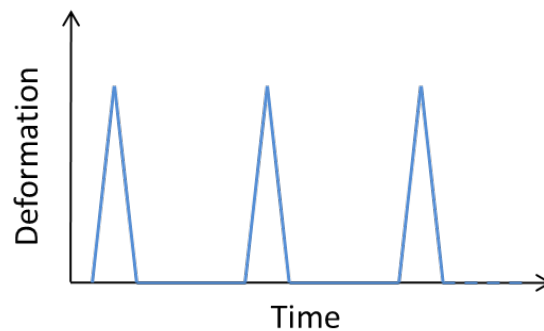


Figure 3 – Schematic representation of change in sample deformation over time as dynamic mechanical stress is applied

Four geometries for the tip of the deformation probe were designed (see Figure 4). Probe A consists of a 35 mm diameter solid cylinder that exerts an out-of-plane deformation on the sample while applying pressure on the NPs. Probe B is identical to probe A, except that it has a slight edge, so that it can deform the sample without applying pressure on the NPs. Probe C has a conical-spherical-tip geometry that can simulate the biaxial deformation of gloves resulting from flexing of the hand and joints (Vu-Khanh et al., 2007). These three probes produce concave deformation of the outside surface of the glove material, where the NPs are applied. Probe D is a 50 mm diameter solid cylinder that, when used in conjunction with a supporting piece (shown in Figure 4), could apply compressive stress to the sample. To offset the reduced volume in the sampling chamber caused by deformation of the sample, the chamber is connected up to an overflow system.

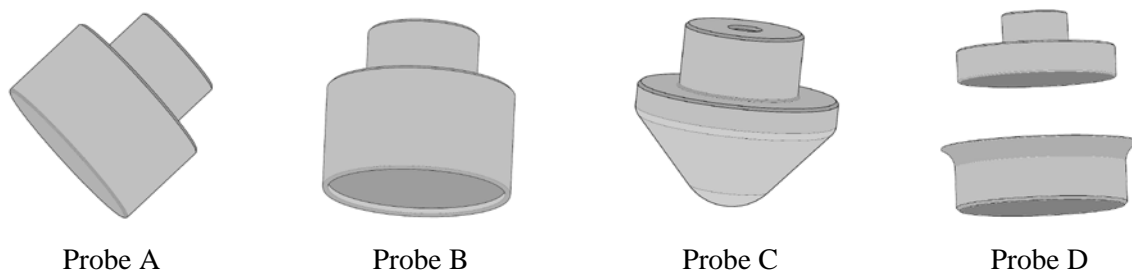


Figure 4 – Tip geometries for deformation probe

The experimental setup and accessories were designed to be handled and operated inside a glove box. Figure 5 shows the setup inside the glove box. Slight negative pressure in the glove box helped ensure that NPs could not leak out. The glove-box vacuum pump was also equipped with a HEPA filter at the outlet. As TiO₂ NPs are highly sensitive to static electricity and therefore have a tendency to stick to the walls of the glove box, the inside surfaces of the box were regularly wiped with a special cloth. To control the temperature in the sampling chamber and simulate the microclimate typically found inside gloves, a heating system with a radiant heat source and a fan was devised for the glove box (Deltombe, 2010). A computer-controlled servo system was used to maintain the sample at a constant temperature ($\pm 1^{\circ}\text{C}$).

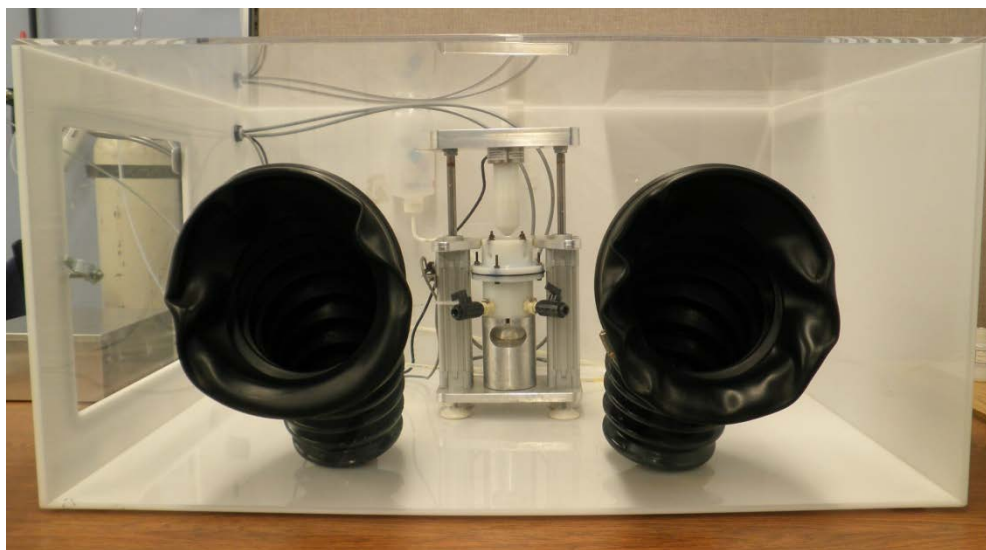


Figure 5 – Experimental setup inside glove box

3.3 System Control, Data Acquisition and Handling Protocol

A software program was written with Labview to control the experimental setup and record the relevant data. It has two interfaces. The first is for setting the sensor parameters (force applied, position and thermocouple) and controlling the displacement of the actuators during the assembly and dismantling of the setup. The second is used to select the test conditions (force or position control mode, static or dynamic mode, height of sample deformation, length of experiment), enter the name of the file for recording the data (time, temperature, force applied, position) and view the results (force applied as a function of time, position as a function of time, and force applied as a function of position). Figure 6 shows a screen shot of the interface used to conduct an experiment.

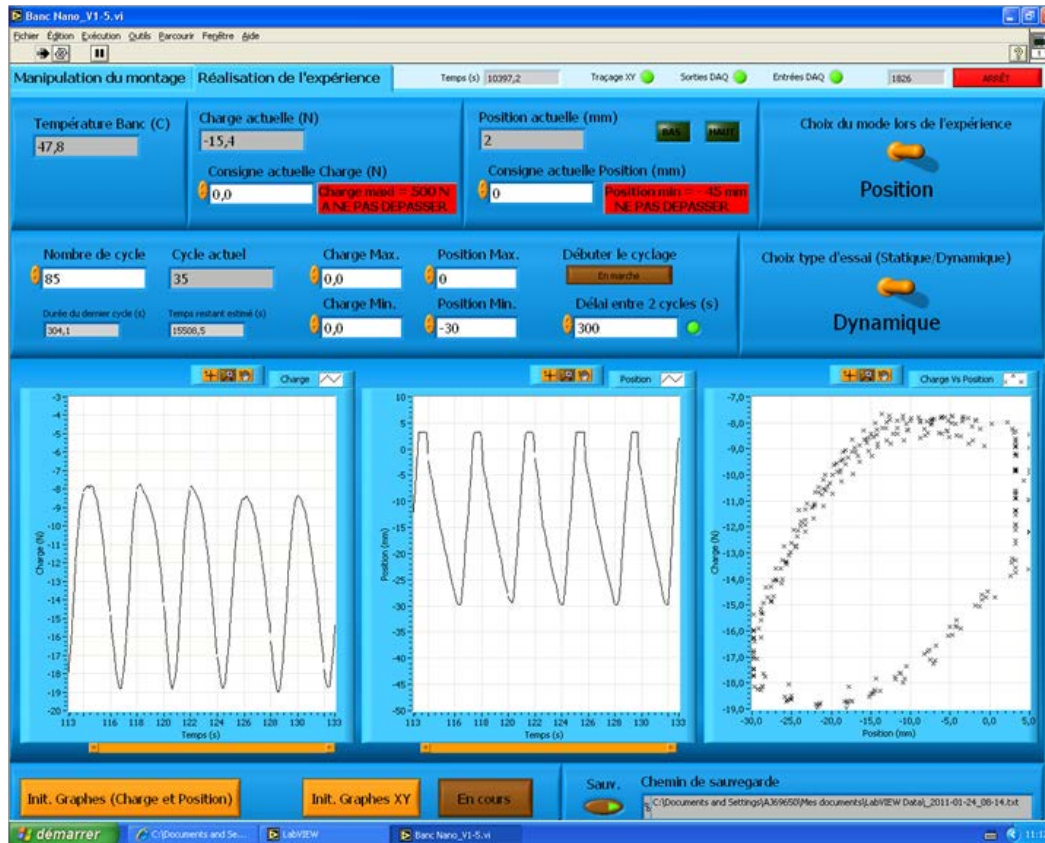


Figure 6 – “Conduct experiment” interface of system control and data acquisition program

A user manual detailing the operating and maintenance protocol for the measurement setup was produced. It covers the following stages:

- Clean sampling chamber and connectors (25% hydrochloric acid and rinse with water)
- Prepare glove sample (and double membrane if NPs in powder)
- Prepare NP sample (powder or colloidal solution)
- Prepare sampling solution (blank + sample) or physiological solution
- Prepare and collect blank (rinsing sampling solution)
- Assemble measurement setup (experimental setup and accessories) and add sample, NPs and sampling solution
- Begin experiment (set operating parameters)
- End experiment (collect sampling solution and dismantle)

A detailed description of these operations is provided in the user manual in Appendix B.

3.4 Analysis Techniques and Sampling Protocol

A significant amount of the work for this study was devoted to identifying analysis techniques for detecting the passage of NPs through glove materials. Two situations had to be taken into consideration: detection in a gaseous medium (air) and detection in a liquid medium (physiological solution).

The first technique evaluated for the direct detection of TiO₂ NPs in a gaseous sampling medium was SMPS. Testing involved the two detection ranges available, 2–150 nm and 10–1000 nm, and air flow velocities of up to 10 L/min. In all cases, nothing was recorded, except for a few isolated events, even when NPs aspirated directly from a spatula disappeared into the SMPS intake pipe. The explanation for this inability to measure TiO₂ powder NPs was found when the end of the pipe was examined. As Figure 7 shows, the inside of the pipe was covered with TiO₂ powder.



Figure 7 – Photograph of SMPS pipe intake after attempt to detect TiO₂ powder NPs

This detection problem was related to the high sensitivity of NPs to electrostatic forces, which causes them to be attracted to nonconducting surfaces (Jankovic et al., 2010). In this case, the presence of graphite in the composition of the SMPS silicone pipe was apparently not sufficient to eliminate the problem with the TiO₂ powder, which could not reach the SMPS's counting module to be detected. One way to overcome the problem would be to use a steel intake pipe for the SMPS. Given that the sampling chamber is made of polyethylene, however, the same static attraction problem would already occur on the walls of the sampling chamber, and so the NPs that might pass through the sample would not have any chance of reaching the SMPS intake pipe. If this technique were used, it would mean that a conducting material would have to be used for the sampling chamber, but this option had been rejected when the setup was designed because of the problem of adsorption of NPs in solution.

A second series of NP detection techniques that was investigated involved the use of microscopy to analyse the inside surface of the glove samples (on the sampling chamber side). In the case of FEG-SEM and AFM, direct observation of NPs at the glove surface proved to be quite inaccurate, owing to the presence of tiny bumps on the elastomer surface that are very similar in size and shape to powdered TiO₂ particles. Figure 8, for instance, shows images of TiO₂ powder

on the surface of nitrile and latex gloves, obtained by FEG-SEM and AFM, respectively. Thanks to a carbon deposit on the surface of the sample, it was possible with FEG-SEM to perceive a chemical contrast by means of backscattered electrons (Figure 9). The resolution was limited, however, which made precise quantitative analysis difficult. The other problems with using these microscopy techniques for the direct detection of TiO₂ NPs on sample surfaces are related to the difficulty of locating a few NPs on a huge surface and the need to eliminate all NPs on the exposed side in order to avoid contamination between the two sides of the sample. In the case of AFM, problems of entrainment of NPs by the probe tip, even in tapping mode, were also encountered.

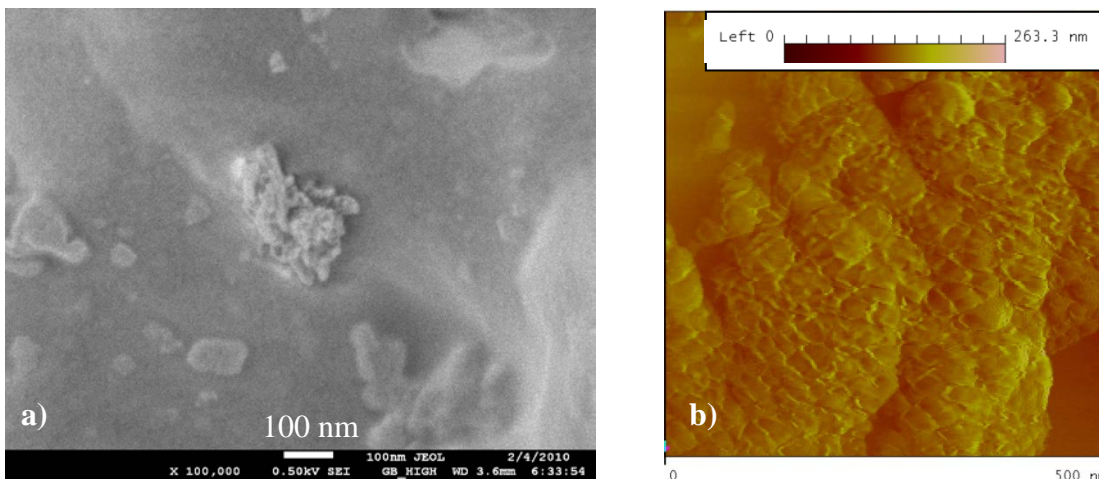


Figure 8 – Images of TiO₂ powder (a) by FEG-SEM on surface of nitrile glove and (b) by AFM on surface of latex glove

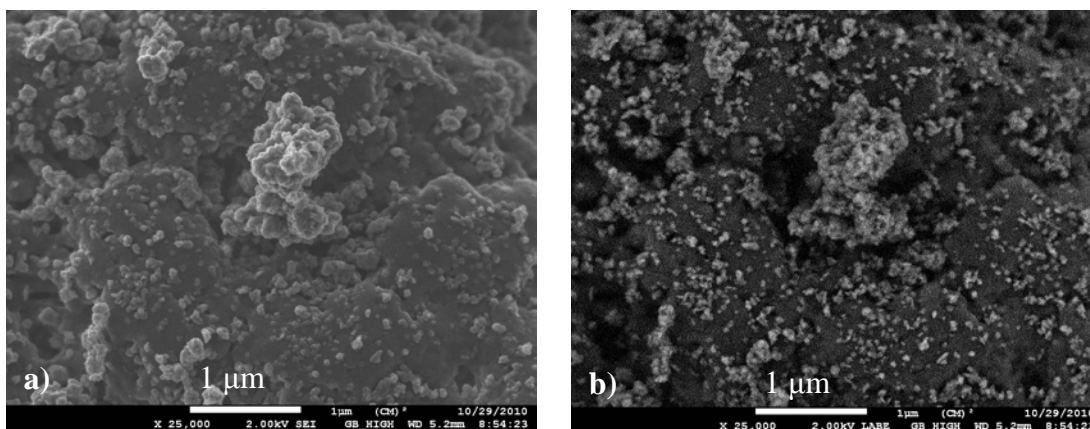


Figure 9 – FEG-SEM images of TiO₂ powder on surface of nitrile glove: (a) secondary electron imaging and (b) backscattered electron imaging

As for TEM, the need to work with very thin samples would require the use of grids stuck to the surface of the samples. But the grids are very fragile and would not withstand the deformations to which the gloves are subjected during testing. Tests might be performed later by positioning electrically charged TEM grids on a support at the bottom of the sampling chamber.

Given that direct detection of NPs in a gaseous medium is quite difficult and in an effort to address the natural tendency of TiO₂ NPs to stick to the walls of the sampling chamber, a sampling protocol tailored to the measurement method was developed. It involved the use of a sampling solution, which was placed in the sampling chamber during assembly of the experimental setup and before the start of the testing (see Figure 10). The height of the sampling solution (generally 10 mm) ensured that it did not come into direct contact with the surface of the sample when the latter was deformed (maximum deformation height of 30 mm corresponding to a 50% deformation of the sample). At the end of the experiment and before the setup was dismantled, the dual-chamber device was carefully tilted and turned so that the liquid rinsed the walls of the sampling chamber. The liquid was then transferred to a flask.

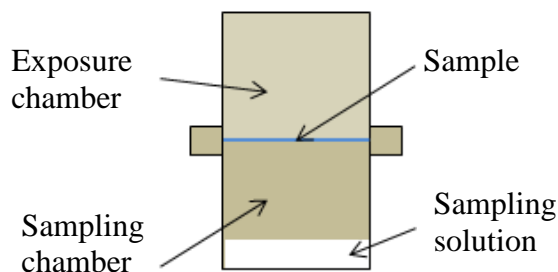


Figure 10 – Diagram of setup, with sampling solution

Once the sampling solution has been collected, various analysis techniques can be used, depending on the formulation of the solution. With a methanol or ultrapure-water sampling solution, ambient temperature centrifugation can be performed at 3,000 rpm for 60 min on carbon-coated copper TEM grids and mica substrates (for analysis by AFM or FEG-SEM) so NPs can be observed and counted (Wilkinson et al., 1999). In addition, the size distribution of the NPs that may be present in the ultrapure-water sampling solution can also be determined by NTA following marking of the NPs. Note that this technique is not sensitive to the nature of the NPs and also counts any that may have been present in the sampling solution at the outset. Lastly, the composition of the sampling solution can be analysed by ICP-MS with a view to detecting the presence of titanium from the TiO₂ NPs. In this case, a sampling solution of 1% nitric acid in ultrapure water was used, following the method proposed by Kaegi et al. (2008).

Given that the sampling solutions are batch tested—which means that the time between when they are collected and when they are analysed differs, depending on the sample—it is crucial to ensure the stability of the solutions over time. To that end, the same sampling solutions were analysed by ICP-MS at approximately three-month intervals. This operation involved over 30 sampling solutions corresponding to different experimental conditions (see Figure 11). The various sets of values for the same samples show perfect agreement. This indicates that the time that elapses between the collection of the sampling solution and its analysis by ICP-MS does not affect the quality of the results.

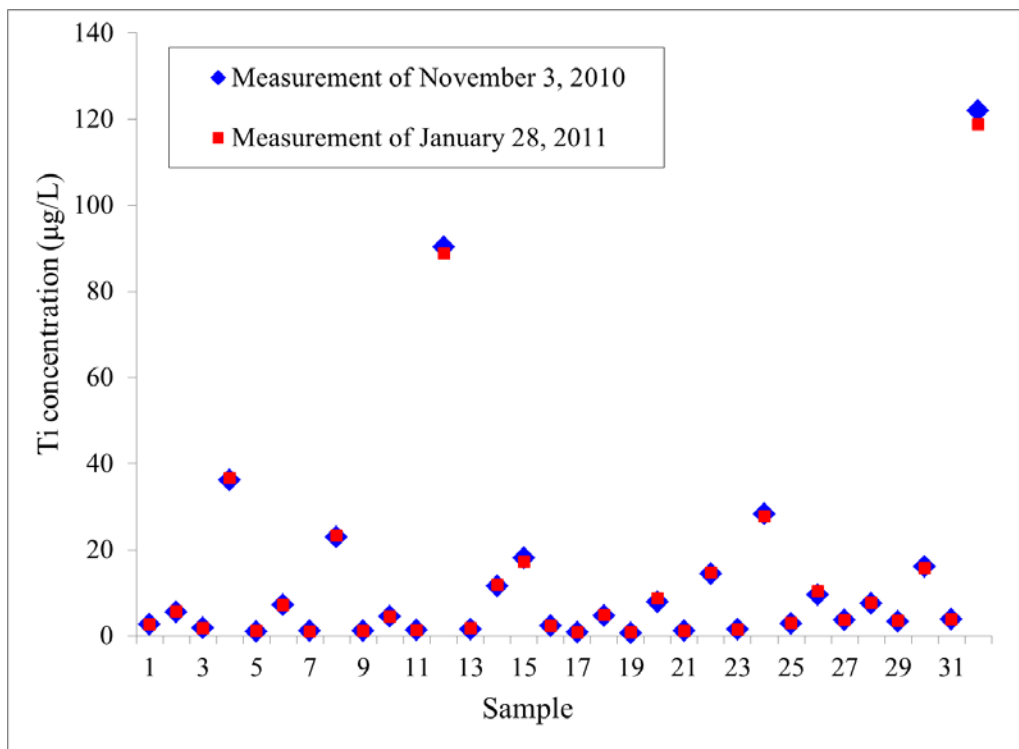


Figure 11 – Comparison of results of sampling solution analyses by ICP-MS done on November 3, 2010, and January 28, 2011

This sampling procedure can also be applied for detecting NPs in a liquid medium, which correspond to the presence of a physiological solution in contact with the surface of the sample in the sampling chamber simulating sweat inside the glove. In this case, the physiological solution serves as the sampling solution and, after it has been collected at the end of the experiment, it can be analysed in the same way, that is, by microscopy (TEM, AFM, FEG-SEM) after centrifugation, by ICP-MS after acidification and by NTA.

Finally, note that in order to detect the presence of possible contaminants and to limit the occurrence of false positives, the operating procedure that was developed, described in detail in Appendix B, includes the production of a blank solution for each experiment. This blank consists of a volume of sampling solution (of the same formulation as that used in the experiment) that is used to make a final rinse of the sampling chamber before the sampling solution for detecting the passage of NPs through the sample is introduced into the chamber. If analysis of the blank indicates NP residue in the sampling chamber, then the results of the experiment are discarded.

4. RESULTS

The experimental results of the study are presented in this section. They include a characterization of the NPs as received and of the glove materials. The assessment of the impact of the different parameters—contact with solvents, mechanical stresses, temperature and contact with physiological solutions simulating sweat—on the glove materials is also reported. Lastly, the results of preliminary tests of NP penetration through the glove materials under various conditions are presented.

4.1 Characterization of Nanoparticles

A detailed characterization of the TiO₂ nanoparticles in powder and colloidal solutions was conducted. The characteristics of the NPs, particularly their agglomeration state, can have a major impact on potential penetration through glove materials.

4.1.1 TiO₂ Powder Nanoparticles

According to the manufacturer’s specifications, the TiO₂ powder was supposed to consist of 15 nm diameter nanoparticles of 99.7% pure anatase. Characterization of the powder was performed by TEM. Powder as received from the manufacturer was deposited on carbon-coated copper TEM grids (3 mm diameter, 200 mesh). Figure 12a shows a typical TEM image. Aggregates of strongly bonded NPs can be seen, as well as agglomerates, where the bonds between the NPs are weaker. In actual fact, very few individual NPs were observed (see Figure 12b).

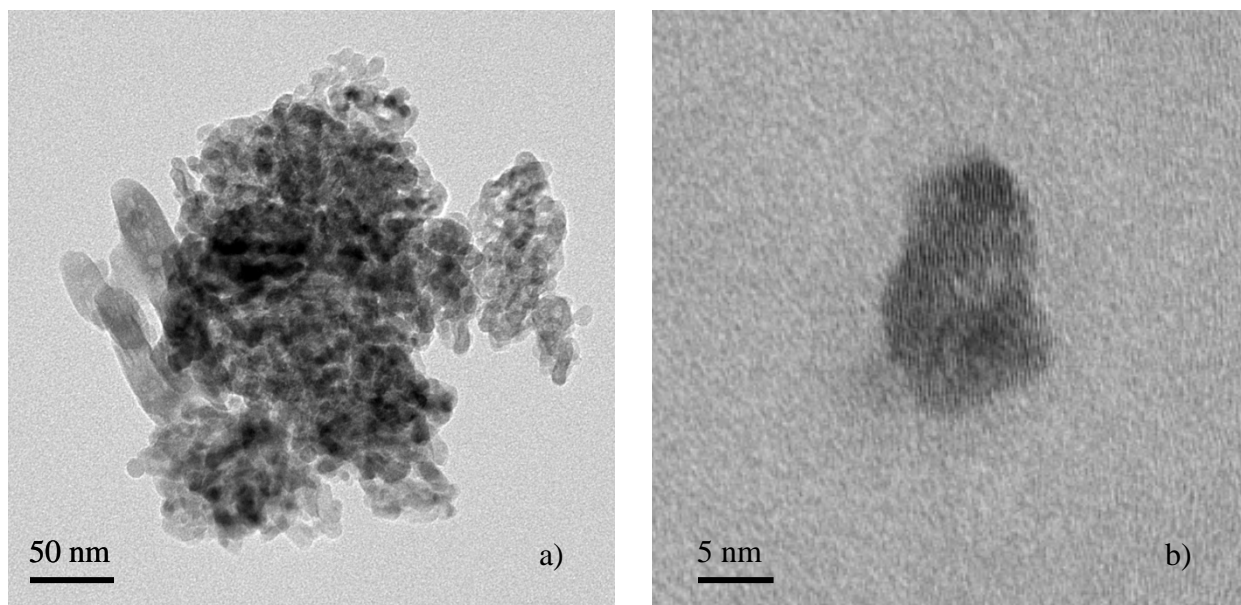


Figure 12 – TEM images of TiO₂ powder: (a) agglomerated NPs, (b) individual NP

It can be seen from Figure 12a that the powder contains NPs of two shapes: spheres and rods. The spherical particles are the anatase allotropic form, i.e., the one specified by the

manufacturer, whereas the rods are rutile, another variety of TiO_2 . On the basis of X-ray diffraction analysis (see Figure 13), the actual proportion of rutile in the TiO_2 powder was estimated to be between 3% and 6%, well above the manufacturer's specifications. The lattice parameter values for the two forms observed were $a = 0.379$ nm and $c = 0.951$ nm for the anatase and $a = 0.459$ nm and $c = 0.296$ nm for the rutile. Both forms have a quadratic crystalline structure (reference: Powder Diffraction File 2 [PDF2, version 1.0, Sept 1994] of the International Centre for Diffraction Data [ICDD]).

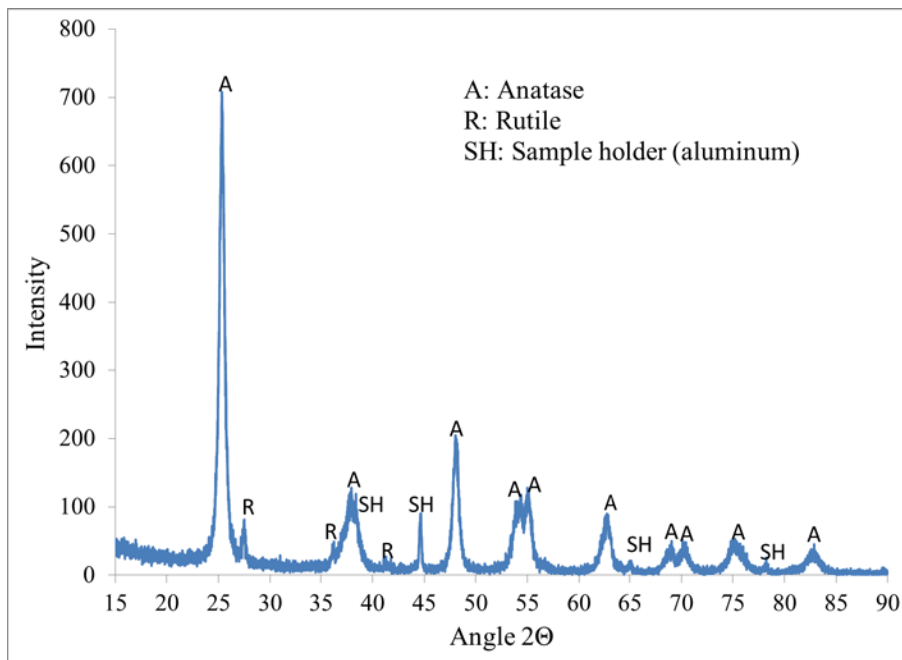


Figure 13 – X-ray diffraction spectrum of TiO_2 powder

Using the TEM's EDS module, the TiO_2 powder was subjected to elementary analysis to see whether any contaminants could be detected. The resulting spectrum, presented in Figure 14, reveals a preponderance of titanium, indicated by the two central peaks at 4.5 and 5 keV, and of oxygen at 0.5 keV. The peaks associated with copper and carbon can be attributed to the sample-holder grids. A very low peak for silicon at 1.7 keV was also noted. These results therefore confirm a high level of purity of the TiO_2 powder.

Lastly, the particle size distribution of the TiO_2 powder was analysed on the basis of the TEM images taken at different magnification levels, following the method described in Noël et al. (2013). A total of 174 particles were included in the statistical analysis. The particles were analysed and counted with Clemex Vision PE software. For each particle, the inner diameter (diameter of largest circle that can fit inside the particle), outer diameter (diameter of smallest circle that can be positioned on outside of the particle) and circular diameter (diameter of disc having same surface as the particle) were calculated. Figure 15 shows the resulting particle size distribution for circular diameter. The preponderance of aggregates between 60 and 200 nm in size can be seen. Agglomerates of up to 1200 nm in diameter were also observed. Only two individual NPs (i.e., smaller than or equal to 20 nm) were found among the 174 particles analysed.

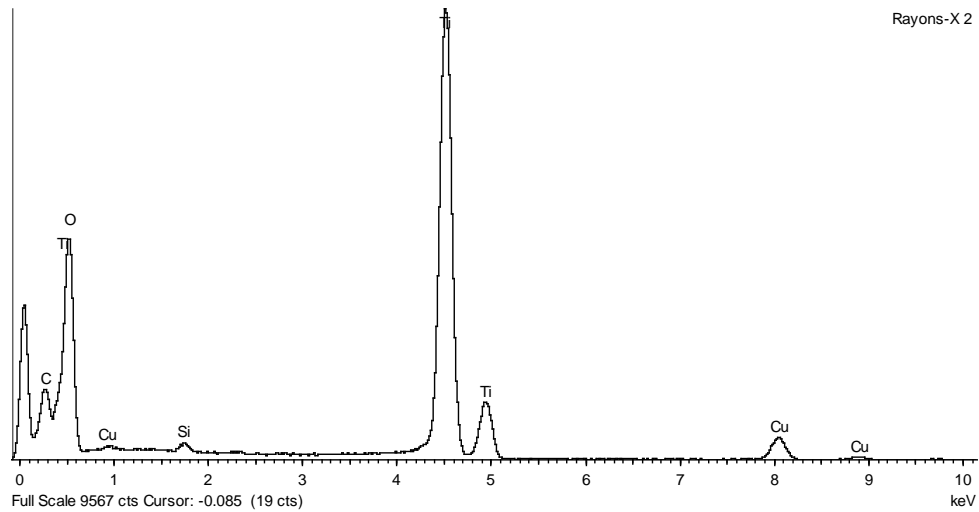


Figure 14 – EDS spectrum of TiO₂ powder

The mean diameter of the particles in the TiO₂ powder was calculated on the basis of the particle size distribution, which follows an inverse Gaussian distribution (see Figure 15). A mean diameter of 217 nm was obtained. This result differs considerably from the figure provided by the manufacturer, which was 15 nm. This discrepancy may be due to the strong tendency of TiO₂ nanoparticles to agglomerate (Witschger et al., 2005).

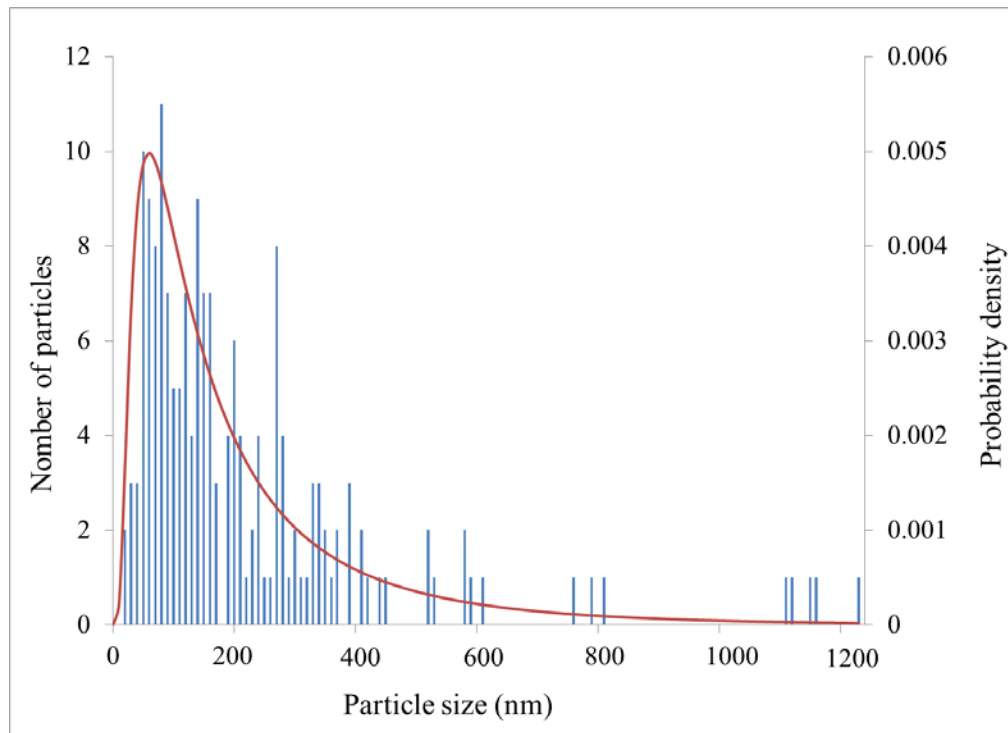


Figure 15 – Particle size distribution of TiO₂ powder based on circular diameter measured from TEM images, with smoothing line by inverse Gaussian distribution

4.1.2 *TiO₂ Nanoparticles in Colloidal Solution*

A characterization of the colloidal solutions of TiO₂ NPs in water, EG and PG was also carried out. The mean size of the NPs was measured by FCS for the colloidal solutions in water and in EG diluted in water: particle diameter values of 21 ± 2 nm for water and 35 ± 3 nm for EG were obtained. These results are close to the manufacturers' data and indicate that the TiO₂ NPs are well dispersed in the commercial colloidal solutions. Note that we were unable to take measurements for the colloidal solutions in PG because the sample-holder basin was made of a material incompatible with the solvent.

Tests using microscopy to observe the NPs contained in the colloidal solutions were conducted, but ultimately failed because of the formation of a viscous film at the surface of the NPs following evaporation of the carrier fluid (water, EG and PG). The film may have formed as a result of additives, such as stabilizing agents, present in the colloidal solutions. In an attempt to detect these additives, the colloidal solutions were examined by thermogravimetric analysis (TGA). The results were compared with the spectra obtained under the same conditions for the solvents used as carrier fluids in the colloidal solutions (technical purity and ultrapure).

Figure 16 shows the results obtained by TGA for the TiO₂ colloidal solution in PG and for technical and ultrapure PG. The curves for the technical PG and the ultrapure PG are identical, indicating similar composition. In contrast, the curve for TiO₂ colloidal solution in PG is shifted toward higher temperatures. The same phenomenon was observed when the curves obtained for TiO₂ colloidal solution in water and for distilled water and ultrapure water were compared. The boiling point was shifted toward higher temperatures because the solvent is absorbed by the NPs, raising the system's vapour pressure. In the case of EG, the same shift toward higher temperatures of the peak corresponding to the TiO₂ colloidal solution was seen in relation to the one for the ultrapure solvent. At the same time, the peak for the technical solvent was also shifted in relation to that for the ultrapure solvent, which indicates a difference in the two levels of purity.

Although the presence of NPs in the TiO₂ colloidal solutions can be seen in the TGA measurements in the form of shifted boiling points, no additional peak in relation to ultrapure solvents—which could have been attributed to additives in the formulation of the colloidal solutions—could be identified in the TGA measurement results. However, this technique may not be sufficiently sensitive, if the additive concentrations in question are too low.

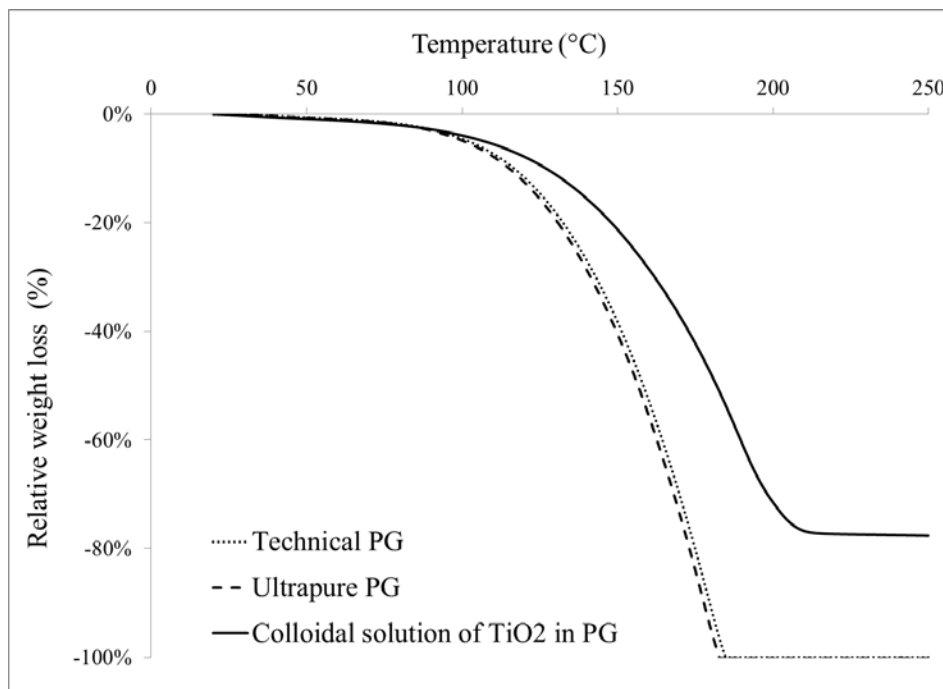


Figure 16 – Relative weight loss as a function of temperature, according to TGA of colloidal solution of TiO₂ NPs in PG and of technical and ultrapure PG

In an attempt to detect possible additives in the three TiO₂ colloidal solutions, FT-IR analyses were also performed. They were done in ATR mode on drops of solution following almost total evaporation of the solvent. No major difference between the spectra of the colloidal solutions, technical solvents and ultrapure solvents was seen for EG and PG. In the case of water, however, the spectrum of the TiO₂ colloidal solution had an additional peak at 1,070 cm⁻¹ in relation to that of ultrapure water (see Figure 17), which may be related to stretching of a C-O bond. This could be an indication of the presence of an alcohol or ether additive, such as ether glycol, in the TiO₂ colloidal solution in water. Note that the EG and PG spectra have a complex structure, which may explain why it is difficult to detect potential additional peaks associated with possible additives. Furthermore, there is a strong likelihood that the peaks characteristic of these possible additives could be very close to the peaks characteristic of the two glycols, which could make it very difficult to detect them.

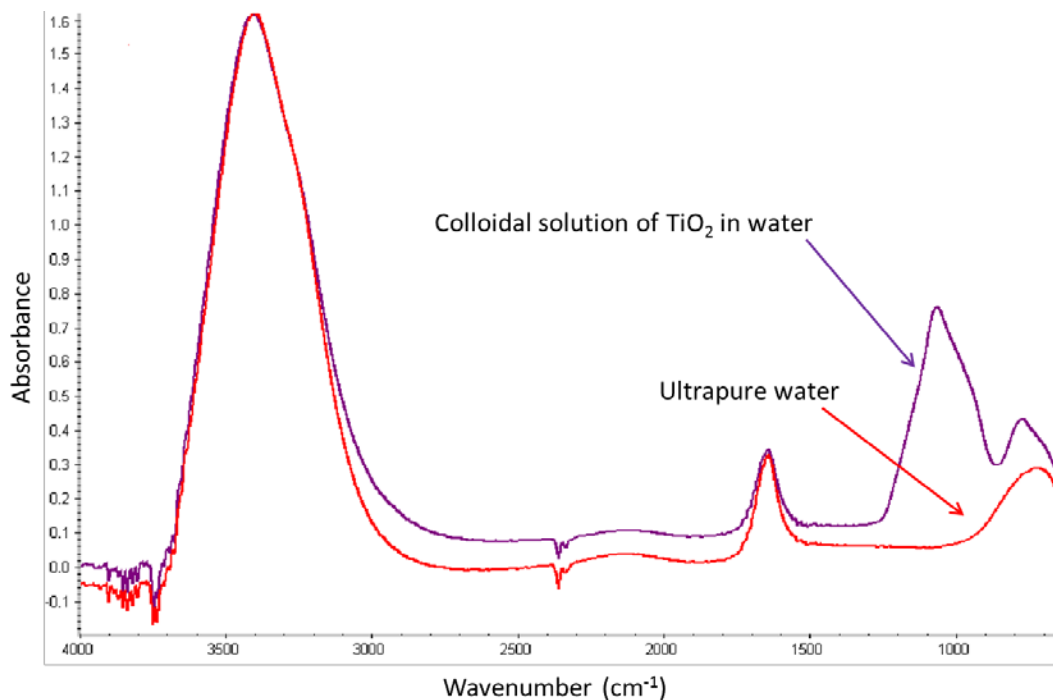


Figure 17 – Comparison of FT-IR spectra of colloidal solution of TiO₂ in water and of ultrapure water

Lastly, the colloidal solutions were analysed by TGA to determine the mass fraction values of NPs in the three solutions (see Table 2). Each value is the mean of two measurements. All values were within 5 percentage points of the values specified by the manufacturers.

Table 2 – Mass fraction of TiO₂ measured by TGA, for three colloidal solutions (water, EG, PG)

	TiO ₂ in water	TiO ₂ in EG	TiO ₂ in PG
Mass fraction measured (%)	14	16	25
Mass fraction according to manufacturer (%)	15	20	20

4.2 Characterization of Glove Materials

Glove materials were likewise characterized in terms of chemical composition, state of the surface and mechanical behaviour.

4.2.1 Chemical Analysis

The main objective of the chemical analysis was to determine whether the gloves contained any TiO_2 , with a view to evaluating any factors that could interfere with the detection of TiO_2 NPs in the sampling solution. Indeed, TiO_2 powder is used in some applications as a reinforcing filler in the polymer matrix. Consequently, for the four models of gloves as well as for a disposable nitrile glove without reinforcing filler (nitrile WRF), measurements were taken on the outer and inner surfaces and in the thickness (cross-section) using the SEM EDS module. Figure 18 shows the spectrum obtained for the outer surface of the nitrile glove. The presence of elements such as zinc, calcium, sulphur, potassium, oxygen and titanium may be due to the use of numerous types of additives—vulcanizing agents, activators, accelerators and reinforcing fillers—in the formulation of the glove materials (Mellström et al., 2005).

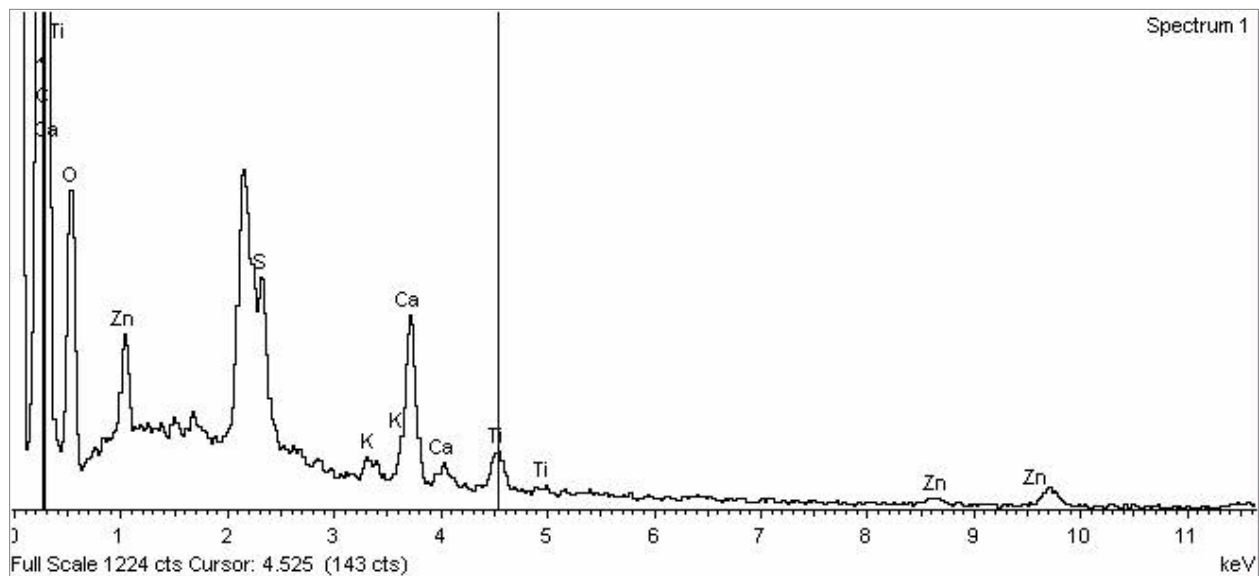


Figure 18 – Example of EDS spectrum of outer surface of nitrile glove

Table 3 gives the mass concentrations of titanium obtained for the five models. Some materials, such as nitrile and neoprene, had non-negligible titanium concentrations. This shows that verification measurements are needed to ensure that any titanium measured in the sampling chamber is not the product of the deterioration of the gloves themselves. Moreover, the slight difference between the results obtained for the two models of nitrile glove suggests that any reinforcing fillers in the model of nitrile glove chosen for the study did not include TiO_2 .

**Table 3 – Mass concentration of titanium in gloves
(outer surface, inner surface and cross-section)**

	Mass concentration of titanium (%)		
	Outer surface	Inner surface	Cross-section
Nitrile	0.51 ± 0.06	0.51 ± 0.08	0.28 ± 0.06
Nitrile WRF	0.23 ± 0.06	0.38 ± 0.06	0.13 ± 0.04
Latex	N/D	N/D	N/D
Neoprene	0.27 ± 0.06	N/D	0.21 ± 0.06
Butyl rubber	N/D	N/D	N/D

N/D: not detectable (detection limit of 100 ppm)

WRF: without reinforcing fillers

4.2.2 State of Surface

The inner and outer surfaces of the gloves were examined by SEM. Figure 19 shows images of the outer surfaces of the four gloves. Micrometric-size pores could be seen on the nitrile surface (Figure 19a), consistent with what Ahn et al. (2006) have reported. The surface of the neoprene glove (Figure 19c) also had fairly long cracks (up to 100 µm) that looked quite deep, as well as a few outcrops of reinforcing particles. Even if these imperfections probably did not go through the full thickness of the glove, they still constitute areas of weakness of the membrane that could become critical in the event of glove deformation. They are also spaces in which NPs could build up (Ahn et al., 2006). The surface of the latex glove (Figure 19b) had a large number of outcropping or semidetached particles. Lastly, the surface of the butyl rubber glove (Figure 19d) appeared to consist of clusters of small plates.

The same type of morphology could be seen on the inner surface of the gloves, except in the case of neoprene, where fibres a dozen micrometres in diameter were also present (see Figure 20). These may be intended to make the gloves easier to get on and off.

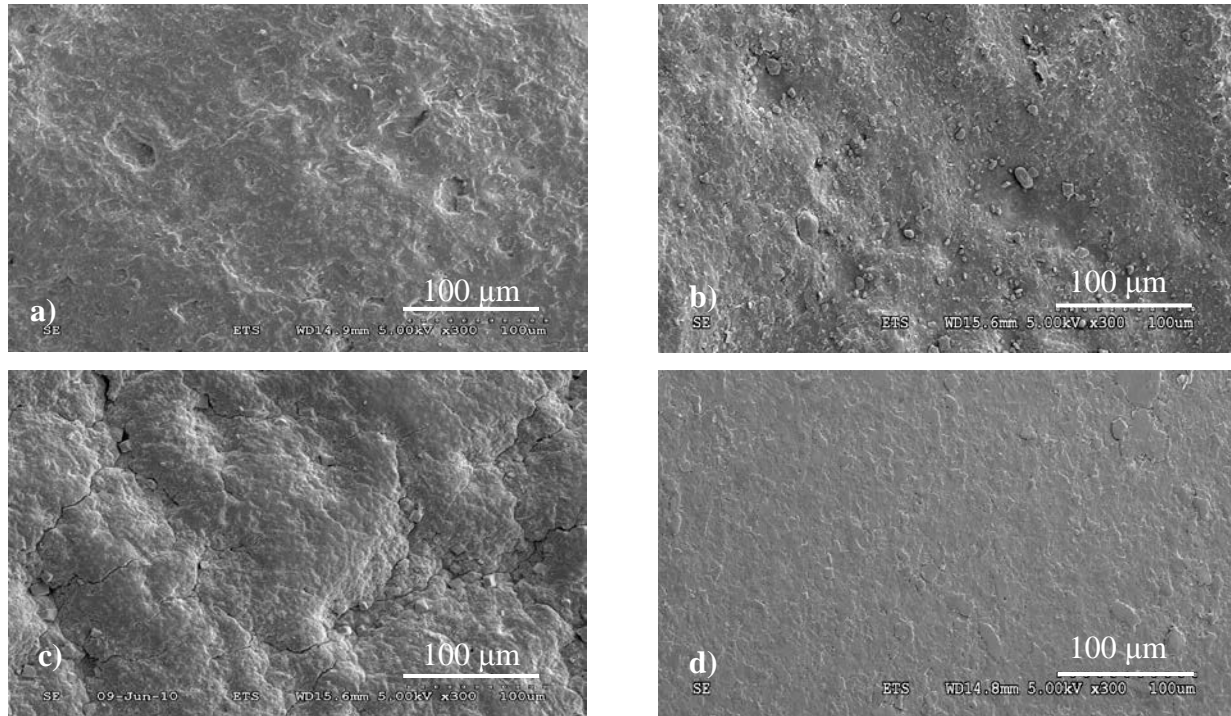


Figure 19 – SEM images of outer surface of gloves: (a) nitrile, (b) latex, (c) neoprene and (d) butyl rubber

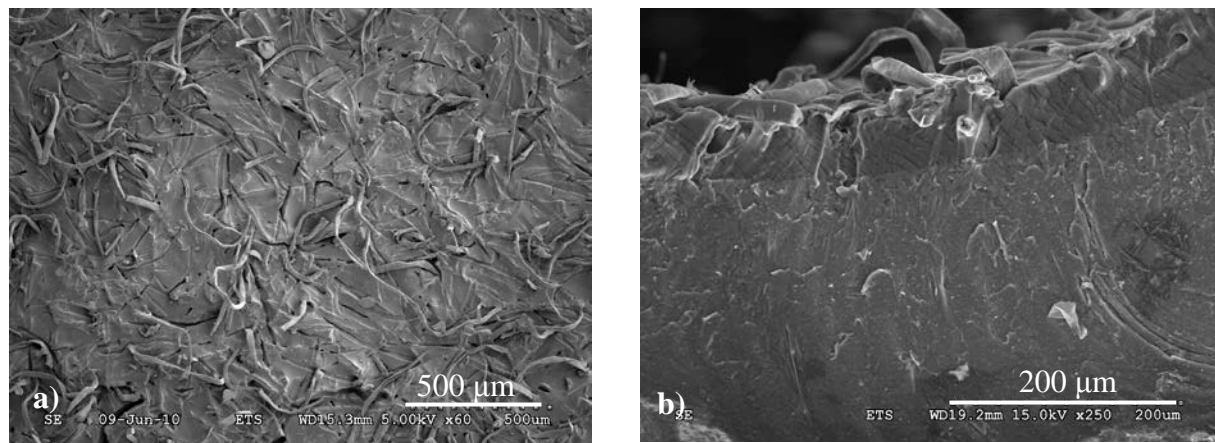


Figure 20 – SEM images of (a) inner surface of neoprene glove and (b) cross-section

4.2.3 Mechanical Behaviour

Given that the gloves are subjected to deformations during NP penetration testing, it was important to characterize their mechanical behaviour. Measurements were taken during both uniaxial stress testing on tensile specimens and during biaxial stress testing using a conical-spherical-tip probe for samples cut from the palms of four types of gloves.

Figure 21 shows an example of uniaxial tension stress-strain curves for samples of nitrile, latex, neoprene and butyl rubber cut crosswise. Non-linear elastic behaviour characteristic of elastomers can be seen in all four materials.

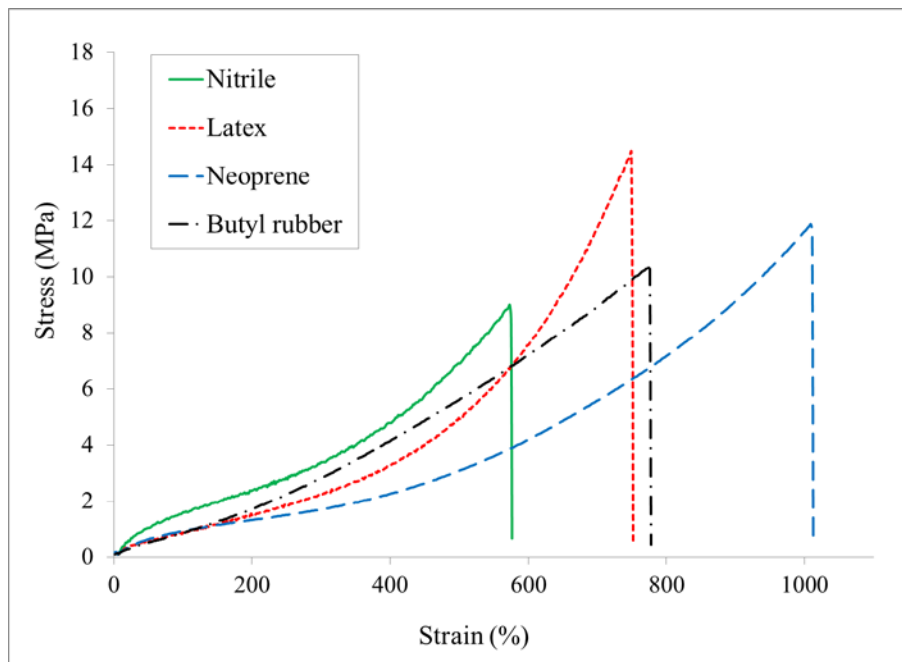


Figure 21 – Stress-strain curves for nitrile, latex, neoprene and butyl rubber when subjected to uniaxial tension (crosswise)

Table 4 gives the results obtained in terms of secant modulus at 100% strain, elongation at break and strength for the four glove materials subjected to uniaxial tensile testing, both lengthwise and crosswise. The results are consistent with the literature on pure vulcanized elastomers with respect to the modulus and elongation at break (Furuta et al., 2005). In the case of tensile strength, the slightly lower values obtained for the gloves may be due to the presence of different additives, especially reinforcing fillers, in their formulations.

For nitrile and latex, differences were seen for elongation at break and tensile strength between the values measured lengthwise and crosswise. This possible anisotropy of some of their mechanical properties may be due to the manufacturing process used for these thin disposable gloves.

Table 4 – Results of lengthwise and crosswise tensile testing of nitrile, latex, neoprene and butyl rubber gloves

	Direction	Secant modulus at 100% (MPa)	Elongation at break (%)	Tensile strength (MPa)
Nitrile	Crosswise	1.9 ± 0.1	595 ± 35	11.4 ± 1.6
	Lengthwise	1.9 ± 0.2	664 ± 8	14.2 ± 0.9
Latex	Crosswise	0.86 ± 0.23	778 ± 50	13.2 ± 1.9
	Lengthwise	0.88 ± 0.02	566 ± 52	9.9 ± 1.5
Neoprene	Crosswise	1.2 ± 0.3	1,002 ± 68	11.9 ± 0.9
	Lengthwise	1.1 ± 0.3	1,096 ± 39	13.7 ± 1.1
Butyl rubber	Crosswise	0.8 ± 0.2	897 ± 37	12.4 ± 0.7
	Lengthwise	0.8 ± 0.4	914 ± 21	11.3 ± 1.2

The mechanical properties of the glove materials when subjected to biaxial strain were also characterized using a flexibility setup (see Section 2.3.2). Figure 22 shows typical examples of force-displacement curves for the four materials. The characteristic shape of the non-linear elastic behaviour observed in uniaxial tension can also be seen in biaxial deformation.

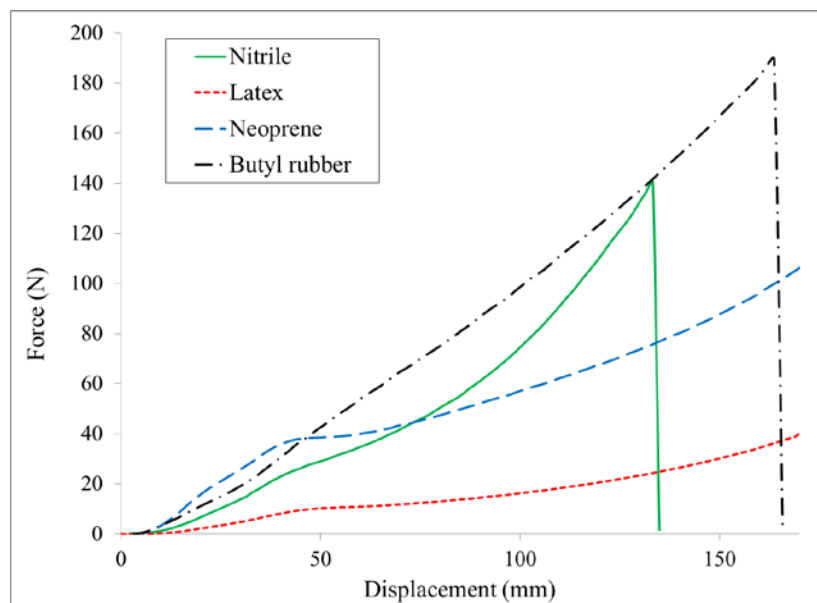


Figure 22 – Force-displacement curves for nitrile, latex, neoprene and butyl rubber when subjected to biaxial strain

Table 5 gives the characteristic mechanical values for the glove materials calculated on the basis of the biaxial deformation data. It can be seen that the maximum deformation that could be applied to the glove samples in the experimental setup, i.e., 80% (probe displacement of 40 mm), was well below the degree of elongation at break for the four materials.

Table 5 – Elongation and force at rupture for nitrile, latex, neoprene and butyl rubber gloves when subjected to biaxial strain

	Elongation at break (%)	Force at break (N)
Nitrile	435 ± 5	66 ± 1
Latex	511 ± 8	41 ± 1
Neoprene	531 ± 40	115 ± 12
Butyl rubber	485 ± 14	211 ± 23

4.3 Characterization of Impact of Deformations on Glove Materials and Nanoparticles

Applying dynamic strain to the samples may progressively affect the mechanical properties of the materials. The deformations may also alter the state of NP agglomeration at the surface of the sample in the exposure chamber when the probe exerts direct pressure on the NPs, as in the case of the biaxial probe.

4.3.1 Impact on Mechanical Behaviour of Glove Materials

To examine the possible effect of dynamic mechanical stress on the properties of the glove materials, testing was conducted with the experimental setup and the residual mechanical performance of the materials was evaluated. More specifically, biaxial dynamic loading of 50% was applied to samples of the four glove materials at a frequency of one deformation every 5 minutes over a total testing time of 7 hours. On the basis of the force-displacement values recorded by the data acquisition system during testing, the work corresponding to a 50% deformation applied to the sample was calculated at regular intervals. Figure 23 shows the results obtained for nitrile and butyl rubber. Similar behaviour was observed for latex and neoprene.

Three phases were identified in the change in work with the number of mechanical stresses undergone. In the initial cycles, a drop in work occurs. Fairly quickly, work reaches a minimum, then increases, which is a sign of rigidification of the material. A final phase corresponding to a drop in work is reached at varying times, depending on the type of material.

In the case of the initial softening, one possible mechanism involved is the Mullins effect, a stress-softening phenomenon resulting from the deformation of rubber that occurs during the initial loading cycles (Mullins, 1969). The Mullins effect has been attributed to the breakage of bonds both between polymer chains and between the matrix and filler particles (Marckmann et al., 2002). The second phase identified in the cyclical loading behaviour of elastomers, i.e., an increase in the rigidity of the material as the number of cycles rises, may be due to a phenomenon of crystallization under stress to which some elastomers are sensitive and which causes an increase in the mechanical performance of the material (Xu et al., 1993). Lastly, the final reduction in work, and therefore in the rigidity of the elastomer, may be due to breakage of the polymer chains.

These results indicate that dynamic loading causes permanent damage to the material, which occurs by various successive mechanisms, depending on the number of deformation cycles. Further study will be required to identify the phenomena involved with certainty.

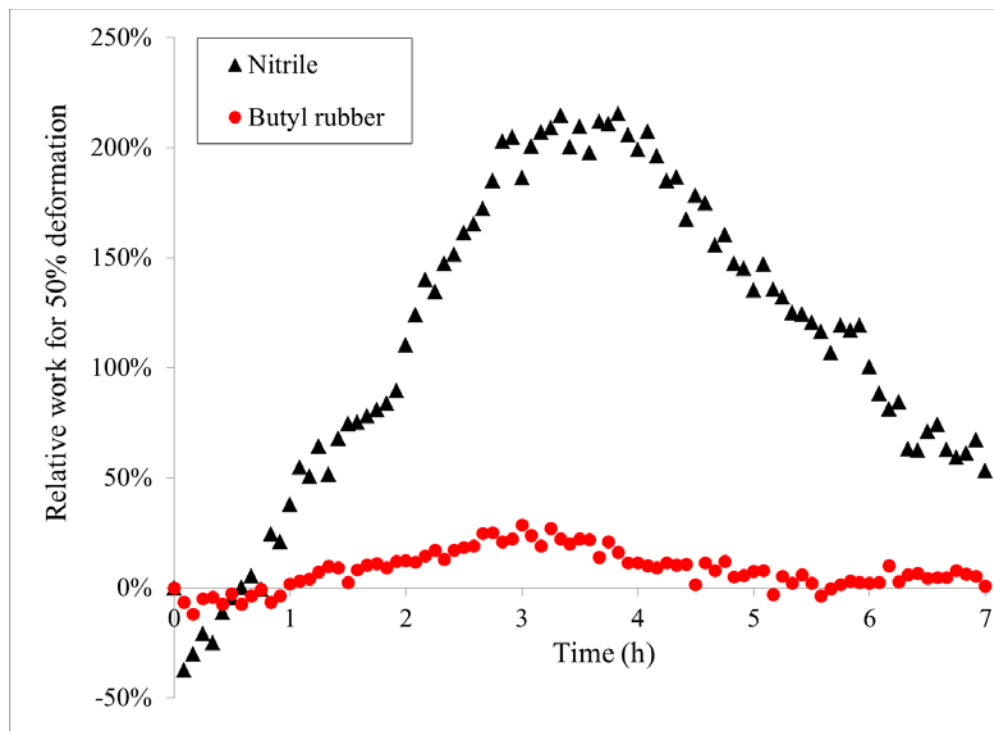


Figure 23 – Relative change in work corresponding to a 50% biaxial deformation of samples of butyl rubber and nitrile, as a function of the duration of exposure to biaxial mechanical loading (one deformation every 5 minutes)

4.3.2 Impact on Nanoparticle Agglomeration State

Similar testing was carried out to assess the effect of biaxial dynamic loading on the NP agglomeration state. TiO₂ powder was deposited on the surface of the sample placed in the experimental setup. A second thin nitrile membrane was placed over the sample to keep the NPs in contact with it. Biaxial dynamic loading of 50% was then applied to the sample at a rate of one deformation every 5 minutes. Following exposure times of 1.5 h, 3 h, 5 h and 7 h to dynamic mechanical stress, the sample was carefully retrieved from the setup and the excess powder removed from the surface. The surfaces of the samples exposed to NPs were then analysed by FEG-SEM.

The images obtained at different magnifications (up to x25,000) of the surface of the samples exposed to NPs were compared. As shown in Figure 24, it would appear that the agglomerates become smaller when the dynamic loading increases from 1.5 h to 7 h. These observations need to be corroborated by rigorous statistical analysis of the images, but that was not possible at the time because of a lack of clear contrast between the NPs and the surface of the gloves. If confirmed, this result would indicate that the particle size distribution of the TiO₂ powder was

changed by the deformations applied to the sample. A reduction of this kind in NP agglomeration could affect penetration of the nanoparticles through the glove materials.

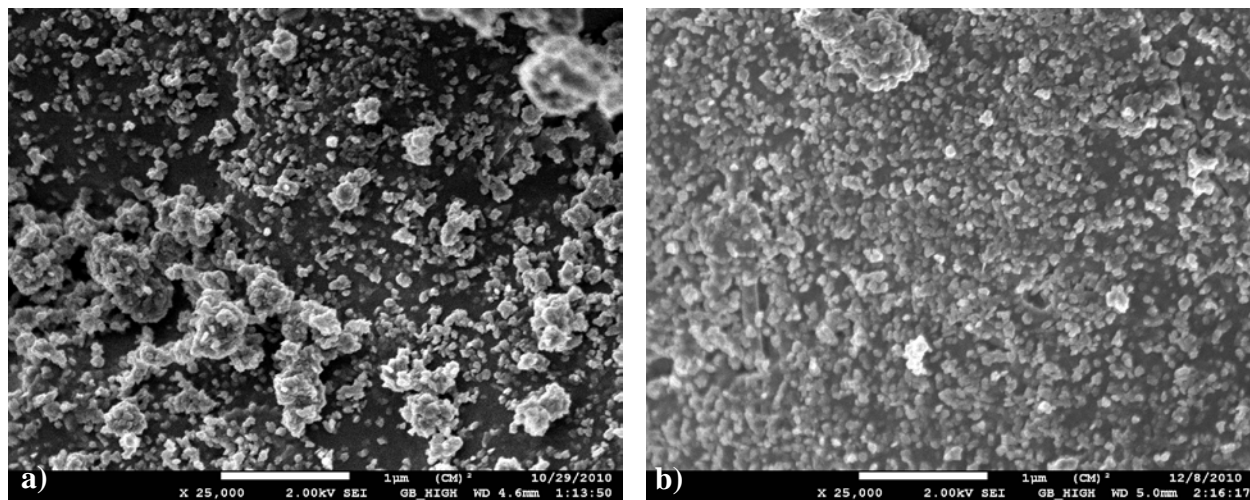


Figure 24 – FEG-SEM images of surface of neoprene samples exposed to TiO_2 powder in conjunction with biaxial dynamic loading of 50% for durations of (a) 1.5 h and (b) 7 h

4.4 Characterization of Impact of Nanoparticle Carrier Fluids in Colloidal Solution on Glove Materials

The elastomers in glove materials can be sensitive to the effects of the carrier fluids of NPs in colloidal solution. The effects can include a swelling of the polymer and a change in its mechanical properties (Rodot, 2006). If solvents penetrate into the elastomer and diffuse through the membrane, they may act as carriers for the NPs and facilitate their passage through the glove. Measurements were therefore taken to characterize the effect of the three carrier fluids of the colloidal solutions—water, EG and PG—on certain physical and mechanical properties of the four glove materials.

4.4.1 Swelling

The mutual solubility of a solvent and a polymer results in a swelling of the polymer. Changes in the solubility of the solvent in the polymer can be quantified by measuring the weight gain and/or the length change of the polymer over time (Perron et al., 2002). These methods can be used to calculate a mean coefficient of diffusion of the solvent in the polymer.

Measurements of weight gain as a function of time of immersion of the glove material in the three colloidal solutions as well as in ultrapure solvents corresponding to the carrier fluids of the solutions were taken for the four glove materials. Immersion times of up to 3 days were used in order to reach the plateau corresponding to maximum swelling. A few comparison tests were also done with disposable nitrile gloves containing no silicone, plasticizers or reinforcing fillers (identified as nitrile WRF).

Figure 25 shows the relative change in the weight of nitrile samples as a function of time of immersion in the TiO₂ colloidal solution in water for the four sets of measurements performed under the same conditions. A gradual increase in weight over time can be seen, with the weight gain reaching 20% after 2 hours of immersion. This 2-hour duration was, however, not sufficient to highlight the plateau indicating that maximum swelling had been reached. Good reproducibility of results among the four sets of measurements was noted, which indicates that the experimental procedure was valid.

To check that the weight gain of the nitrile samples following immersion in the TiO₂ colloidal solution in water was not caused by a build-up of NPs in the surface pores of the membrane, swelling measurements were also taken in ultrapure water. Figure 26 presents the comparative results of weight gain for nitrile in ultrapure water and in the colloidal solution of TiO₂ in water. Perfect consistency can be seen for the entire 8-hour duration of the experiment. This indicates that the weight gain of the nitrile samples through immersion in the colloidal solution of TiO₂ in water was indeed due to water swelling the nitrile. Diffusion of water through nitrile, latex and vinyl gloves within a period of less than 12 hours has also been shown with tritium markers (Golanski et al., 2010).

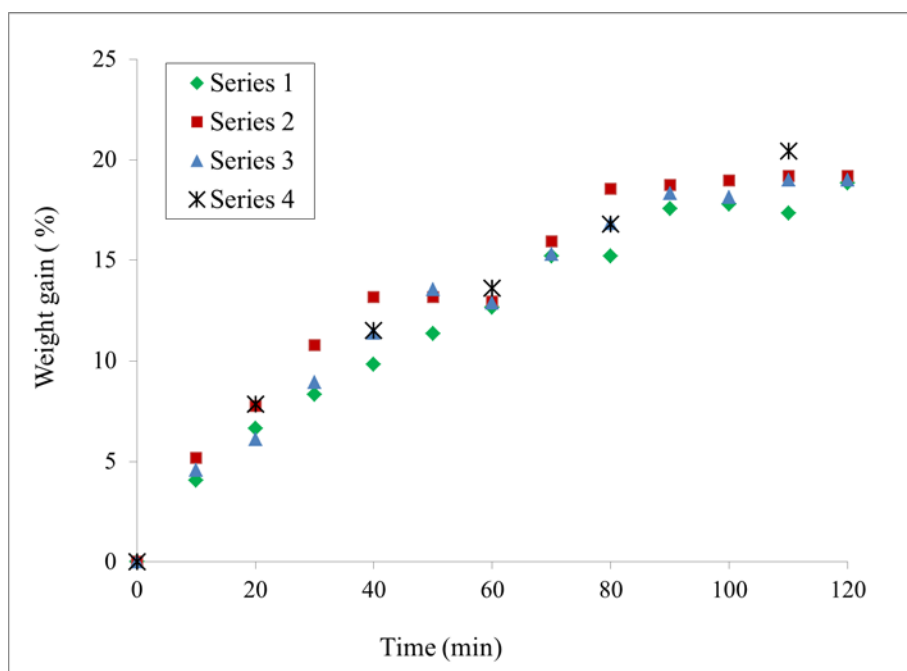


Figure 25 – Weight gain as a function of immersion time of nitrile in colloidal solution of TiO₂ in water, with four repeats

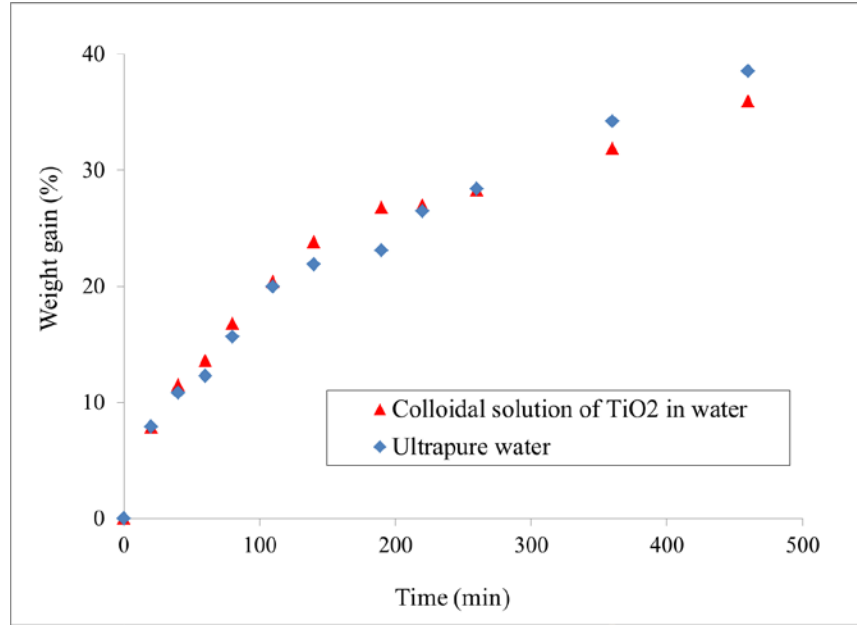


Figure 26 – Weight gain as a function of immersion time of nitrile in colloidal solution of TiO₂ in water and in ultrapure water

To ensure that the results obtained for the nitrile glove model selected for the project were representative of the behaviour of disposable nitrile gloves in general, measurements of swelling in ultrapure water were also taken with another model of glove from another manufacturer. These gloves were advertised as containing no silicone, plasticizers or reinforcing fillers (nitrile WRF). Figure 27 shows the results for the nitrile glove selected for the project and the WRF nitrile glove for comparison purposes. A difference in absolute value can be seen between the swelling behaviours of the two models of gloves. It can be attributed to a difference in formulation and in particular to the presence of reinforcing particles in the composition of the nitrile glove selected for the project. However, the tendency observed, i.e., progressive weight gain right from the start of the immersion and the reaching of a plateau after long immersion times, is the same. The maximum rate of swelling in water is approximately 100% for nitrile gloves with reinforcing fillers, and 60% for gloves made of nitrile WRF. Nitrile gloves therefore appear to be sensitive to swelling by water, regardless of the proportion of reinforcing filler. The disposable nitrile gloves used in the workplace do generally contain reinforcing fillers, hence the appropriateness of the model selected for the study.

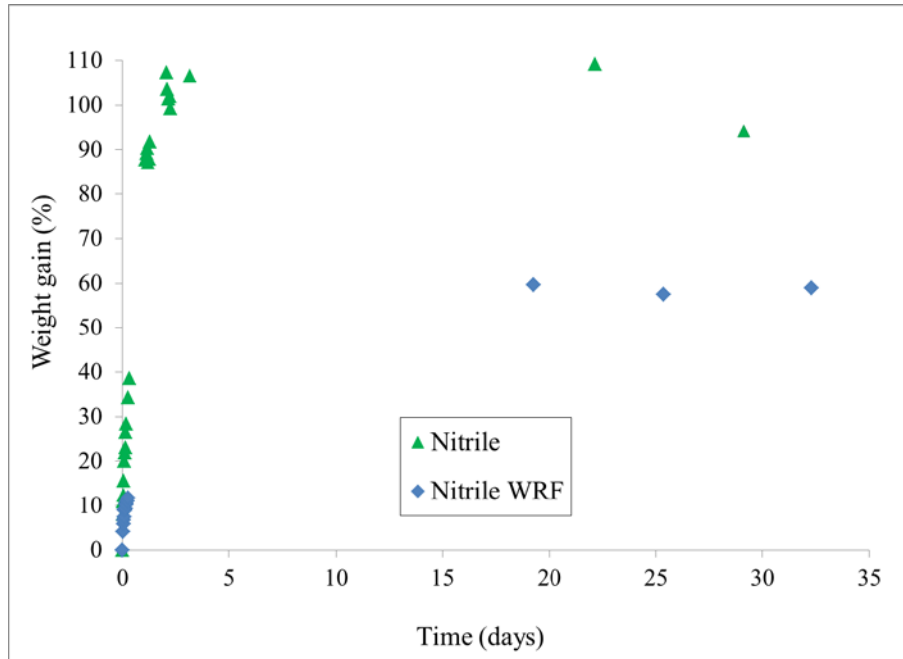


Figure 27 – Weight gain as a function of immersion time of nitrile and of nitrile WRF in ultrapure water

The swelling behaviour of nitrile in the other two colloidal solutions, i.e., with EG and PG as a carrier fluid, was also measured. Figure 28 compares the weight gain recorded for nitrile immersed in colloidal solutions of TiO₂ in water, EG and PG. The same tendency can be seen for the three solutions, i.e., a gradual increase in weight and failure to reach maximum swelling after 8 hours of immersion. The curves for EG and PG are superimposed, indicating a similar affinity of the two colloidal solutions for nitrile. This may be due to the fact that the two solvents (EG and PG) belong to the same chemical family, which is one of the parameters that control the rate of swelling of elastomers by solvents (Nohilé et al., 2008). On the other hand, there is a stark difference between the weight gain for nitrile in colloidal solution of TiO₂ in water as opposed to in EG or PG: swelling values approximately twice as high were recorded for the colloidal solution of TiO₂ in water. This contrast between the swelling of nitrile in water and its swelling in glycols may be due to a number of factors, including differences in viscosity, molecular size and structure, and polarity of the two families of solvents.

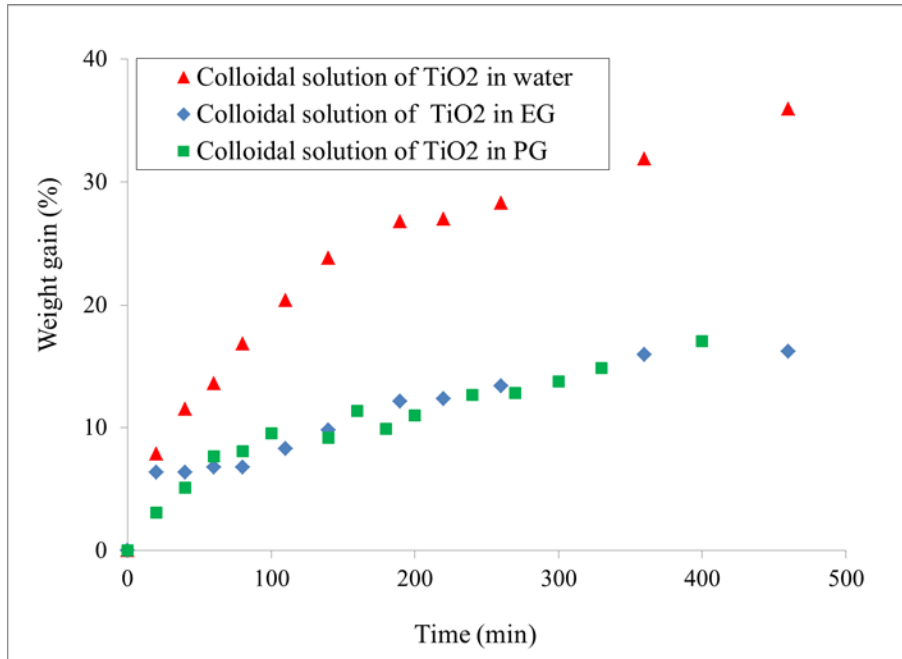


Figure 28 – Weight gain as a function of immersion time of nitrile in colloidal solutions of TiO₂ in water, EG and PG

The swelling behaviour of the four glove materials in colloidal solutions of TiO₂ in water, EG and PG was also compared. Figure 29 shows weight gain as a function of immersion time of nitrile, latex, neoprene and butyl rubber in a colloidal solution of TiO₂ in water. Significant differences in swelling behaviour between the four glove materials can be seen. After two hours, the weight gain of the nitrile reached close to 20%, whereas that of the latex peaked at 7% and the neoprene at 4%. In all three cases, the weight gain was gradual and began right from the start of the immersion. This indicates chemical diffusion, involving the NP carrier fluid, in nitrile, latex and neoprene. For the butyl rubber samples, no significant weight gain was measured. Butyl rubber therefore does not appear to be susceptible to swelling in a colloidal solution of TiO₂ in water, in contrast to the other three materials.

To monitor the maximum swelling that could be reached by nitrile, latex or neoprene gloves in the colloidal solutions of TiO₂ in water, EG and PG, measurements were taken over a longer time. Figure 30 shows the results for an immersion period of 79 hours (just over 3 days) in the colloidal solution of TiO₂ in water. It can be seen that the classification of the materials by maximum degree of swelling attained remains the same as after 2 hours of swelling, i.e., nitrile swells up much more than latex, which swells up slightly more than neoprene. The maximum swelling rates recorded for this period are 79% for nitrile gloves, 27% for latex and 23% for neoprene.

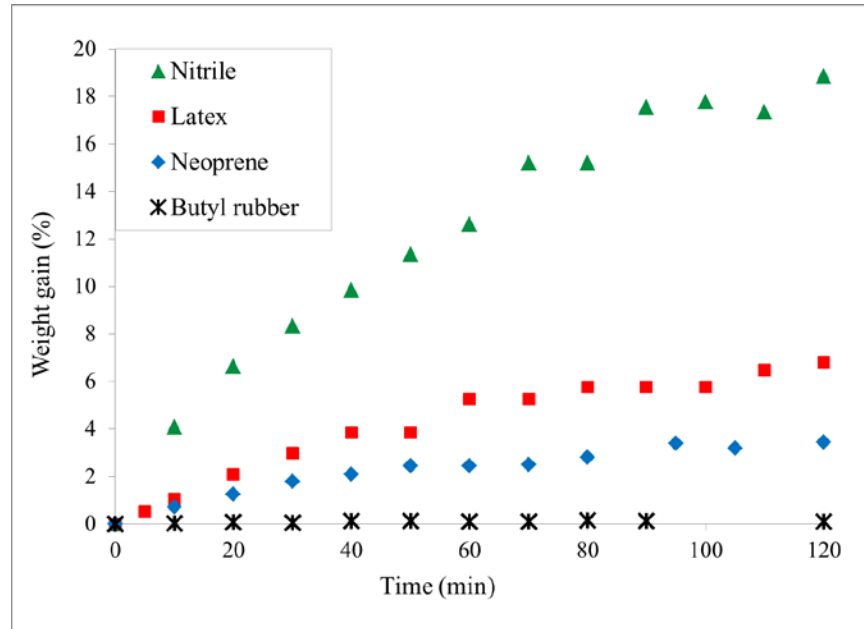


Figure 29 – Weight gain of nitrile, latex, neoprene and butyl rubber as a function of immersion time in colloidal solution of TiO₂ in water

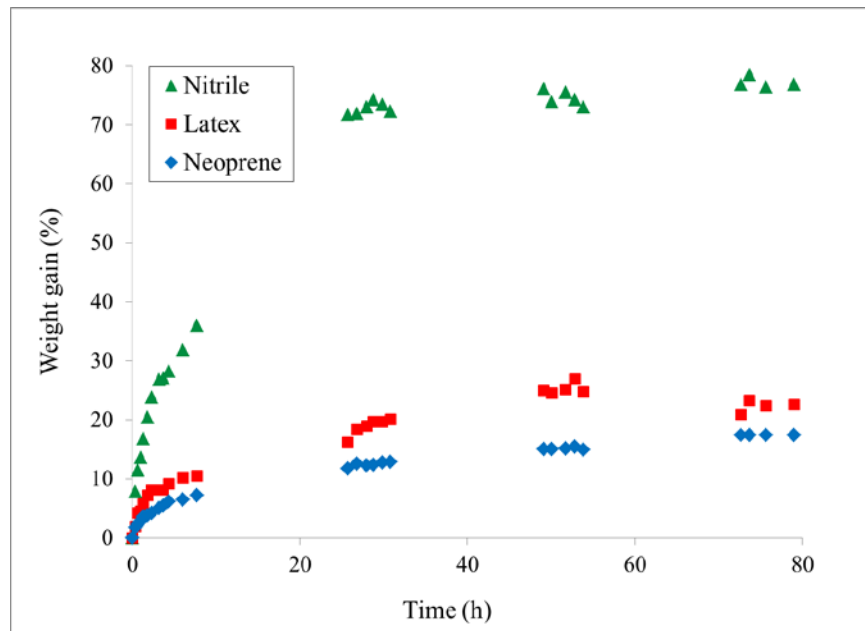


Figure 30 – Weight gain of nitrile, latex and neoprene for long immersion times in colloidal solution of TiO₂ in water

The values for maximum weight gain measured over immersion periods of up to 37 days for the four glove materials and the three colloidal solutions of TiO₂ are summarized in Table 6. The ranking of the four materials by swelling rate for the three solutions is the same, i.e., the nitrile swells up much more than the latex, which swells up a little more than the neoprene. Butyl rubber did not swell in any of the three solutions. This indicates that gloves made of nitrile, latex

or neoprene are indeed affected by being in contact with colloidal solutions of TiO₂ in water, EG or PG.

Table 6 – Maximum rate of weight gain for four glove materials (nitrile, latex, neoprene and butyl rubber) in three colloidal solutions of TiO₂ (in water, EG and PG)

	Maximum rate of swelling (%)		
	Colloidal solution of TiO ₂ in water	Colloidal solution of TiO ₂ in EG	Colloidal solution of TiO ₂ in PG
Nitrile	79	73	94
Latex	27	14	26
Neoprene	23	11	11
Butyl rubber	0	0	0

For the three colloidal solutions of TiO₂ (in water, EG and PG), the values of the mean coefficient of diffusion D in nitrile, latex and neoprene were calculated from the weight gain data using the following approximation (Perron et al., 2002):

$$D \approx \frac{0,04919 e^2}{t_{1/2}^2}$$

where e is the thickness of the membrane and $t_{1/2}$ is the half-life calculated from the linear regression of the change in $(M_t - M_0)/(M_\infty - M_0)$ as a function of \sqrt{t} at $(M_t - M_0)/(M_\infty - M_0) = 1/2$. M_0 , M_t and M_∞ are, respectively, the mass values of the sample at time 0, time t and infinite time (maximum swelling). The mean coefficient of diffusion in butyl rubber was not calculated because no weight gain was recorded.

These mean coefficients of diffusion are given in Table 7. Higher mean coefficients of diffusion were measured for neoprene with the three colloidal solutions of TiO₂ (in water, EG and PG), which implies that in neoprene, carrier fluid diffusion occurs faster. This may be due to its moderate resistance to chemicals (Dolez et al., 2010). Nitrile and latex, on the other hand, are very similar to each other in their behaviour. Major differences among the three colloidal solutions of TiO₂ can also be seen, with the solution in water diffusing faster than that in EG, which in turn diffuses faster than the solution in PG. This tendency is the same for the three glove materials. Note that these mean coefficient of diffusion values are lower than what may be measured with other, more powerful solvents (Perron et al., 2002).

Table 7 – Mean coefficients of diffusion in nitrile, latex and neoprene, for three colloidal solutions of TiO₂ (in water, EG and PG)

	Mean coefficient of diffusion (cm ² /s)		
	Colloidal solution of TiO ₂ in water	Colloidal solution of TiO ₂ in EG	Colloidal solution of TiO ₂ in PG
Nitrile	1.6 10 ⁻¹⁰	7.0 10 ⁻¹¹	5.0 10 ⁻¹¹
Latex	1.4 10 ⁻¹⁰	10.4 10 ⁻¹¹	4.0 10 ⁻¹¹
Neoprene	1.0 10 ⁻⁹	6.9 10 ⁻¹⁰	1.5 10 ⁻¹⁰

Mean coefficients of diffusion for ultrapure water and PG were also calculated. Values similar to those measured for the corresponding colloidal solutions were obtained for water in the three elastomers and for PG in latex. In contrast, ultrapure PG diffused slightly faster in nitrile and in neoprene than the colloidal solution of TiO₂ in PG did. This difference in behaviour may be due to the presence of additives in the colloidal solution of TiO₂ in PG, which alter the diffusion process (Perron et al., 2002).

In Figure 30, a slight decrease in the weight of latex for longer durations of immersion in the colloidal solution of TiO₂ in water can be seen. This weight loss was confirmed by measurements taken after very long immersion times (22, 28 and 35 days, see Figure 31). A similar, but far more noticeable phenomenon was seen with colloidal solutions of TiO₂ in EG and PG. After 30 days of immersion, the weight gain of latex samples had fallen from 14% (at maximum swelling) to 5% for EG, and from 26% to 6% for PG (see Figure 31). A drop in weight gain was also seen for nitrile after lengthy immersion in EG, sliding from 73% at maximum swelling to 63% after 28 days of immersion. This weight loss may be due to a deterioration of the elastomers from the effect of the colloidal solutions of TiO₂ in the various solvents (Rodot, 2006). This long-term deterioration of the materials in colloidal solutions of TiO₂ was confirmed by weight losses in relation to the initial weight measured for these samples immersed for 40 days then dried under a hood (see Table 8). The deterioration should eventually stabilize, as seen in the case of latex and the colloidal solution of TiO₂ in water, where a plateau appears to have been reached at 27 days (Figure 31). In the case of colloidal solutions of TiO₂ in EG or PG, another phenomenon that prevents the plateau from being reached may come into play. This may be related to the hygroscopic nature of the two carrier fluids, which absorb water from the surrounding air, with the water taking the place of the solvents in the polymer matrix. Since water has a lower mass and volume than EG and PG, a gradual loss of mass may occur. However, this phenomenon is entirely reversible and does not result in any difference in weight after drying.

The phenomenon of deterioration of latex and nitrile in colloidal solutions of TiO₂ in water, EG and PG, which occurs with immersion times far longer than a workday, is not relevant to the problem of protecting against NPs by wearing gloves. The deterioration may, however, need to be taken into consideration for products intended for storing NPs in colloidal solutions.

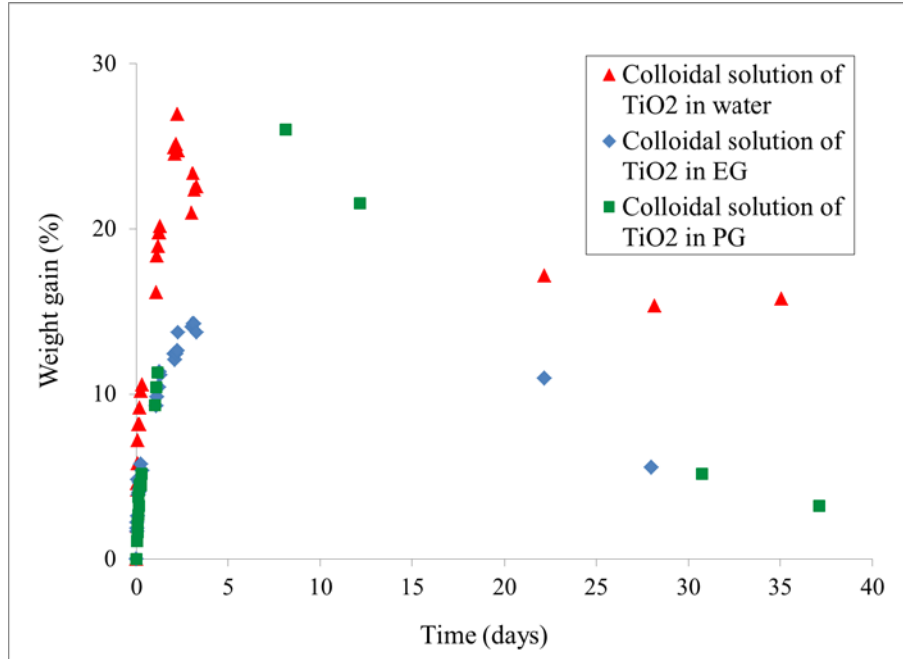


Figure 31 – Weight gain of latex as a function of immersion time (days) in colloidal solutions of TiO₂ in water, EG and PG

Table 8 – Change in weight in relation to initial weight, for samples of nitrile, latex and neoprene immersed for 40 days in three colloidal solutions of TiO₂ (in water, EG and PG) then dried under a hood

	Change in weight (%)		
	Colloidal solution of TiO ₂ in water	Colloidal solution of TiO ₂ in EG	Colloidal solution of TiO ₂ in PG
Nitrile	0.4	-5.5	-9.0
Latex	-10.8	-14	-14.4
Neoprene	-2.4	-2.9	-3.1

The swelling of glove materials from the effect of colloidal solutions of TiO₂ in water, EG and PG was also characterized by length change measurements of lengthwise and crosswise samples cut from the palm of gloves. Significant increases in the length of samples following immersion in the three colloidal solutions of TiO₂ were noted for nitrile and latex. Figure 32, for instance, shows the variation in relative length of crosswise samples of nitrile as a function of immersion time in colloidal solutions of TiO₂ in water and PG. Just as swelling was noticeable in terms of weight gain, it could also be seen in a gradual increase in length that began right from the time the samples were immersed in the solutions. Similar changes in the length of samples were also measured with the technical and ultrapure solvents corresponding to the carrier fluids of the colloidal solutions of TiO₂ in water, EG and PG. These results confirm the sensitivity of the

glove materials to the carrier fluids of the three colloidal solutions, which resulted in diffusion of the solvent in the elastomer.

It should be noted that major differences between lengthwise and crosswise elongation were seen in the case of nitrile and latex, with the crosswise elongation being far greater (Dolez et al., 2011). This anisotropic dimensional swelling was attributed to the anisotropy measured for certain mechanical properties of the two materials (see Section 4.2.3).

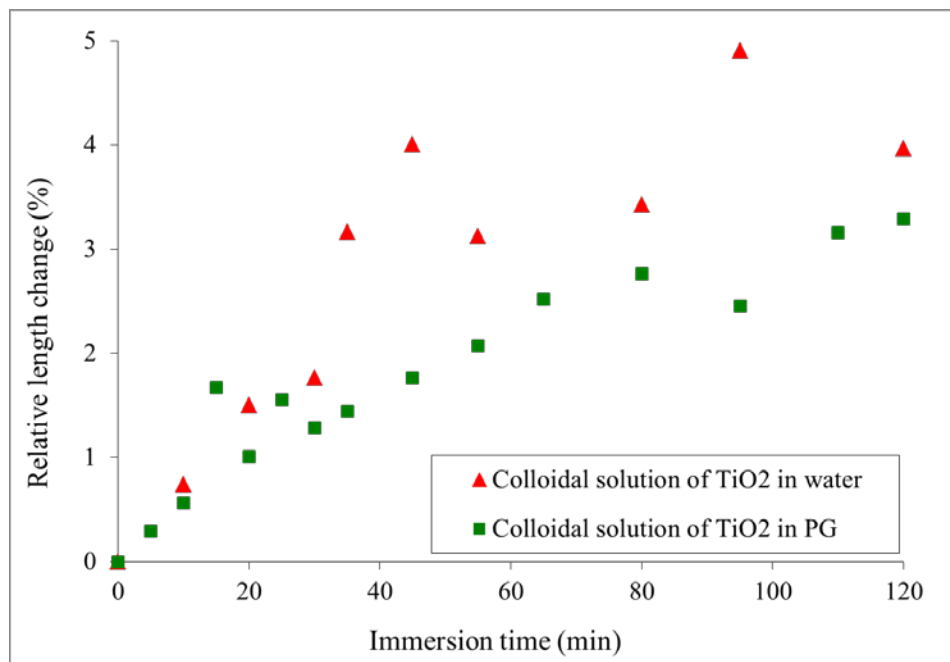


Figure 32 – Relative length change of nitrile (crosswise) as a function of immersion time in colloidal solutions of TiO₂ in water and in PG

To characterize more precisely the mechanisms involved in this process of swelling of the glove materials from the effect of the carrier fluids of the colloidal solutions of TiO₂, the swelling residue was analysed by FT-IR and EDS. To that end, glove samples were left immersed in solvents corresponding to the carrier fluids of the colloidal solutions of TiO₂ for a week. It was noted that the swelling solution (water, EG or PG), which was initially colourless, gradually turned yellowish as the immersion time of the samples increased. Then a drop of swelling liquid was deposited on a microscope slide, which was left under a hood until the solvent evaporated. The residue that remained was then analysed. Figure 33 shows the FT-IR spectrum obtained for neoprene immersed in EG for 7 days. Most of the peaks can be associated with bonds present in the EG solvent, such as C-O at 3,342 and 1,029 cm⁻¹ and C-H at 2,935 cm⁻¹. In contrast, the peak at 754 cm⁻¹ is characteristic of N-H bonds. It could indicate the presence in the neoprene swelling solution of an amine, such as diaminodiphenylmethane, which is used as a vulcanizing agent in the manufacture of neoprene (Wallace, 2008), or a phenylenediamine used as an antioxidant (Mellström et al., 2005). The peak around 1,600 cm⁻¹ is associated with chlorine, present in the monomer of neoprene, chloroprene.

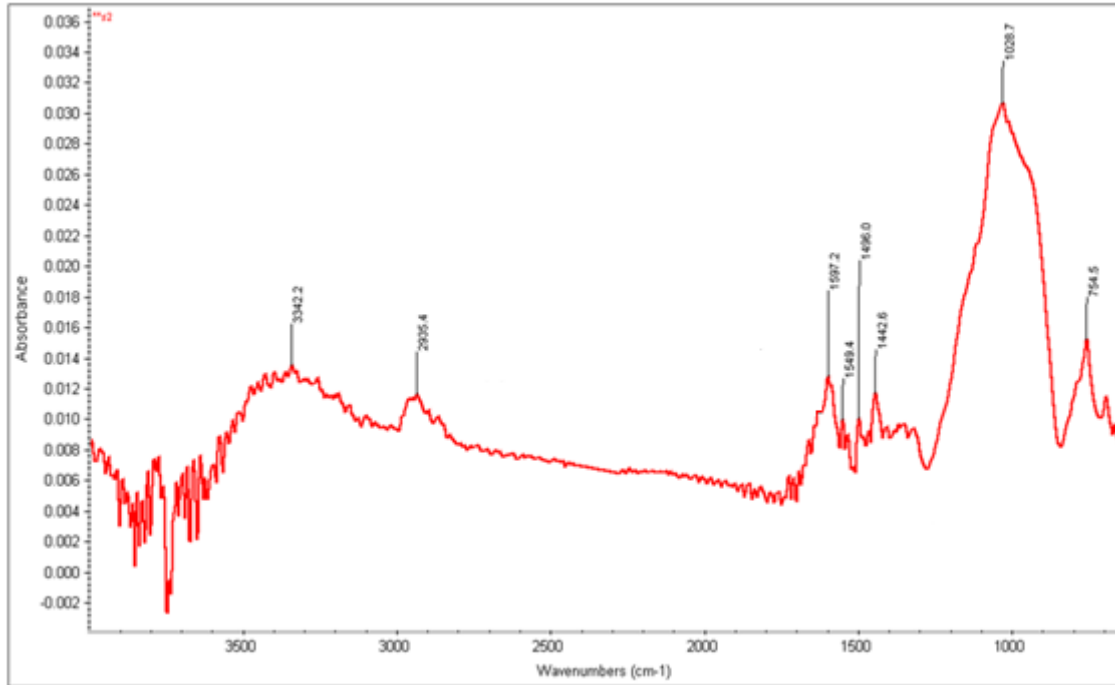


Figure 33 – FT-IR spectrum for residue from swelling of neoprene in EG for 7 days

The results of the EDS analysis of the same swelling residue from neoprene immersed in EG for 7 days are presented in Figure 34. Peaks associated with zinc, calcium, chlorine, sulphur, aluminum, magnesium, sodium, oxygen and carbon can be seen. Zinc and magnesium are used in oxide form as vulcanizing agents in the manufacture of neoprene, whereas calcium and aluminum are reinforcing filler constituents (DuPont Dow Elastomers, 2004). Sulphur is a vulcanizing accelerator. Sodium bicarbonate is one of the potential ingredients in the manufacture of neoprene.

The analyses of the composition of the swelling residue from glove materials due to the effect of the solvents used as carrier fluids in the colloidal solutions of TiO_2 therefore indicate that in parallel to the diffusion of the solvents in the elastomer shown by the measurements of increase in weight and length, immersion of the gloves in colloidal solutions of TiO_2 also causes an extraction of chemical species, additives, reinforcing fillers and non-polymerized monomer molecules from the polymer matrix. This extraction can lead to a change in the composition and physical and mechanical properties of the membrane (Nohilé, 2010) and can affect its resistance to the penetration of NPs.

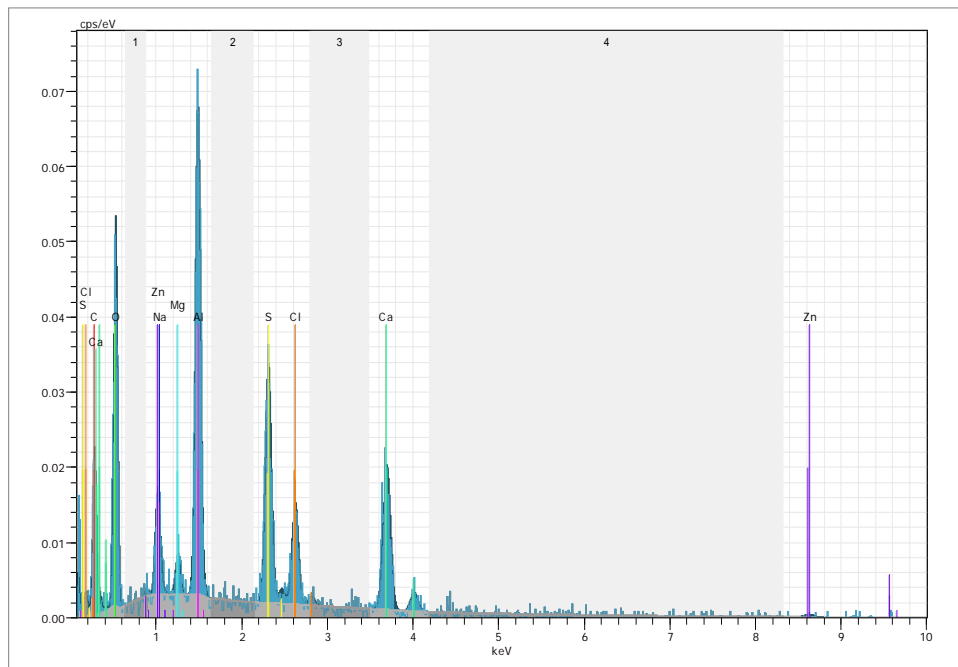


Figure 34 – EDS spectrum of analysis of residue from swelling of neoprene in EG for 7 days

4.4.2 Impact on Dynamic Mechanical Behaviour

To study the effect of contact with colloidal solutions of TiO₂ on the dynamic mechanical behaviour of glove materials, tests were conducted with the experimental setup by simultaneously exposing the samples to the colloidal solutions and subjecting them to biaxial dynamic loading of 50% (one deformation every 5 minutes) for a total of 7 hours. The residual mechanical performances of the materials were evaluated at regular intervals on the basis of force-displacement values recorded by the data acquisition system during testing by calculating the work required to cause a 50% deformation of the sample. The results obtained were compared with the data corresponding to the application of the mechanical deformations alone. Figure 35 shows the results for nitrile exposed to the colloidal solution of TiO₂ in water.

The condition corresponding to simultaneous exposure to the colloidal solution of TiO₂ in water and to dynamic mechanical loading elicits the same behavioural response as in the case of the application of dynamic loading alone, i.e., that a slight decrease in work occurs first, which is then followed by an increase, due to a rigidification of the material, and finally a decline in mechanical performance. The same behavioural similarity was also observed for the other materials. Contact with the colloidal solution, especially its carrier fluid, does not appear to affect the nature of the mechanisms involved in the gradual damaging of the glove materials as a result of the dynamic loading. The increase in relative work seen in the case of the contact of nitrile with the colloidal solution of TiO₂ in water could perhaps be due to a mechanical reinforcement effect produced by nanoparticles that have diffused into the membrane. This hypothesis needs to be tested by a more in-depth study of the phenomenon.

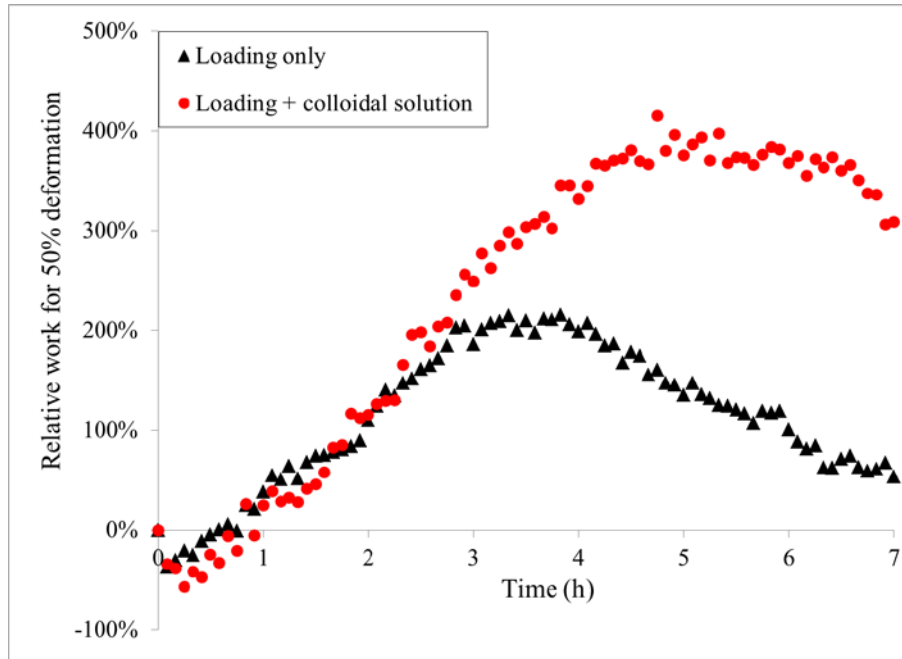


Figure 35 – Relative change in work required for a 50% biaxial deformation of samples of nitrile as a function of the duration of exposure to biaxial mechanical loading (one deformation every 5 minutes) in conjunction or not with exposure to colloidal solution of TiO₂ in water

4.5 Characterization of Impact of Deformations and Nanoparticle Carrier Fluids on State of Glove Surfaces

An analysis was conducted to observe the impact of dynamic loading and contact with the carrier fluids of the colloidal solutions of TiO₂ on the state of the surface of the gloves, especially with respect to the imperfections identified for each of the materials (see Section 4.2.2). These observations were noted on the outer and inner surfaces of the glove samples imaged by SEM after the samples had been subjected to dynamic mechanical deformations (one 50% deformation with the biaxial probe every 5 minutes) and/or had had their outer surface brought into contact with the solvents corresponding to the carrier fluids of the three colloidal solutions of TiO₂. The testing was conducted using the setup developed for the study, for varying durations.

Figure 36 compares the surfaces of nitrile glove samples when new and after 7 hours of deformation. A major change in the state of the surface can be seen. In particular, it appears that the number, diameter and depth of the pores have increased. This may indicate an embrittlement of the membrane as a result of the dynamic mechanical loading. A greater number of NPs may also build up in these more numerous, deeper imperfections.

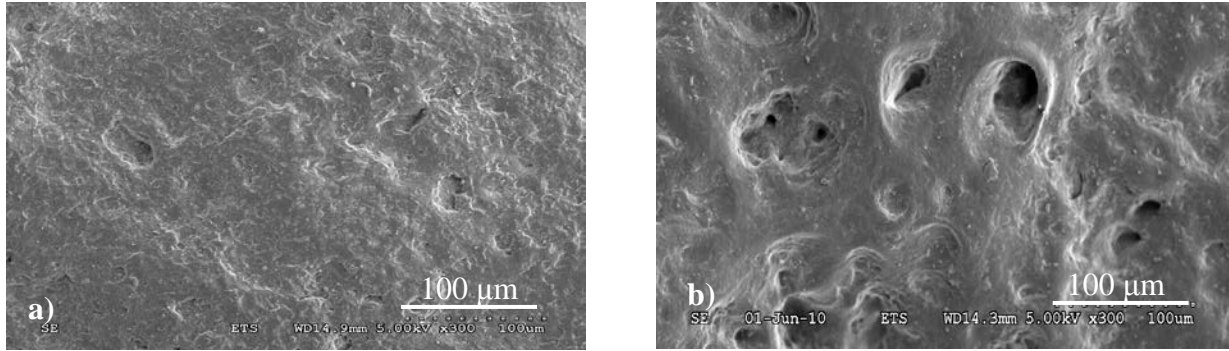


Figure 36 – SEM images of outer surface of nitrile gloves: (a) when new, (b) after 7 hours of biaxial deformations

In order to quantify the effect of these conditions on the state of the surface of the gloves, the images were analysed using ImageJ software, focusing on the area of imperfections characteristic of each material: pores for nitrile, cracks for neoprene, raised particles for latex and clusters of small plates for butyl rubber (see Section 4.2.2). Figure 37 shows the change in the area of imperfections as a function of the duration of biaxial dynamic loading for nitrile and neoprene (outer surface). A slight upward trend can be seen as the duration of the stress increases. For nitrile, a sudden jump between 5 and 7 hours may be associated with reaching a critical threshold of damage to the membrane.

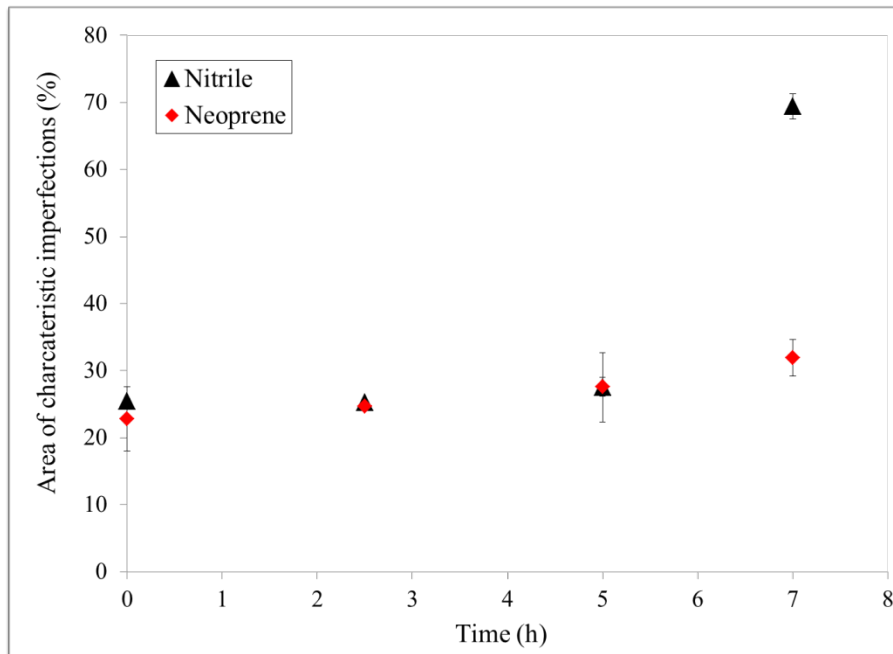


Figure 37 – Change in area of imperfections in nitrile and neoprene (outer surface) as a function of duration of biaxial dynamic loading

The compiled results of the analysis of the outer surface of the four glove materials after 7 hours of exposure to PG, 7 hours of biaxial dynamic loading and the simultaneous application of the

two conditions (deformed gloves in contact with PG in the exposure chamber) are presented in Figure 38. Both the mechanical deformations and the contact with the solvent appear to have a strong impact on the outer surface of the latex gloves and, to a lesser degree, of the butyl rubber gloves. However, only the mechanical deformations seem to increase the area of imperfections of the other two materials, with the impact on nitrile being more significant impact than that on neoprene. A similar tendency was seen with EG as a solvent.

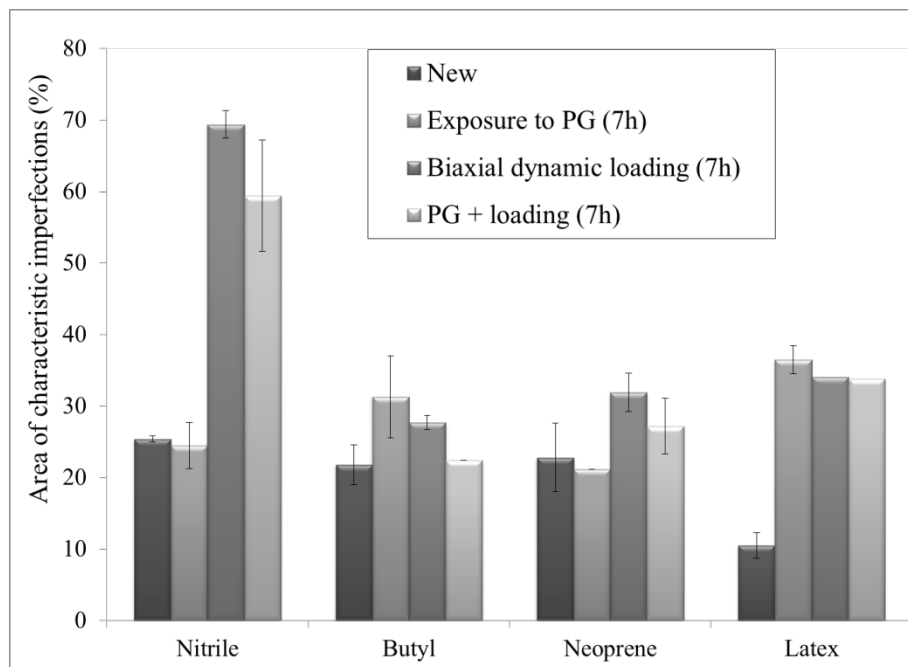


Figure 38 – Impact of 7 hours of exposure to PG, biaxial dynamic loading and the combination of the two on the area of imperfections of nitrile, butyl rubber, neoprene and latex gloves (outer surface)

Regarding the impact of the deformations on the outer surface of the gloves, abrasion caused by the deformation probe rubbing on the surface of the sample may have contributed to the changes seen in the state of the sample surface. This hypothesis is supported by the fact that the area of imperfections is systematically reduced when the mechanical deformations are combined with exposure to PG, where the solvent acts as a lubricant. The abrasion may increase if NPs are present, as the TiO_2 particles, much harder than the elastomers, may act as a grinding powder.

In the case of contact with the solvents used as carrier fluids in the colloidal solutions of TiO_2 , no correlation was found between the effect on the surface imperfections and the swelling. This may indicate either that the two phenomena are not linked, or that the swelling affects surface imperfections of different materials differently.

The same analysis of the effect on the four glove materials of contact with PG for 7 hours, the application of biaxial dynamic loading for 7 hours and the simultaneous application of both conditions (solvent + deformations for 7 hours) was also conducted for the inner surfaces of the samples, i.e., the reverse side from the exposed surface. A comparison of the results for the inner surfaces (Figure 39) and those for the outer surfaces (Figure 38) shows that the effects on the

inner surface are far less extensive than those on the outer surface, which is directly in contact with the deformation probe and/or solvent. In the case of nitrile and neoprene gloves, the differences between the conditions on the inner surfaces fall within the range of measurement uncertainty. In contrast, for latex, significant changes in relation to the “new” condition were seen for both contact with the solvent and application of the deformations, as well as for the combined effect of the two. This was the same tendency as noted for the outer surface. For latex, then, this indicates that the impact of the chemical and mechanical stresses applied to the outer surface can even be seen on the inner surface, which shows the extent of the effect produced. Finally, for butyl rubber, further testing and analysis will be needed to explain the results regarding the impact of the stresses on the inner surface.

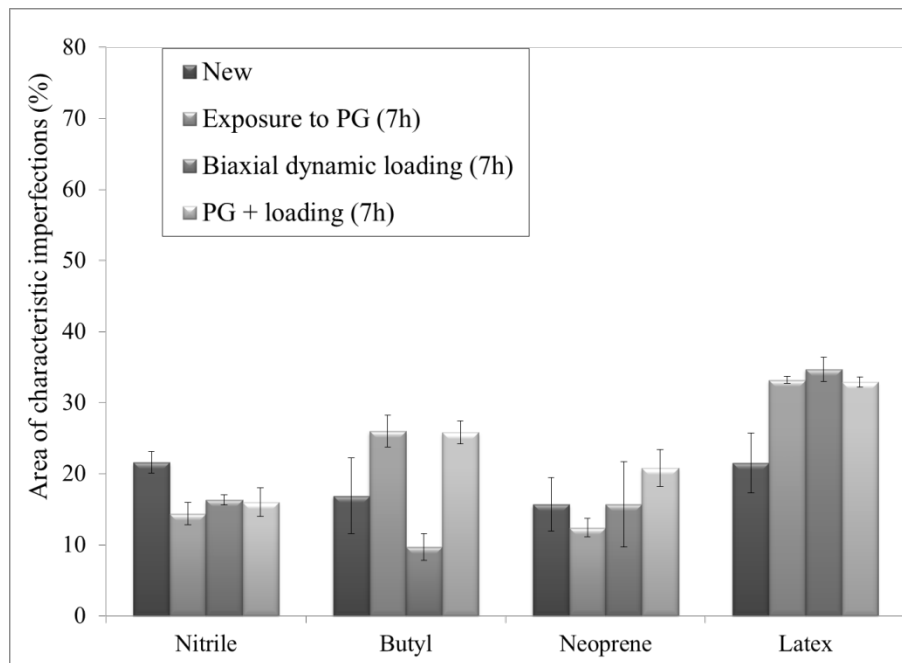


Figure 39 – Impact of 7 hours of exposure to PG, biaxial dynamic loading and the combination of the two on the area of imperfections of nitrile, butyl rubber, neoprene and latex gloves (inner surface)

4.6 Characterization of Impact of Environmental Stresses on Glove Materials

To determine the possible influence of the environmental stresses typical of the microclimate inside protective gloves on the resistance of the gloves to NP penetration, measurements were taken to characterize the impact of temperature and immersion in physiological solutions simulating sweat on glove materials.

4.6.1 Impact of Temperature on Mechanical Behaviour of Glove Materials

To assess the effect of temperature on the mechanical behaviour of the gloves, uniaxial tensile measurements were taken at 40°C and the results were compared with the properties determined at ambient temperature (see Section 4.2.3). The results are presented in Table 9. On account of the limited height of the testing machine oven and the extreme extensibility of the glove materials, only the modulus values could be determined for the tests at 40°C.

Table 9 – Comparison of values of secant modulus at 100% for nitrile, latex, neoprene and butyl rubber, measured at 25°C and 40°C

	Direction	Secant modulus at 100% (MPa)	
		25°C	40°C
Nitrile	Crosswise	1.9 ± 0.1	2.8 ± 0.4
	Lengthwise	1.9 ± 0.2	3.3 ± 0.3
Latex	Crosswise	0.86 ± 0.23	3.2 ± 0.3
	Lengthwise	0.88 ± 0.02	2.7 ± 0.3
Neoprene	Crosswise	1.2 ± 0.3	1.16 ± 0.03
	Lengthwise	1.1 ± 0.3	1.17 ± 0.03
Butyl rubber	Crosswise	0.8 ± 0.2	1.00 ± 0.07
	Lengthwise	0.8 ± 0.4	1.10 ± 0.05

For all materials except neoprene, the modulus increased to varying degrees when the temperature was raised from 25°C to 40°C. The rigidification at 40°C of nitrile, latex and, to a lesser extent, butyl rubber can be attributed to the entropic nature of elasticity in elastomers. The force that binds the ends of the chains is proportional to temperature, and an increase in temperature will cause a contraction of the material (McCrum et al., 1997). In the case of neoprene, no difference in modulus was seen for the measurements taken at 25°C and 40°C.

4.6.2 Swelling of Glove Materials in Physiological Solutions

Length change measurements were carried out on rectangular samples of the four glove materials cut crosswise and immersed in solutions made to simulate sweat (pH of 4 and 6). Figure 40 shows the results for nitrile. For comparison purposes, length change measurements taken following immersion of the samples in ultrapure water (pH of 6.3) are included in Figure 40. In all three cases, a significant increase in length of the nitrile was noted, indicating swelling, i.e., diffusion of the solvent in the elastomer. A close match between the values obtained for the physiological solution of pH 6 and those for ultrapure water can be seen. The results for the physiological solution of pH 4 are just slightly lower. It would therefore seem that the contact of

the gloves with the sweat produced on the skin in the glove may well have an effect on the nitrile, even over relatively short periods (less than two hours). This swelling of the nitrile may affect the behaviour of the material when it interacts with NPs. Measurements of NP penetration involving the presence of a physiological solution in contact with the glove sample therefore need to be conducted for nitrile.

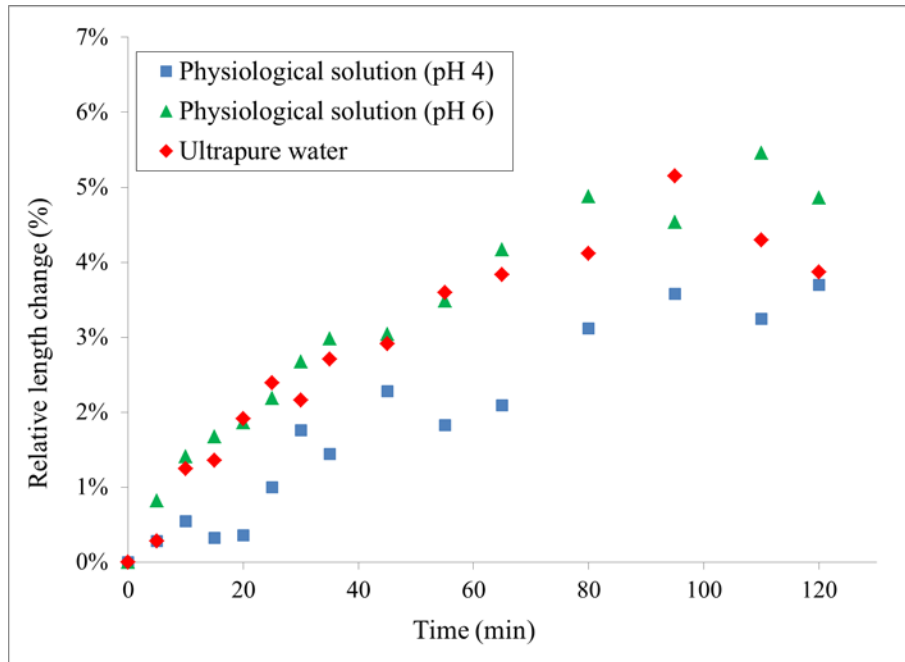


Figure 40 – Relative length change of nitrile as a function of immersion time in physiological solutions of pH 4 and pH 6 and in ultrapure water

Swelling was also observed with latex. In this case, the values measured for the two physiological solutions and ultrapure water were different. Lastly, no change in length of neoprene or butyl rubber in physiological solutions was seen over a period of two hours.

4.7 Measurement of Penetration of Nanoparticles through Glove Materials

A few preliminary measurement results for TiO₂ NP penetration of the four glove materials were obtained using the experimental setup described in Section 3.2 and the sampling protocol outlined in Section 3.4. The measurements were for NPs in both powder form and in colloidal solution. Mechanical loading was applied to the samples using a conical-spherical-tip probe (probe C), which can simulate the biaxial deformations to which gloves are subjected at the joints, for instance, and in the palm. These biaxial deformations were applied dynamically, with one 50% deformation (corresponding to a probe displacement of 30 mm) every 5 minutes. This figure of 50% for the applied deformation was equivalent to 60% of the maximum rate of deformation measured at the back of the hand on disposable nitrile gloves (Vu-Khanh et al., 2011). Further work will be required to determine the extent of deformation that gloves undergo

at the palm. These experiments were conducted over variable durations of up to 7 hours. The following characterization techniques were used: ICP-MS, NTA, TEM and AFM.

For each condition, a blank was produced and analysed in accordance with the sampling protocol. If analysis of the blank revealed that residual NPs might be present in the sampling chamber before the start of the experiment, the test was deemed invalid and the result of the analysis of the corresponding sampling solution was excluded. A number of validation tests designed to ensure that any NPs detected in the sampling solution had indeed passed through the glove sample were also conducted.

4.7.1 Results for TiO₂ Powder

Two series of tests involving the four glove materials, TiO₂ powder NPs and 50% biaxial dynamic loading for up to 7 hours were conducted, with measurements taken by ICP-MS, using an acid sampling solution. For the second series, an additional seal was added above the sample. This 2-cm wide, flat circular seal made of butyl rubber was designed to ensure that NPs could not get from the exposure chamber to the sampling chamber by way of the four holes pierced in the sample for the cell-retaining screws. The results for nitrile and butyl rubber are presented in Figure 41. The point at the origin corresponds to the mean value of the blanks measured for the series. A major difference between the two data sets can be seen for both nitrile and butyl rubber. The difference was attributed to the use of the additional seal in series 2. It would appear to indicate that there was a problem with a defective seal between the exposure and sampling chambers in series 1. The additional seal was used systematically for all subsequent measurement series.

To make sure that the titanium concentrations detected in the sampling solutions were indeed related to NPs passing from the exposure chamber to the sampling chamber, the results of the ICP-MS measurements for the series 2 tests combining TiO₂ powder and biaxial dynamic loading were compared with the results of tests conducted with no NPs in the exposure chamber, but with the same deformations applied to the samples. The results for nitrile and butyl rubber are presented in Figure 42.

In Figure 42, there does not seem to be any clear difference between the concentration measurements with and without NPs in the case of butyl rubber. It would therefore appear that the butyl rubber glove material is impermeable to the TiO₂ powder NPs used, even following application of biaxial dynamic loading of 50% for 7 hours. This result, which will need to be confirmed by further measurements, is very significant, given that butyl rubber is the preferred material for glove box gloves, which are used to handle NPs while keeping the risks of exposure to a minimum. This absence of penetration by TiO₂ powder, if confirmed, may be due to the fact that butyl rubber offers good resistance to gases, with which NPs can be associated because they are so small.

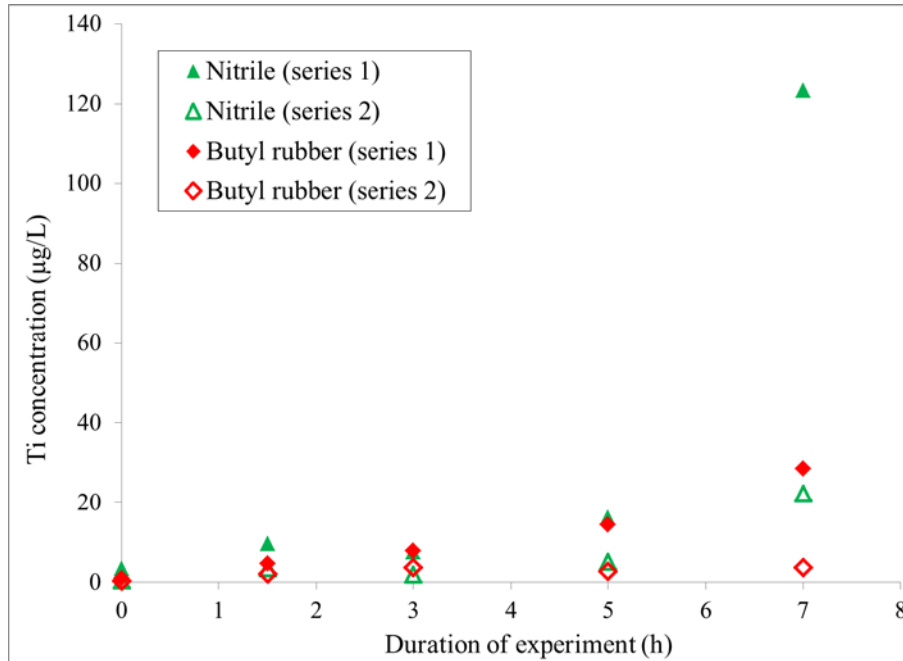


Figure 41 – ICP-MS measurements of titanium in sampling solution as a function of experiment duration, for nitrile and butyl rubber exposed simultaneously to TiO₂ powder and biaxial dynamic loading: comparison of two series of tests

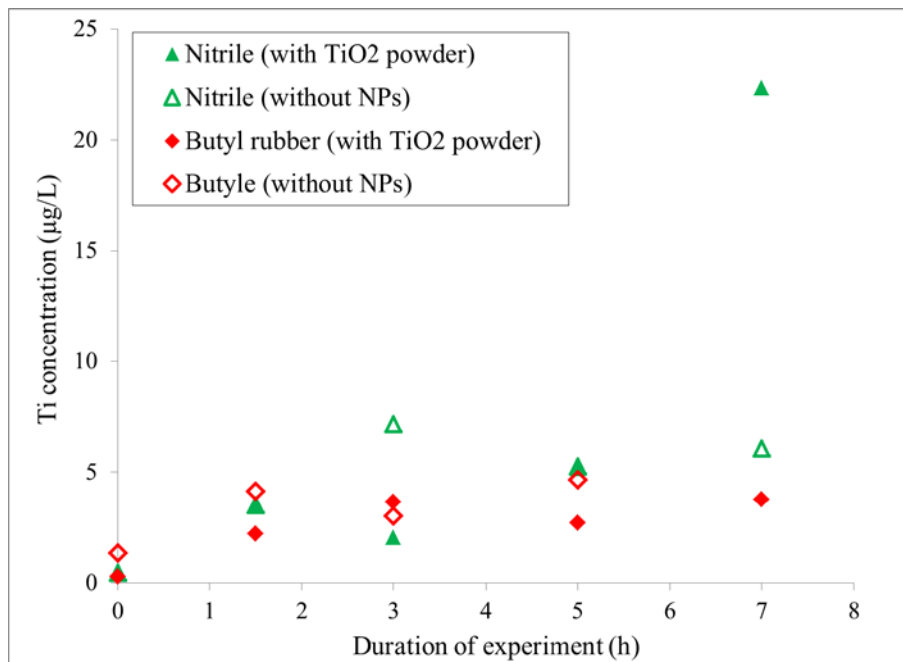


Figure 42 – ICP-MS measurements of titanium in sampling solution as a function of experiment duration, for nitrile and butyl rubber exposed or not to TiO₂ powder in addition to biaxial dynamic loading

In the case of nitrile, in contrast, the concentration value corresponding to 7 hours of repeated deformation is much higher in the presence of NPs (Figure 42). This would seem to indicate that it might be possible for TiO₂ powder to pass through nitrile gloves after exposure to biaxial dynamic loading of 50% for durations of more than 5 hours. Below 5 hours, no obvious difference between the conditions with and without NPs was seen. This sudden change in the resistance of nitrile to the passage of NPs between 5 hours and 7 hours of the application of biaxial dynamic loading may be associated with a major increase in the area of imperfections on the outer surface of the gloves seen between 5 and 7 hours of deformations (see Figure 37). This tendency was also seen with the results of the series 1 tests (Figure 41), in which penetration of NPs through the nitrile glove combined with penetration through the defective seal.

For neoprene, higher values for the condition with NPs than for that without NPs were observed for 5 and 7 hours of biaxial dynamic loading. These results, which need to be confirmed, would seem to indicate the possibility of TiO₂ powder passing through neoprene gloves when the gloves are subjected to biaxial dynamic loading of 50% for longer than 3 hours at a frequency of one deformation every 5 minutes. This result is a cause for concern, given that some glove boxes are equipped with neoprene gloves. Lastly, in the case of latex, no conclusions can be drawn about the possibility of TiO₂ powder passing through the material because of a number of aberrations in the measurement results.

Sampling solutions in ultrapure water from series 1, i.e., with no additional flat seal, were also produced for NTA analysis. The fact that there was a higher NP concentration in the sampling solutions than in the corresponding blanks can be seen in the results presented in Table 10. No value is given for nitrile on account of a problem with contamination of the sampling chamber, indicated by a very high NP value in the blank. Even if the resulting data cannot be used, owing to the problem with the defective seal highlighted by the ICP-MS analyses (see Figure 41), the fact that TiO₂ NPs were detected in the sampling solutions by this technique indicates its application potential for the method developed to measure the penetration of NPs through glove materials. It should be noted, however, that this technique does not discriminate with respect to the nature of the NPs measured.

Table 10 – NP concentrations measured by NTA in blank and in sampling solution, for latex, neoprene and butyl rubber exposed simultaneously to TiO₂ powder and to biaxial dynamic loading for 7 hours (results for series 1, with defective seal)

Material	NP concentration (10 ⁸ /ml)	
	Blank	Sampling solution
Latex	1.50	2.52
Neoprene	1.16	2.44
Butyl rubber	0.69	2.73

A few TEM observations of samples prepared by centrifugation of sampling solutions in pure water and in methanol were also made. No NPs were identified on the images. However, no conclusions could be drawn about the applicability of the technique to the measuring method

developed due to a labelling problem which prevented us from being able to match the TEM observations with those made by other techniques.

Lastly, samples corresponding to 7-hour tests with biaxial dynamic loading (50%) and TiO₂ powder were prepared by centrifugation of sampling solutions in pure water on mica substrates, which were then analysed by AFM. Figure 43 shows the result for an experiment conducted with a nitrile glove sample. It can be seen that NPs are spread homogeneously across the mica surface. By comparison, the samples corresponding to blanks did not show any significant presence of NPs. This result indicating possible penetration of TiO₂ powder NPs through nitrile gloves following dynamic loading of 50% for 7 hours is consistent with the data from the ICP-MS analyses of the sampling solutions (see Figure 42).

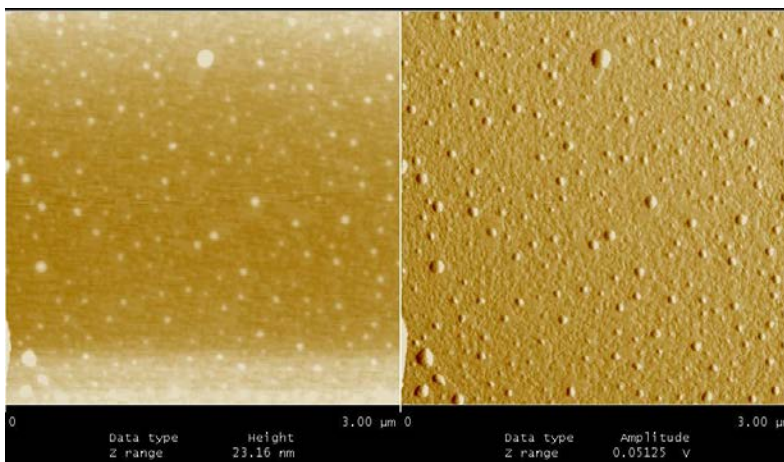


Figure 43 – AFM image (scale of 3 μm) of a sampling solution in pure water centrifuged on a mica substrate from a nitrile sample subjected for 7 hours to biaxial dynamic loading (50%) and to TiO₂ powder

Figure 44 shows a more highly magnified image of the same sample as in Figure 43. The NPs visible on the mica substrate appear to have a diameter of around 70 nm. This value is less than the mean diameter of the TiO₂ particles measured in the powder as it was received from the manufacturer. This may be related to the disagglomeration of the powder that might occur when mechanical deformations of the gloves combine with pressure on the NPs (see Figure 24).

Tests to measure the penetration of NPs in powder through the glove materials were also conducted without any deformations, and the sampling solutions were analysed by ICP-MS. The results are presented in Table 11. The titanium concentrations measured in the sampling solutions without any deformations being applied to the sample are of the same order of magnitude as those obtained in the absence of NPs (6 μg/L on average for the data obtained with application of deformations for 7 h). This indicates that no TiO₂ powder seems to pass through the glove materials if they are not subjected to deformations. This result may be due to the agglomeration state of the NPs in the TiO₂ powder, when their mean diameter is more on the micrometric scale (see Figure 15).

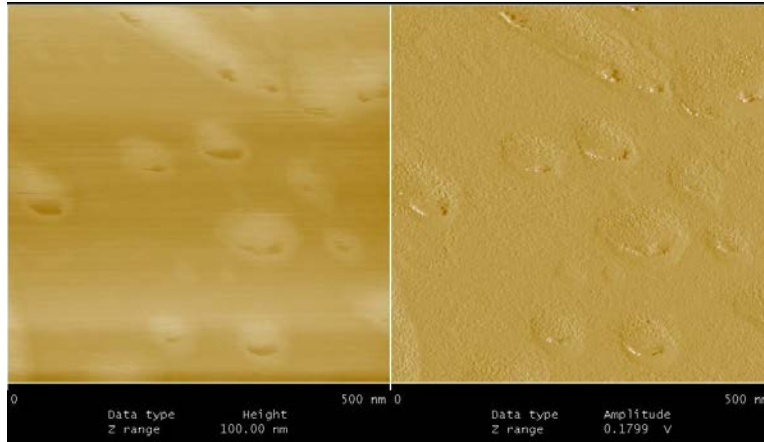


Figure 44 – AFM image (scale of 500 nm) of a sampling solution in pure water centrifuged on a mica substrate from a nitrile sample subjected for 7 hours to biaxial dynamic loading (50%) and to TiO₂ powder

Table 11 – Titanium concentrations measured by ICP-MS in sampling solution, for nitrile, latex, neoprene and butyl rubber exposed to TiO₂ powder for 7 hours, without deformation of the sample

	Ti concentration (µg/L)
Nitrile	2.07
Latex	3.37
Neoprene	6.89
Butyl rubber	2.97

4.7.2 Results for Colloidal Solutions of TiO₂

A few tests to measure the penetration of TiO₂ NPs in colloidal solution through glove materials were conducted with a colloidal solution of TiO₂ in water. Titanium concentrations in the sampling solutions after an exposure time of 7 hours without deformation of the sample were measured by ICP-MS, and the results are presented in Table 12. It can be seen that these values are systematically higher than what was measured, also without deformation, with the TiO₂ powder (Table 11). Even if measurements at intermediate exposure times will need to be carried out to complete the results, the data in Table 12 seem to indicate that NPs could penetrate the glove materials following 7 hours of exposure of the samples to a colloidal solution of TiO₂ in water, without deformation.

Table 12 – Titanium concentrations measured by ICP-MS in sampling solution, for nitrile, latex, neoprene and butyl rubber exposed to colloidal solution of TiO₂ in water for 7 hours, without deformation of the sample

	Ti concentration (µg/L)
Nitrile	7.62
Latex	5.91
Neoprene	54.1
Butyl rubber	10.39

Tests were also conducted by combining exposure to NPs in colloidal solution with the application of biaxial dynamic loading to the glove samples. The sampling solutions in acidic water were analysed by ICP-MS. The results for nitrile and butyl rubber exposed to the colloidal solution of TiO₂ in water are presented in Figure 45. For comparison purposes, the titanium concentrations in the sampling solutions for gloves deformed without any exposure to colloidal solution are included. In the case of butyl rubber, a slight increase in the titanium concentration in the sampling solutions following combined exposure to the colloidal solution of TiO₂ in water and biaxial dynamic loading may be observable in comparison with the condition without colloidal solution, but it needs to be confirmed by further testing. In the case of nitrile, the sharp contrast is undeniable for 5 and 7 hours of deformation. Significant differences were also measured for latex. The data would appear to indicate possible penetration of NPs as a result of combined exposure of the glove materials to a TiO₂ colloidal solution and to biaxial dynamic loading.

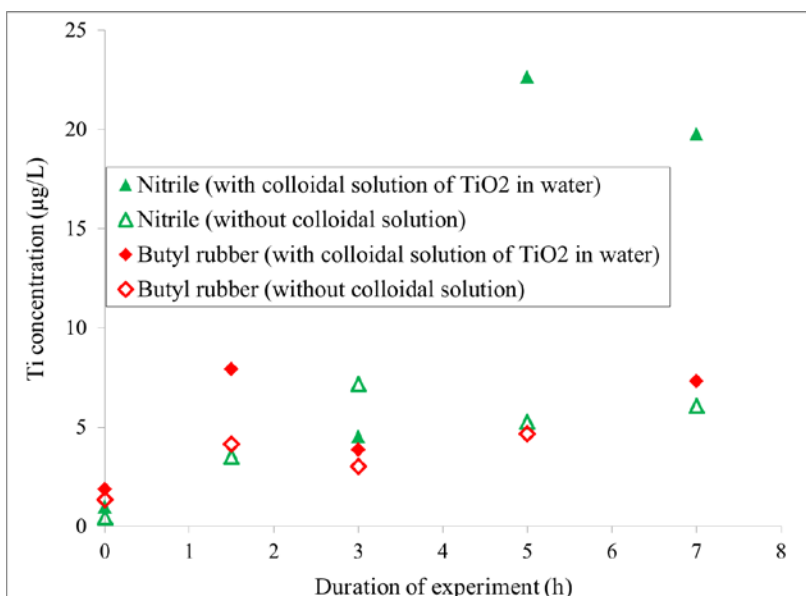


Figure 45 – ICP-MS measurements of titanium in sampling solution as a function of experiment duration, for nitrile and butyl rubber exposed or not to colloidal solution of TiO₂ in water in addition to biaxial dynamic loading

5. DISCUSSION

5.1 Method Chosen to Measure Penetration of Nanoparticles through Glove Materials

The main objective of this study was to develop a method for measuring nanoparticle penetration through glove materials under conditions simulating how gloves are used in the workplace. To that end, an experimental setup was designed, built and tested with the NPs and glove materials selected for the study.

It was shown that the experimental setup can accommodate TiO₂ NPs in both powder form and in colloidal solution thanks to the choice of setup material that prevents the effects of adsorption of NPs in colloidal solution, and the addition of a flat seal on top of the sample in order to limit the risks of NPs in powder form passing directly from the exposure chamber to the sampling chamber.

Experiments were also conducted by simulating stresses corresponding to conditions of glove use in the workplace. In particular, mechanical stresses were applied to the glove materials in the form of 50% biaxial dynamic loading of the samples at a rate of one deformation every 5 minutes. These deformation values are relevant for disposable gloves, for which maximum deformation rates of 80% at the back of the hand have been measured (Vu-Khanh et al., 2011). The typical rates of deformation that thicker protective gloves, such as those made of neoprene or butyl rubber, undergo are in all likelihood lower than this and so could easily be applied by the experimental setup. Other probe geometries have also been designed to simulate other types of deformations, such as compression, and have been tested with glove materials (Jambou, 2009). Regarding microclimate effects in gloves, although no experiments involving measurement of the penetration of NPs through gloves have yet been done under these conditions, the setup could accommodate physiological solutions thanks to its overflow system and its ability to maintain the temperature of the sample at physiological levels, i.e., up to 40°C (Deltombe, 2010).

The concave configuration which was used for the simultaneous application of NPs and mechanical loading corresponds to specific circumstances under which the gloves are used in the workplace, including exposure of the palm and fingers to NPs. There are other cases where the hand deforms the opposite side of the material to the one exposed to the NPs, in other words, in a convex shape in relation to the NPs. The difference between the two configurations involves, firstly, the pressure applied on the NPs by the deformation probe, which may lead to a disagglomeration of the particles through shearing. The potential influence of the pressure applied to the NPs on their penetration through the gloves could be verified by comparing the results obtained with deformation probes A and B (see Figure 4). The other possible effect of the difference between the two configurations is related to the state of stress on the two sides of the sample. As the convex side of the glove is under tension, it is more susceptible to the formation of cracks in which NPs can become deposited than is the concave configuration chosen for the tests, in which the glove surface is under compression. More advanced analyses are needed to assess the impact of this difference in configuration.

The third requirement of the study specifications concerned the sampling system. The sampling chamber was designed so that an inline analyser, such as an SMPS, could be connected to it, or on completion of the test, a liquid could be collected from it which could then be analysed to determine whether it contained any NPs. Special attention was given to minimizing the risks of false positives resulting from NPs passing directly from the exposure chamber to the sampling chamber. To that end, a system of rectangular cross-sectioned seals and flat seals positioned on both sides of the sample was designed, and its effectiveness demonstrated experimentally (see Figure 41). In addition, to limit the impact of contamination of the sampling chamber by residual NPs (such as from the previous experiment), the sampling protocol developed includes the systematic production of a blank for each experiment conducted, which takes the form of a final rinse of the sampling chamber and analysis of the rinse liquid at the same time as the analysis of the sampling solution collected at the end of the experiment.

Lastly, the safety of the procedure was ensured by using a glove box to house the experimental setup during operation, as well as during assembly, dismantling and cleanup. The glove box was equipped with a HEPA filter at the outlet from the pump intended to maintain the glove box at slightly negative pressure in order to prevent any NPs from escaping into the ambient air. Special attention was also given to management of waste materials containing NPs. They were recovered and stored separately before being collected by a company specializing in the handling and treatment of hazardous waste.

Another major component of the measurement method consisted of the techniques used to detect NPs in the sampling chamber. Regarding FEG-SEM, the combined use of secondary and backscattered electrons after depositing carbon on the surface of the sample made it possible to satisfactorily detect NPs that could otherwise have been confused with the relief of the glove surface when the exposed side of deformed gloves was examined (see Figure 9). This is a very appropriate observation technique because, in view of the possible migration of NPs toward the unexposed surface of the gloves, it could prove to be an effective tool in confirming the penetration of particles through the gloves. It should be noted, however, that it is not possible for the time being to conduct automated quantitative analysis of these images. The combined contrasts of the relief and the differences in atomic number make the images difficult to analyse with a software program. It would be possible to identify the NPs on the images manually in order to quantify their size, number, etc., but that would take much longer. The other problem that needs to be addressed regarding direct observation of the passage of NPs using microscopic analysis of the unexposed surface of the gloves is related to the need to eliminate all NPs from the exposed surface in order to avoid transferring contamination from one side of the sample to the other. Efforts are under way to try to find a solution to this problem.

As an alternative to direct observation of the unexposed surface of the gloves, a specific sampling protocol was developed. It is based on the use of a small volume of sampling solution in the sampling chamber for the duration of the testing, and analysing it a posteriori by various techniques. The applicability of several different combinations of sampling solution formulations and analysis techniques was investigated. Positive results were obtained with a sampling solution made of ultrapure water acidified by 1% nitric acid and analysed by ICP-MS, an ultrapure-water-based sampling solution analysed by NTA, and an ultrapure water sampling solution combined with centrifugation on a mica substrate and analysed by AFM. Other analytical techniques were

also considered, including TEM observation of grid samples produced by centrifugation and atomic absorption spectrometry.

Identifying several NP detection techniques that can be applied to the method developed for this study for measuring nanoparticle penetration through protective gloves has a number of advantages. First, not being limited to a single analysis technique expands the potential use of the method, as users can opt for the most readily available technique or techniques. Furthermore, the possibility of combining the results provided by several techniques means that the limits of any one technique can be addressed by using another, for instance, the lack of discriminative capability of NTA and AFM regarding the nature of the NPs observed and the lack of information provided by ICP-MS with respect to the fine structure of the NPs present in the sampling solution. Lastly, given the complexity of the handling and detection of NPs and the potential impact of positive results for the penetration of NPs through gloves, the possibility of confirming results by means of several analysis techniques increases the reliability of the method and helps ensure the quality of the conclusions.

Note, however, that the results provided in the report using the identified techniques remain fairly preliminary and that further work is needed, for instance, to establish how effective they are. For ICP-MS, for example, the concentration of titanium detected in relation to the concentration of TiO₂ NPs in the solution should be quantified so that the need to subject the solution samples to TiO₂ NP digestion treatment can be assessed.

Another aspect of NP detection techniques that needs to be further studied concerns the applicability of the techniques to the configuration simulating the microclimate inside the gloves, in which a physiological solution is in contact with the inner surface of the sample. For instance, it will be necessary to substantiate that the chemicals used in the formulation of the physiological solutions do not interfere with the analysis techniques and/or the sample preparation treatments.

With further regard to the techniques for detecting NPs in the sampling chamber, the work so far has focused on titanium dioxide because of its extensive use in industrial and commercial applications. Similar testing needs to be done with other types of NPs that are also widely used and potentially biologically active, such as carbon nanotubes. Research should therefore be conducted to assess whether the already identified detection techniques are applicable to these other NPs and possibly to propose other techniques better suited to the various types of NPs.

One final aspect concerns the choice of the measurement method with regard to its relevance to conditions simulating workplace use. These conditions refer in particular to the application of the NPs, in powdered form or as colloidal solution, and the mechanical and environmental stresses to which the gloves are subjected. Regarding the NPs, even if the results of this study are too preliminary to be able to draw any quantitative conclusions about the effect of the presence of the NP colloidal solution carrier fluids on the mechanisms and kinetics of NP transport through gloves, it nonetheless appears very clear that the carrier fluids have a major impact on the elastomers used in gloves and that testing of the effectiveness of protective gloves against NPs must be conducted with NPs both in powder form and in colloidal solution in the various types of carrier fluids used.

As regards the effect of the mechanical stresses applied to glove materials, the results obtained clearly show the significance of the impact of the deformations on NP penetration. The mechanical loading program used for the purpose of measuring the penetration of NPs through the gloves in this study consisted in applying biaxial dynamic loading of 50%, at a rate of one deformation every 5 minutes, while simultaneously applying pressure on the NPs. The degree of deformation chosen corresponds to 60% of the maximum rate of deformation measured at the back of the hand for disposable gloves (Vu-Khanh et al., 2011). The relevant values for thicker gloves, such as those made of neoprene or butyl rubber, may be slightly lower and will need to be determined. Other types of mechanical stresses may also be involved, such as the compression that corresponds to the application of a gripping force. A probe and a sample holder were designed for this purpose. Cylindrical probes, with and without edges, are also available for studying the impact of the compression applied to the NPs, in combination with the deformation of the sample.

Lastly, regarding the effect of the microclimate inside the gloves, preliminary measurements showed that both temperature and contact with physiological solutions affect the glove materials differently and, in some cases, fairly significantly. For instance, a rigidification of nitrile, latex and, to a lesser extent, butyl rubber, was measured at 40°C. Swelling of nitrile and latex in physiological solutions with different pH values was also seen. This indicates how important it is to take into consideration the effect of the microclimate inside the gloves when conducting measurements to test the effectiveness of protective gloves against NPs.

5.2 Penetration of Nanoparticles in Powder through Glove Materials

Some measurements of the penetration of TiO₂ powder NPs through the four glove models chosen for the study were conducted. They will obviously need to be replicated and validated in order to be corroborated. A few preliminary conclusions may nevertheless be drawn on the basis of these results.

First, it appears that NPs in powder do not pass through the glove materials without the application of mechanical stress (Table 11). This may be due to the dense agglomeration of the NPs in the TiO₂ powder, where they take the form of intermediate-sized (200 nm) aggregates and agglomerates rather than individual NPs (Figure 15).

In contrast, as shown by ICP-MS measurements of titanium concentrations in the sampling solution (Figure 42) and by AFM observations of samples centrifuged on mica substrates (Figure 43), when gloves are deformed dynamically, NPs in powder may be able to pass through the membrane after a certain length of time, particularly in the case of thin gloves like disposable nitrile models. This penetration may be related to damage to the elastomer membrane from repeated mechanical deformations; the damage was visible on the surface of the samples (see Section 4.5) and was highlighted by the measurements of residual mechanical performance (see Section 4.3.1). The penetration may also be due, in part, to a reduction in the size of the TiO₂ powder particles, which seems to occur when the mechanical deformations of the gloves are combined with pressure on the NPs (Figure 24).

The fact that no NPs passed through the butyl rubber gloves, according to our measurements, may be associated with butyl rubber's high impermeability to gases (Jin et al., 2010). As NPs are extremely small, some researchers have likened their behaviour to that of gas molecules (Balazy et al., 2004; Schneider, 2007).

5.3 Penetration of Nanoparticles in Colloidal Solution through Glove Materials

Preliminary measurements of the penetration of TiO₂ NPs in colloidal solution in water through the four glove models chosen for the study were conducted. Possible penetration of NPs was detected, particularly when biaxial dynamic loading was applied to the samples. This result may be associated with the significant effects the NP carrier fluids were observed to have on the glove materials, not only in terms of swelling (Section 4.4.1), but also mechanical behaviour (Section 4.4.2) and surface state (Section 4.5).

In particular, substantial swelling after short immersion times was measured for nitrile, latex and neoprene in the three TiO₂ colloidal solutions. The swelling is a sign of diffusion of the NP carrier fluid in the elastomer. As the solvent diffuses, it may entrain the NPs of the colloidal solution with it through the membrane and thus facilitate their penetration through the gloves.

The other phenomena that may be involved when glove materials swell up with the carrier fluids of TiO₂ colloidal solutions are extraction of soluble additives such as plasticizers and reinforcing particles (see Figure 33 and Figure 34) and long-term deterioration of the chemical structure of the material (Figure 31). These processes may also interact with the mechanism whereby NPs penetrate through the gloves.

5.4 Applicability of Method to Other Types of Research

The method developed for this study was intended for protective gloves. It was designed to enable relatively significant degrees of deformation like those that gloves undergo at the joints (Vu-Khanh et al., 2011). The non-porous nature of the elastomer membranes was taken into account in selecting the techniques for detecting NPs in the sampling chamber, i.e., very low NP concentrations.

However, this method could also prove useful for studying the penetration of NPs through the textiles used in protective clothing. Preliminary work has been done in this area using the experimental setup developed for this project (Testori, 2011). More specifically, cotton knit fabric, cotton/polyester lab coat fabric and polyolefin-based non-woven membrane (ProShield[®]) were subjected to exposure to TiO₂ powder NPs and to the application of a level of dynamic mechanical deformations suited to the type of material. As higher amounts of NPs were expected to pass through these materials, the detection of titanium in the sampling solutions was done by atomic absorption spectrometry.

This provides an indication of the significant potential that the NP penetration measurement method developed for this study holds for the assessment of protective materials used in

occupational health and safety. The method could also prove useful in other fields where the penetration of NPs through porous or non-porous membranes is an issue, such as NP packaging, storage and transportation.

6. CONCLUSIONS, PROSPECTS AND RECOMMENDATIONS

The purpose of this project was to develop a method for measuring the penetration of NPs through protective glove materials under conditions simulating glove use in the workplace. A secondary objective was to collect preliminary data on the effectiveness of these glove materials in providing protection against NPs.

The proposed method consists of an experimental setup for exposing glove samples to NPs in powdered form and in colloidal solution, while at the same time subjecting them to static or dynamic mechanical loading, under conditions simulating the microclimate inside the gloves. The setup is connected to a data acquisition and control system. To complete the method, a sampling protocol was developed, and a series of NP detection techniques were selected. The measurement method was used to conduct tests on four models of protective gloves of different thicknesses, made of nitrile, latex, neoprene and butyl rubber, by exposing them to commercially available TiO₂ NPs in powdered form and in colloidal solution. The setup's mechanical loading capacity was also explored in the experiments.

Preliminary results were obtained regarding the effectiveness of the four models of gloves tested for protection against NPs. In the case of TiO₂ powder NPs, penetration through nitrile gloves appears to occur after 7 hours of repeated biaxial dynamic deformation. This penetration may be associated with damage to the membrane resulting from mechanical loading, as well as with a possible reduction in the agglomeration state of the NPs in the powder. Butyl rubber, in contrast, seems to be impermeable to the penetration of powder TiO₂ NPs under the experimental conditions. It should be noted that no penetration of powder NPs through any of the glove materials was measured when no deformation was applied.

For NPs in commercial colloidal solution, the possibility of penetration through gloves was detected, especially when the samples were subjected to biaxial dynamic deformation. This possible penetration may be due to the significant swelling caused by the colloidal solution carrier fluids in all the glove materials except butyl rubber. A change in the mechanical behaviour and surface state of the glove materials following contact with these solvents was also measured, with potential consequences for glove resistance to NP penetration.

These results underscore the value of the work done and the importance of pursuing research in this field. Many questions remain unanswered, and the preliminary conclusions of this report, regarding the possibility of NPs penetrating through protective glove materials, will need to be validated and extended to other types of mechanical deformations and configurations (with and without pressure on the NPs), to the effect of environmental stresses, to other types of NPs, to other types of gloves, etc. In particular, measurements will need to be taken in configurations and with experimental parameter values that best simulate the various situations encountered in the workplace. It will also be important to assess the influence of NP characteristics—especially chemical nature, aspect ratio, propensity to agglomeration, and physical and mechanical properties—on their capacity to penetrate protective gloves. Some changes to the experimental setup are also being considered in order to allow the use of other detection techniques, such as substituting a conductive polymer for parts of the setup, in order to reduce static electricity problems and make it possible to detect NPs with an SMPS, and to improve its reliability,

including by means of a single electrical actuator instead of the two pneumatic actuators currently being used.

This project also showed that MEB-FEG allows NPs to be observed at the exposed surface of gloves and might be used to detect NPs that have migrated through gloves. However, images obtained using this technique do not lend themselves to quantitative image analysis, which would only be possible after manual identification of the NPs.

Another spinoff of this project was the establishment of a formal collaboration with the nanomaterials chemistry and safety laboratory (LCSN) team of the Commissariat à l'énergie atomique et aux énergies alternatives (CEA) in Grenoble, France. A joint research project on the barrier properties of polymer and textile membranes against NPs in a liquid medium is currently under way. It will benefit from the two research teams' complementary expertise in this area, as well as from new advances and tools resulting from the work.

Finally, even if the results on the effectiveness of protective gloves against NPs are still very preliminary, the possibility of NP penetration through gloves that they seem to indicate is sufficient reason to recommend caution with regard to the choice and conditions of use of protective gloves when possible exposure to NPs exists. More specifically, given the significant impact of mechanical stresses on the gloves, they should be replaced regularly, especially thin models. Similarly, gloves that come into contact with NPs in a colloidal solution should be changed promptly. Further work is needed before more specific recommendations can be made about the protection levels provided and about conditions for safe use of the gloves in case of NP exposure.

BIBLIOGRAPHY

- Afsset. (2006). Les nanomatériaux - effets sur la santé de l'homme et sur l'environnement. Agence française de sécurité sanitaire de l'environnement et du travail, Maisons-Alfort, France.
- Afsset. (2008). Les nanomatériaux : Sécurité au travail. Agence française de sécurité sanitaire de l'environnement et du travail, Maisons-Alfort, France.
- Afsset. (2010). Évaluation des risques liés aux nanomatériaux pour la population générale et pour l'environnement. Groupe de travail Nanomatériaux - exposition du consommateur et de l'environnement, Agence française de sécurité sanitaire de l'environnement et du travail, Maisons-Alfort, France. Saisine 2008/005.
- Ahn, K., Ellenbecker, M. J. (2006). « Dermal and respiratory protection in handling nanomaterials at the center for high-rate nanomanufacturing (CHN) ». AIHce Conference. Chicago, IL.
- Amoabediny, G. H., Naderi, A., Malakootikhah, J., Koohi, M. K., Mortazavi, S. A., Naderi, M., Rashedi, H. (2009). « Guidelines for safe handling, use and disposal of nanoparticles », Journal of Physics: Conference Series 170(1), p. 012037.
- ASTM. (2002). Standard Test Method for vulcanized Rubber and Thermoplastic Elastomers - Tension, American Society for Testing and Materials. ASTM D 412-98, p. 44-57.
- Balazy, A., Podgórski, A., Gradon, L. (2004). « Filtration of nanosized aerosol particles in fibrous filters. I - experimental results », Journal of Aerosol Science 35(Supplement 2), p. 967-980.
- Bard, D., Mark, D., Mohlmann, C. (2009). « Current standardisation for nanotechnology », Journal of Physics: Conference Series 170(1), p. 012036.
- Beaupré, L.A., Salehi, F., Zayed, J., Plamondon, P., L'Espérance, G. (2004). « Physical and Chemical Characterization of Mn Phosphate/Sulfate Mixture Used in an Inhalation Toxicology Study », Inhalation Toxicology, 16(4), p. 231-244.
- Bloch, D. (2006). « Exposition aux nanoparticules », CEA Grenoble, Service de santé au travail.
- BSI. (2007). « Nanotechnologies - Part 2: Guide to safe handling and disposal of manufactured nanomaterials », British Standards Institution. PD 6699-2:2007.
- Burlett, D. J. (2004). « Thermal techniques to study complex elastomer/filler systems », Journal of Thermal Analysis and Calorimetry 75(2), p. 531-544.
- Carr, R. (2007). « Direct visualisation and analysis of nanoparticles using a new laser-based, single particle tracking system », NTNE2007 - NanoTechnology Northern Europe (Congress and Exhibition), 27-29th March, Helsinki, Finland.
- CEN. (1998). « Reference test method for release of nickel from product intended to come in direct and prolonged contact with the skin », European Committee for Standardisation, Brussels. EN 1811.
- CEST. (2006). « Éthique et nanotechnologies: se donner les moyens d'agir », AVIS, Commission de l'éthique de la science et de la technologie.
- Dalla Via, R. (2008). « Overview of ISO TC 229 Nanotechnology standardization activities in the field of health, safety and the environment », INNO 2008. Montréal.
- De Kee, D., Chan Man Fong, C.F., Pintauro, P., Hinestroza, J., Yuan, G., Burczyk, A. (2000). « Effect of temperature and elongation on the liquid diffusion and permeation characteristics

- of natural rubber, nitrile rubber, and bromobutyl rubber », *Journal of Applied Polymer Science* 78(6), p. 1250-1255.
- Deltombe, F. (2010). « Étude de la pénétration des nanoparticules à travers les gants de protections », Internship report, École de technologie supérieure, Montréal (QC) Canada.
- Dolez, P. I., Bodila, N., Lara, J., Truchon, G. (2010a). « Personal protective equipment against nanoparticles », *International Journal of Nanotechnology* 7(1), p. 99-117.
- Dolez, P., Soulati, K., Gauvin, C., Lara, J., Vu-Khanh, T. (2010b). « Document d'information pour la sélection des gants de protection contre les risques mécaniques », Technical guide RG-649. Institut de recherche Robert-Sauvé en santé et en sécurité du travail, Montréal (QC) Canada. 65pp.
- Dolez, P., Vinches, L., Wilkinson, K., Plamondon, P., Vu-Khanh, T. (2011). « Development of a test method for protective gloves against nanoparticles in conditions simulating occupational use », *Journal of Physics: Conference Series*, 304: 012066. NanoSafe 2010, Grenoble, France, Nov. 16-18, 2010.
- Domingos, R.F., Tufenkji, N., Wilkinson, K.J. (2009). « Aggregation of titanium dioxide nanoparticles: role of natural organic matter », *Environ. Sci. Technol.* 43, p. 1282-1286.
- Domingos, R.F., Peyrot, C., Wilkinson, K.J. (2010). « Aggregation of titanium dioxide nanoparticles: role of calcium and phosphate », *Environmental Chemistry*. 7, p. 61-66.
- DuPont Dow Elastomers. (2004). « A guide to grades, compounding and processing of neoprene rubber », NPE-H77650-00-D0140.
- Edgren, C. S., R. G. Radwin, Irwin, C.B. (2004). « Grip force vectors for varying handle diameters and hand sizes », *Human Factors* 46(2), p. 244-251.
- Ellenbecker, M. J., Tsai, S.-J. (2010). « Exposure assessment for engineered nanoparticles: A review of the state-of-the-art », NanoSafe 2010, Grenoble, France.
- Furuta, I., Kimura, S.-I., Masamichi I. (2005). « Physical Constants of Rubbery Polymers ». In: *Polymer Handbook*. J. Brandrup, E. Immergut, H., E. A. Grulke, A. Abe and D. R. Bloch (Eds), John Wiley & Sons, p. V/1-V/7.
- Giacobbe, F., Minica, L., Geraci, D. (2009). « Nanotechnologies: Risk assessment model », *Journal of Physics: Conference Series* 170(1), p. 012035.
- Golanski, L., Guiot, A., Tardif, F. (2008a). « Are conventional protective devices such as fibrous filter media, respirator cartridges, protective clothing and gloves also efficient for nanoaerosols ? », NanoSafe: European Strategy for Nanosafety.
- Golanski, L., Guiot, A., Tardif, F. (2008b). « Experimental evaluation of personal protection devices against graphite nanoaerosols: fibrous filter media, masks and protective clothing », *Proceedings of the Nanotechnology Conference and Trade Show Nanotech 2008*, NanoScience and Technology Institute (NSTI). Boston, MA, Hune 1-5, 2008.
- Golanski, L., Guoit, A., Tardif, F. (2009a). « Experimental evaluation of individual protection devices against different types of nanoaerosols: graphite, TiO₂ and Pt », *Journal of Physics: Conference Series* 170.
- Golanski, L., Guiot, A., Rouillon, F., Pocachard, J., Tardif, F. (2009b). « Experimental evaluation of personal protection devices against graphite nanoaerosols: fibrous filter media, masks, protective clothing, and gloves », *Human and Experimental Toxicology* 28(6-7), p. 353-359.

- Golanski, L., Brouard, C., Motellier, S., Auger, A., Tardif, F. (2010). « Set-up of new measurement methods for polymeric membrane and textile barrier properties against nano-hydrosols », NanoSafe 2010, Grenoble, France.
- Goldstein, J., Newbury, D.E., Joy, D.C., Lyman, C.E., Echlin, P., Lifshin, E., Sawyer, L., Michael, J.R. (2003). « Scanning Electron Microscopy and X-ray Microanalysis », Springer, New York, 3rd edition, p. 195-203.
- Hallock, M. F., Greenley, P., DiBerardinis, L., Kallin, D. (2009). « Potential risks of nanomaterials and how to safely handle materials of uncertain toxicity », *Journal of Chemical Health & Safety* 16(1), p. 16-23.
- Hanley, J. T. (2006). « Aerosol system and swatch testing of chemical protective garments », Elevated Wind Studies International Conference, Arlington, VA, Sept. 25-26, 2006.
- Hansen, S. F. (2009). « Regulation and risk assessment of nanomaterials - Too little, too late ? », Department of environmental engineering, Technical University of Denmark. Ph. D. dissertation, 111 p.
- Harrabi, L., Dolez, P.I., Vu-Khanh, T., Lara, J. (2008). « Evaluation of the flexibility of protective gloves », *International Journal of Occupational Safety and Ergonomics* 14(1), p. 61-68.
- Hayden, G., Milne, H. C., Patterson, M.J., Nimmo, M.A. (2004). « The reproducibility of closed-pouch sweat collection and thermoregulatory responses to exercise-heat stress », *European Journal of Applied Physiology* 91(5-6), p. 748-751.
- Hervé-Bazin, B. (2007). « Les nanoparticules: Un enjeu majeur pour la santé au travail ? », *EDP Sciences*. 704 p.
- Hofacre, K. C. (2006). « Aerosol penetration of fabric swatches », Elevated Wind Studies International Conference. Arlington, VA, Sept. 25-26, 2006.
- Huang, S.-H., Huang, Y.-H., Chen, C. -W., Chang, C. -P. (2007). « Nanoparticle penetration through protective clothing materials », *Proceedings of the 3rd International Symposium on Nanotechnology, Occupational and Environmental Health, Taipei, Taiwan, Aug. 29 - Sept. 1, 2007*. p. 290-291.
- ICTA. (2007). « International coalition calls for strong oversight of nanotechnology », *Ohs online*. International Center for Technology. Aug. 6, 2007.
- ISO. (2008). « Nanotechnologies - Health and safety practices in occupational settings relevant to nanotechnologies », Technical report/ISO/TR 12885. International Organization for Standardization.
- Jackson, N., Lopata, A., Elms, T., Wright, P. (2009). « Engineered nanomaterials: Evidence of the effectiveness of workplace controls to prevent exposure », *Safe Work Australia*. 75 p.
- Jambou, A. (2009). « Conception d'un montage pour tester la pénétration des nanoparticules à travers les gants de protection », Internship report, École de technologie supérieure, Montréal (QC) Canada.
- Jankovic, J. T., Hall, M.A., Zontek, T.L., Hollenbeck, S.M., Ogle, B.R. (2010). « Particle loss in a scanning mobility particle analyzer sampling extension tube », *International Journal of Occupational and Environmental Health* 16(4). p. 429-433.
- Jin, J., Nguyen, V., Weiqiang, G., Brian, J.E., Douglas, L.G. (2005). « Cross-linked lyotropic liquid crystal-butyl rubber composites: Promising "breathable" barrier materials for chemical protection applications », *Chemistry of Materials* 17(2), p. 224-226.

- Kaegi, R., Ulrich, A., Sinnet, B., Vonbank, R., Wichser, A., Zuleeg, S., Simmler, H., Brunner, S., Vonmont, H., Burkhardt, M., Boller, M. (2008). « Synthetic TiO₂ nanoparticle emission from exterior facades into the aquatic environment », *Environmental Pollution* 156, p. 233-239.
- Kaluza, S., Kleine Balderhaar, J., Orthen, B., Honnert, B., Jankowska, E., Pietrowski, P., Rosell, M.G., Tanarro, C., Tejedor, J., Zugasti, A. (2009). « Workplace exposure to nanoparticles », J. Kosk-Bienko (Ed.). European Agency for Safety and Health at Work.
- Kurabayashi, H., Tamura, K., Machida, I., Kubota, K. (2002). « Inhibiting bacteria and skin pH in hemiplegia: Effects of washing hands with acidic mineral water », *American Journal of Physical Medicine and Rehabilitation* 81(1), p. 40-46.
- Larivière, C., Tremblay, G., Nadeau, S., Harrabi, L., Dolez, P., Vu-Khanh, T., Lara, J. (2010). « Do mechanical tests of glove stiffness provide relevant information relative to their effects on the musculoskeletal system ? A comparison with surface electromyography and psychophysical methods », *Applied Ergonomics* 41, p. 326-334.
- Li, Y., De Kee, D., Chan Man Fong, C.F., Pintauro, P., Burczyk, A. (1999). « Influence of external stress on the barrier properties of rubbers », *Journal of Applied Polymer Science* 74(6), p. 1584-1595.
- Mahé, S. (2009). « Conception d'un montage expérimental pour la mesure de la pénétration des nanoparticules à travers les matériaux de gants de protection », Internship report, École de technologie supérieure, Montréal (QC) Canada.
- Marckmann, G., E. Verron, Gornet, L., Chagnon, G., Charrier, P., Fort, P. (2002). « A theory of network alteration for the Mullins effect », *Journal of the Mechanics and Physics of Solids* 50(9), p. 2011-2028.
- Maynard, A. (2005). « Nanotechnology and occupational health », EPA, June 13, 2005.
- McCrum, N. G., Buckley, C. P., Bucknall, C. B. (1997). « Principles of Polymer Engineering », New York, Oxford University Press.
- Meiling, T. T., Lohmannsroben, H.-G., Kon, K., Karthaus, O. (2010). « Solvent Effect of the Adsorption of Titanium Dioxide Nanoparticles onto Microporous Polymer Films », *e-Journal of Surface Science and Nanotechnology* 8, p. 309-3012.
- Mellstrom, G. A. and A. S. Boman (2005). « Gloves: Types, materials and manufacturing. Protective gloves for occupational use », A. S. Boman, T. Estlander, J. E. Wahlberg and H. I. Maibach (Eds). Boca Raton, London, New York, Washington DC, CRC Press. p. 15-28.
- Meyer, J. P., Flenghi, D., Turpin-Legendre, E. (2001). « Force maximale de préhension: Intérêts, méthode de recueil et valeurs de référence », *Archives des maladies professionnelles et de médecine du travail* 62(6), p. 493-522.
- Muller, C., L'Espérance, G., Plamondon, P., Kennedy, G., Zayed, J. (2008). « Characterization of beryllium particles from CAISiFrit », *Journal of Toxicology and Environmental Health, Part A*, 71, p. 1091-1099.
- Mullins, L. (1969). « Softening of rubber by deformation », *Rubber Chemistry and Technology* 42(1), p. 339-362.
- Nanotechnology Workgroup. (2007). « Nanotechnology White Paper », Science Policy Council, United States Environmental Protection Agency. EPA 100/B-07/001.

- Nicolay, C. W., Walker, A. L. (2005). « Grip strength and endurance: Influences of anthropometric variation, hand dominance, and gender », *International Journal of Industrial Ergonomics* 35(7), p. 605-618.
- NIOSH. (2005). « Strategic plan for NIOSH nanotechnology research - Filling the knowledge gap: Draft », Nanotechnology Research Program, National Institute for Occupational Safety and Health, Center for Disease Control and Prevention.
- NIOSH. (2006). « Final Combined Presentations for the October 13, 2006 NPPTL meeting ».
- NNI. (2006). « Environmental, health, and safety research needs for engineered nanoscale materials », The National Nanotechnology Initiative, Nanoscale science, engineering, and technology subcommittee, Committee on technology, National science and technology council.
- Noël A, L'Espérance G, Cloutier Y, Plamondon P, Boucher J, Philip S, Dion C, Truchon G, Zayed J. 2013. Assessment of the contribution of electron microscopy to nanoparticle characterization sampled with two cascade impactors. *Journal of Occupational and Environmental Hygiene*, 10: 155-172.
- Nohilé, C. (2010). « Étude de l'effet du gonflement par les solvants sur les propriétés du caoutchouc butyle ». Ph.D. dissertation. École de technologie supérieure, Montréal (QC) Canada. 201 p.
- Nohile, C., Dolez, P.I., Vu-Khanh, T. (2008). « Parameters controlling the swelling of butyl rubber by solvents », *Journal of Applied Polymer Science* 110(6), p. 3926-33.
- NRC. (2007). « Progress toward safe nanotechnology in the workplace », Nanotechnology Research Center, CDC - Workplace Safety and Health. DNNS (NIOSH) # 2007-123.
- NTRC. (2009). « Progress toward safe nanotechnology in the workplace - Project updates for 2007 and 2008 », NIOSH nanotechnology research center, Department of Health and Human Services - CDCP - NIOSH. #2010-104. 102 p.
- OECD. (2010). « Current developments/activities on the safety of manufactured nanomaterials - Tour de table at the 7th meeting of the working party on manufactured nanomaterials », Series on the safety of manufactured nanomaterials. Organisation for Economic Co-operation and Development. Paris, France. ENV/JM/MONO(2010)42.
- Ostiguy, C., Roberge, B., Ménard, L., Endo, C. (2008a). « Guide de bonnes pratiques favorisant la gestion des risques reliés aux nanoparticules de synthèse », Technical guide/R-586. Institut de recherche Robert-Sauvé en santé et en sécurité du travail, Montréal (QC) Canada.
- Ostiguy, C., Soucy, B., Lapointe, G., Woods, C., Ménard, L. (2008b). « Les effets sur la santé reliés aux nanoparticules », Report R-558, Institut de recherche Robert-Sauvé en santé et en sécurité au travail, Montréal (QC) Canada.
- Ostiguy, C., Roberge, B., Woods, C., Soucy, B. (2009). « Les nanoparticules de synthèse - Connaissances actuelles sur les risques et les mesures de prévention en SST », Report R-646, Institut de recherche Robert-Sauvé en santé et en sécurité au travail, Montréal (QC) Canada. 159 pp.
- Paik, S. Y., Zalk, D.M., Swuste, P. (2008). « Application of a pilot control banding tool for risk level assessment and control of nanoparticle exposures », *Annals of Occupational Hygiene* 52(6), p. 419-428.
- Papp, T., Schiffmann, D., Weiss, D., Castranova, V., Vallyathan, V., Rahman, Q. (2008). « Human health implications of nanomaterial exposure », *Nanotoxicology* 2(1), p. 9-27.

- Park, J. H. and D. Kim (2001). « Preparation and characterization of water-swelling natural rubbers », *Journal of Applied Polymer Science* 80(1), p. 115-121.
- PCAST. (2010). « Report to the President and Congress on the Third Assessment of the National Nanotechnology Initiative », President's Council of Advisors on Science and Technology, National Nanotechnology Initiative, Executive Office of the President of the United-States. 96 p.
- Perron, G., Desnoyers, J.E., Lara, J. (2002). « Résistance des vêtements de protection aux mélanges de solvants industriels - Développement d'un outil de sélection », Report R-305. Institut Robert-Sauvé en santé et en sécurité du travail, Montréal (QC) Canada. 65 p.
- Prabhakar, R. S., Raharjo, R., Toy, L.G., Lin, H., Freeman, B.D. (2005). « Self-consistent model of concentration and temperature dependence of permeability in rubbery polymers », *Industrial and Engineering Chemistry Research* 44(5), p. 1547-1556.
- Purvis, A. J. and N. T. Cable (2000). « The effects of phase control materials on hand skin temperature with gloves of soccer goalkeepers », *Ergonomics* 43(10), p. 1480-1488.
- Ricaud, M. (2009). « Nanomatériaux - Risques pour la santé & mesures de prévention », Institut national de recherche et de sécurité pour la prévention des accidents du travail et des maladies professionnelles. ED 6064. 6 p.
- Robichaud, C. O., Uyar, A.E., Darby, M.R., Zucker, L.G., Wiesner, M.R. (2009). « Estimates of upper bounds and trends in nano-TiO₂ production as a basis for exposure assessment », *Environmental Science and Technology* 43, p. 4227-4233.
- Rodot, M. (2006). « Chemical protective gloves from performances to service time prediction », *Proceedings of the 3rd European Conference on Protective Clothing and Nokobetef* 8, Gdynia, Poland.
- Rouse, J. G., Yang, J., Ryman-Rasmussen, J.P., Barron, A.R., Monteiro-Riviere, N.A. (2007). « Effects of mechanical flexion on the penetration of fullerene amino acid-derivatized peptide nanoparticles through skin », *Nano Letters* 7(1), p. 155-160.
- Ryman-Rasmussen, J. P., Riviere, J.E., Monteiro-Riviere, N.A. (2006). « Penetration of intact skin by quantum dots with diverse physicochemical properties », *Toxicol. Sci.* 91(1), p. 159-165.
- Santé Canada. « Éthylène glycol : classification relative à la toxicité aiguë, Questions reliées à des substances spécifiques », (Accessed Dec. 15, 2010). <http://www.hc-sc.gc.ca/ewh-semt/occup-travail/whmis-simdut/substance-fra.php#a3>.
- Schmid-Wendtner, M. H., Korting, H. C. (2006). « The pH of the skin surface and its impact on the barrier function », *Skin Pharmacology and Physiology* 19(6), p. 296-302.
- Schneider, T. (2007). « Evaluation and control of occupational health risks from nanoparticles », *Nordic Council of Ministers. TemaNord 2007*. 581 p.
- Schulte, P. A., Salamanca-Buentello, F. (2007). « Ethical and scientific issues of nanotechnology in the workplace », *Environmental Health Perspectives* 115(1). p. 5-12.
- Schulte, P., Geraci, C., Zumwalde, R., Hoover, M., Kuempel, E. (2008). « Occupational Risk Management of Engineered Nanoparticles », *Journal of Occupational and Environmental Hygiene* 5(4), p. 239 - 249.
- Shvedova, A. A., Castranova, V., Kisin, E.R., Schwegler-Berry, D., Murray, A.R., Gandelsma, V.Z., Maynard, A., Baron, P. (2003). « Exposure to carbon nanotube material: Assessment of

- nanotube cytotoxicity using human keratinocyte cells », *Journal of Toxicology and Environmental Health-Part A* 66(20), p. 1909-1926.
- Singh, A., Mukherjee, M. (2003). « Swelling dynamics of ultrathin polymer films », *Macromolecules* 36(23), p. 8728-8731.
- Sombatsompop, N. (1998). « Swelling characteristics of some natural rubber based elastomers », *Progress in Rubber and Plastics Technology* 14(4), p. 208-225.
- Sullivan, P. J., Mekjavic, I. B. (1992). « Temperature and humidity within the clothing microenvironment », *Aviation, space, and environmental medicine* 63(3), p. 186-192.
- Testori, N. (2011). « Étude de la pénétration des nanoparticules à travers des textiles de protection utilisés en santé et sécurité au travail », Internship report, École de technologie supérieure, Montréal (QC) Canada.
- Truchon, G., Noël, A., Cloutier, Y., Maghni, K., Gautrin, D., Hallé, S., Dufresne, L., Dolez, P., Tardif, R. (2008). « La recherche en nanotoxicologie: Par où commencer ? » *Travail et Santé* 32(2), p. 32-35.
- Van Niftrik, M., Verbist, K. (2010). « Stoffenmanager 1.0: An online control banding tool for the prioritization of risks related to working with manufactured nano objects », *NanoSafe 2010*, Grenoble, France.
- Volynskii, A. L., Grokhovskaya T.Y., Sanchez, A., Lukovkin, G.M., Bakeyev, N.F. (1988). « Mechanism of the migration of a low molecular weight component in the system natural rubber vulcanizate-low molecular weight hydrocarbon », *Polymer Science USSR (English Translation of Vysokomolekulyarnye Soyedineniya Series A)* 30(10), p. 2220-2227.
- Vu-Khanh, T., Dolez, P., Harrabi, L., Lara, J., Larivière, C., Tremblay, G., Nadeau, S. (2007). « Caractérisation de la souplesse des gants de protection par des méthodes mécaniques et biomécaniques », Report R-506. Institut Robert-Sauvé en santé et en sécurité du travail, Montréal (QC) Canada. 90 p.
- Vu-Khanh, T., Dolez, P., Thang Nguyen, C., Gauvin, C., Lara, J. (2011). « Caractérisation de la résistance des gants à la piqûre par les aiguilles - Mise au point d'une méthode d'essai », Report R-711. Institut Robert-Sauvé en santé et en sécurité du travail, Montréal (QC) Canada, 123 p.
- Wallace, R. B. (2008). « Wallace/Maxcy-Rosenau-Last Public health and preventive medicine », McGraw-Hill Professional.
- Wang, G., Li, M., Chen, X. (1999). « Effects of fillers on mechanical properties of a water-swelling rubber », *Journal of Applied Polymer Science* 72(4), p. 577-584.
- Wang, X., Kalinitchenko, I. (2010). « Principles and performance of the Collision Reaction Interface for the Varian 820-MS », *Advantage Note, Varian*. p. 1-4.
- West, P., Starostina, N. (2006). « AFM capabilities in characterization of particle nanocomposites: From angstroms to microns », 2006 Multifunctional Nanocomposites International Conference, Sep 20-22 2006, American Society of Mechanical Engineers, New York, NY 10016-5990, United States. 2006, p. 5.
- Wilkinson, K. J., Balnois, E., Leppard, G.G., Buffle, J. (1999). « Characteristic features of the major components of freshwater colloidal organic matter revealed by transmission electron and atomic force microscopy », *Colloids and Surfaces A: Physicochemical and Engineering Aspects* 155(2-3), p. 287-310.

- Witschger, O., Fabries, J.-F. (2005a). « Particules ultra-fines et santé au travail 2- Sources et caractérisation de l'exposition », Institut National de Recherche et de Sécurité. ND 2228-199-05.
- Witschger, O., Fabries, J.-F. (2005b). « Particules ultra-fines et santé au travail: 1 - Caractéristiques et effets potentiels sur la santé », Hygiène et sécurité au travail - Cahiers de notes documentaires, INRS. ND 2227-199-05.
- Xu, P. and J. E. Mark (1993). « Strain-induced crystallization in stretched polyisobutylene elastomers », Polymer Preprints, Division of Polymer Chemistry, American Chemical Society 34(2), p. 556.
- Zhang, L. W. and N. A. Monteiro-Riviere (2008). « Assessment of quantum dot penetration into intact, tape-stripped, abraded and flexed rat skin », Skin Pharmacology and Physiology 21(3), p. 166-180.

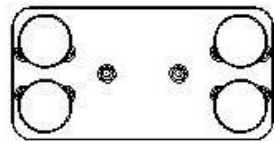
APPENDIX A: DRAWINGS OF EXPERIMENTAL SETUP

List of plates

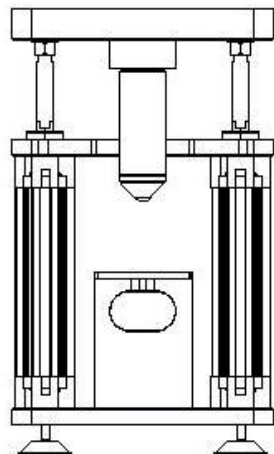
- Overview – Nano Bench
- Lower plate
- Beam
- Cell support
- Centre plate
- Sampling chamber
- Exposure chamber
- Exposure chamber ring
- Probe rod
- Solid tip with compression A
- Solid tip without compression B
- Conical-spherical tip C
- Compression tip D
- Support for compression test measurements

Glossary for plates:

Aluminium	Aluminum
Bague chambre exposition	Exposure chamber ring
Banc Nano	Nano bench
Cadre	Frame
Cellule	Cell
Chambre d'échantillonnage	Sampling chamber
Chambre d'exposition	Exposure chamber
Coupe	Cross-section
Échelle	Scale
Fléau	Beam
Plateau central	Centre plate
Plateau inférieur	Lower plate
Polyéthylène	Polyethylene
Sonde	Probe
Support de la cellule	Cell support
Support mesure en compression	Support for compression test measurements
Tête conique-sphérique	Spherical-conical probe tip
Tête de compression	Compression probe tip
Tête plane avec compression	Solid probe tip with compression
Tête plane sans compression	Solid probe tip without compression
Tige de la sonde	Probe rod
Vue de derrière	Rear view
Vue de dessous	Bottom view
Vue de dessus	Top view
Vue de droite	Right side view
Vue de face	Front view
Vue de gauche	Left side view
Vue globale	Overview
Vue isométrique	Isometric view

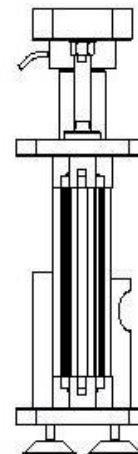


Vue de dessous
Echelle : 1:5

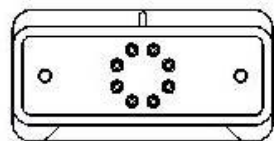
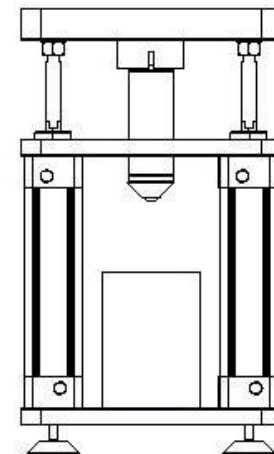


Vue de face
Echelle : 1:5

Vue de gauche
Echelle : 1:5

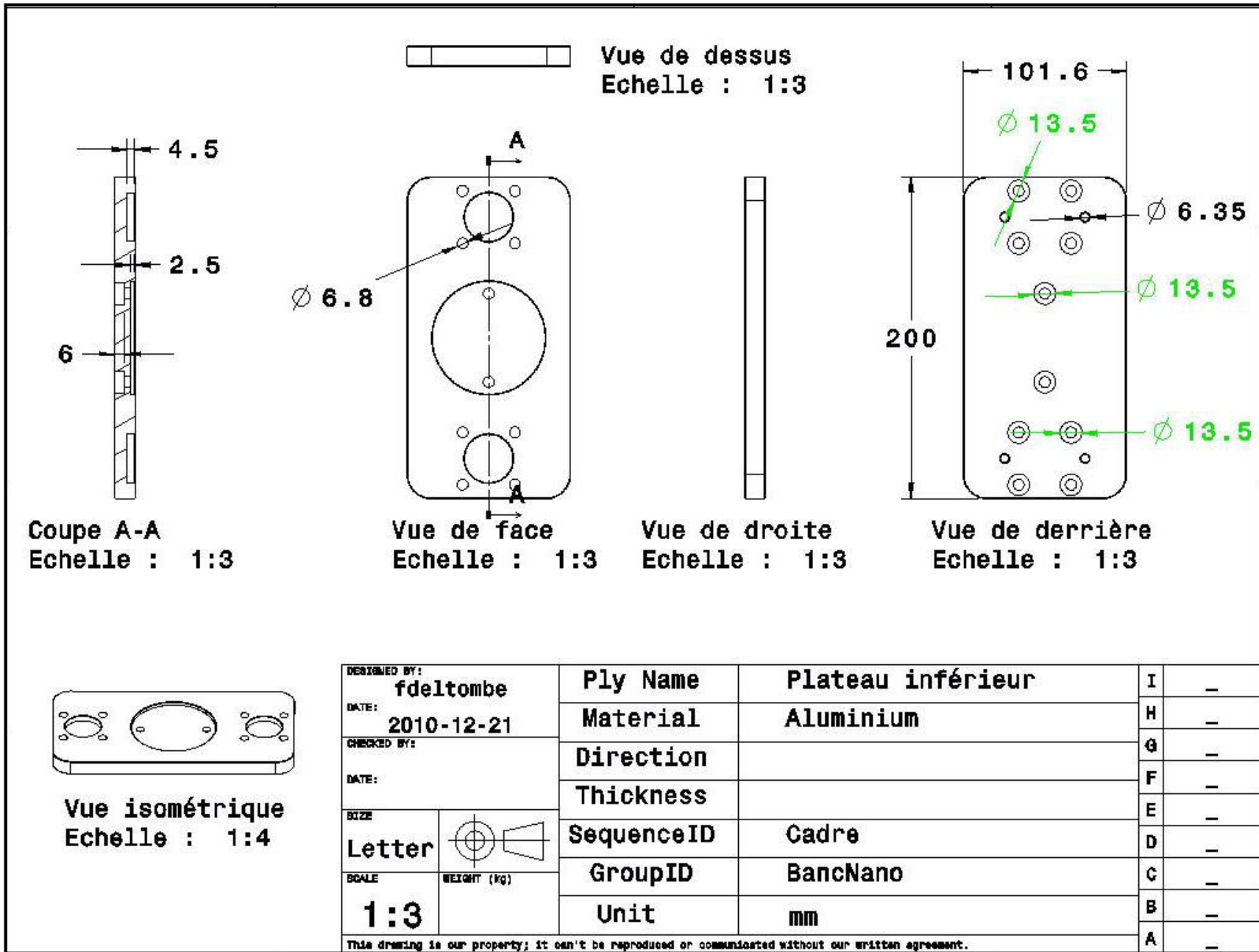


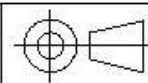
Vue de derrière
Echelle : 1:5

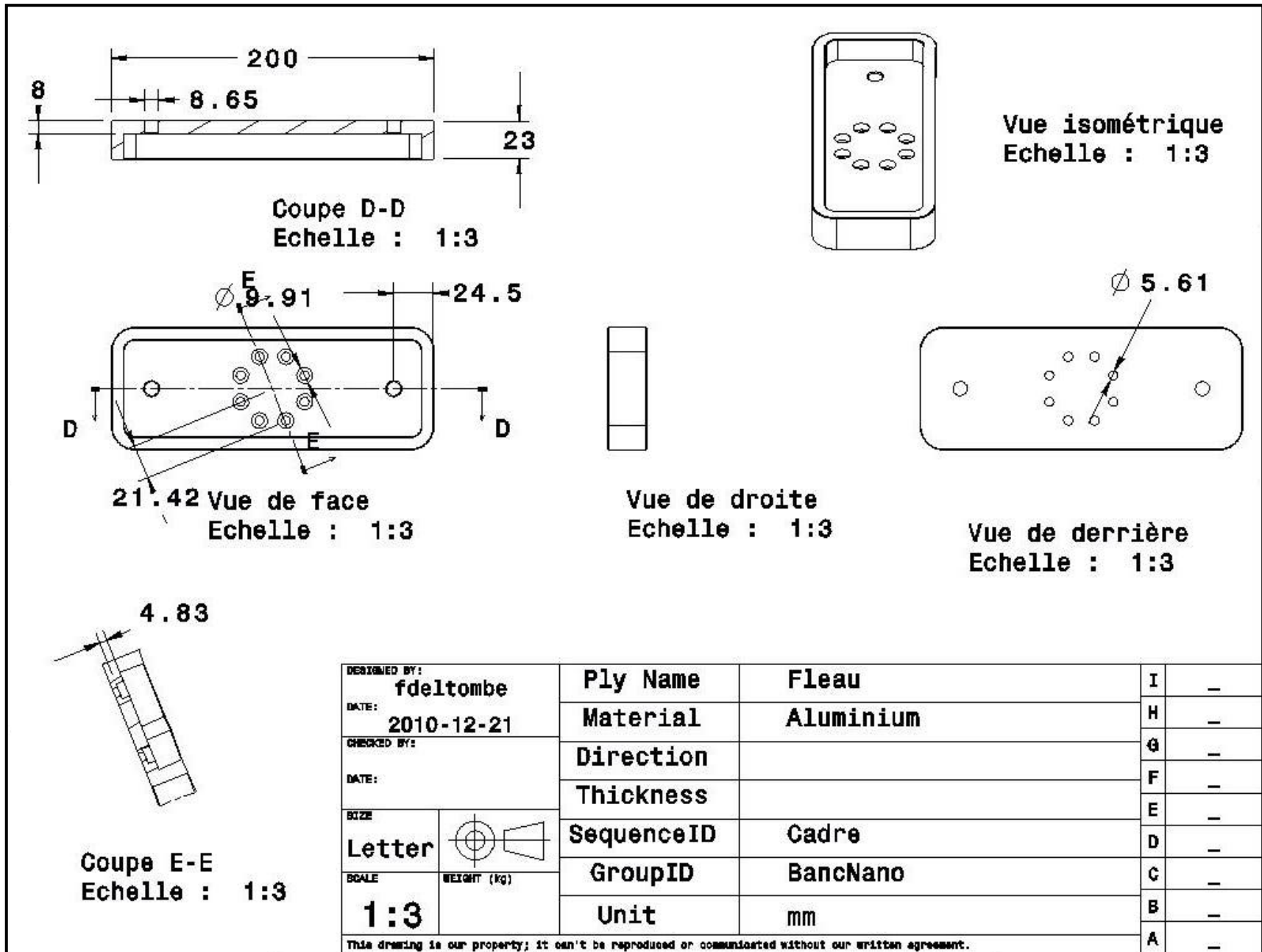


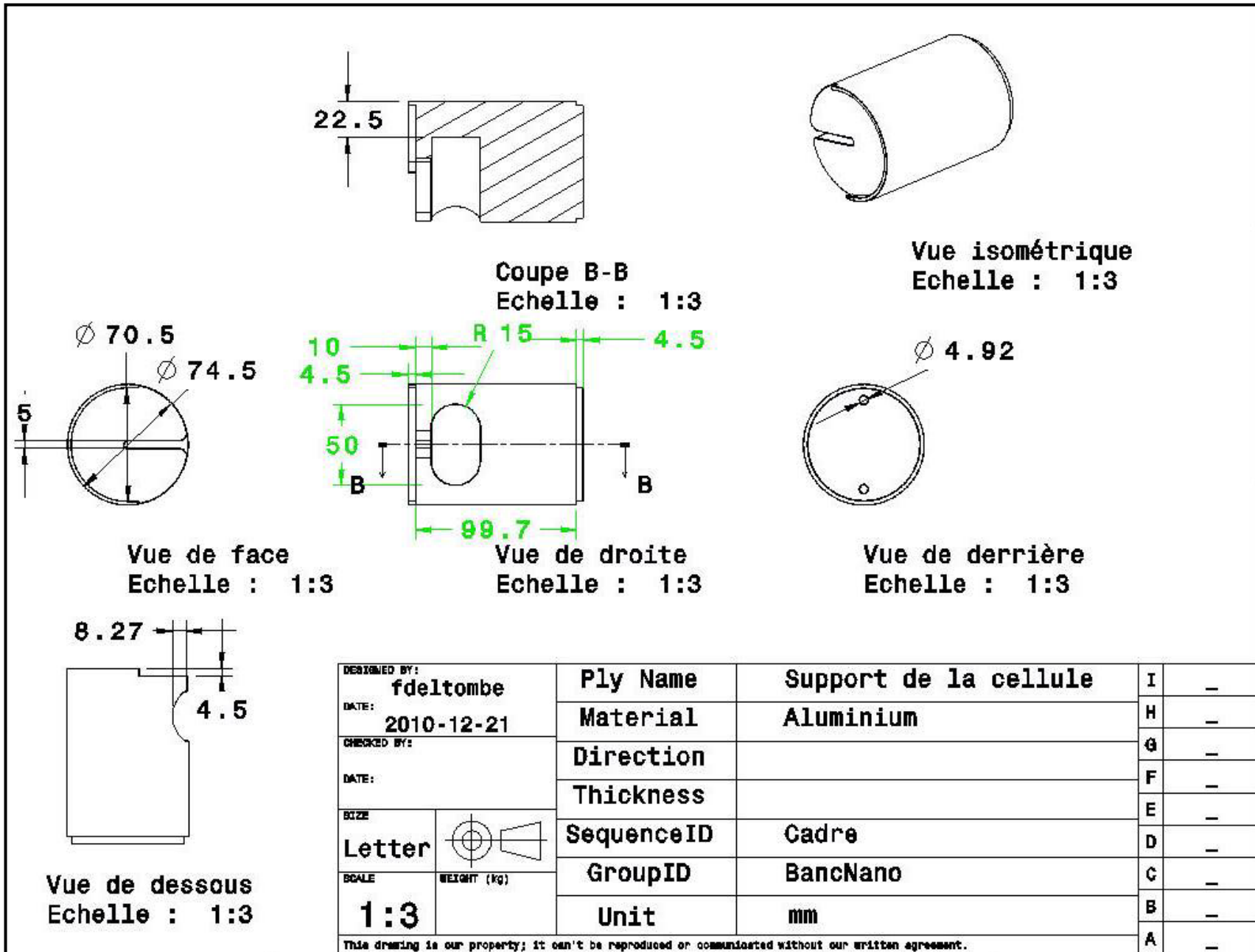
Vue de dessus
Echelle : 1:5

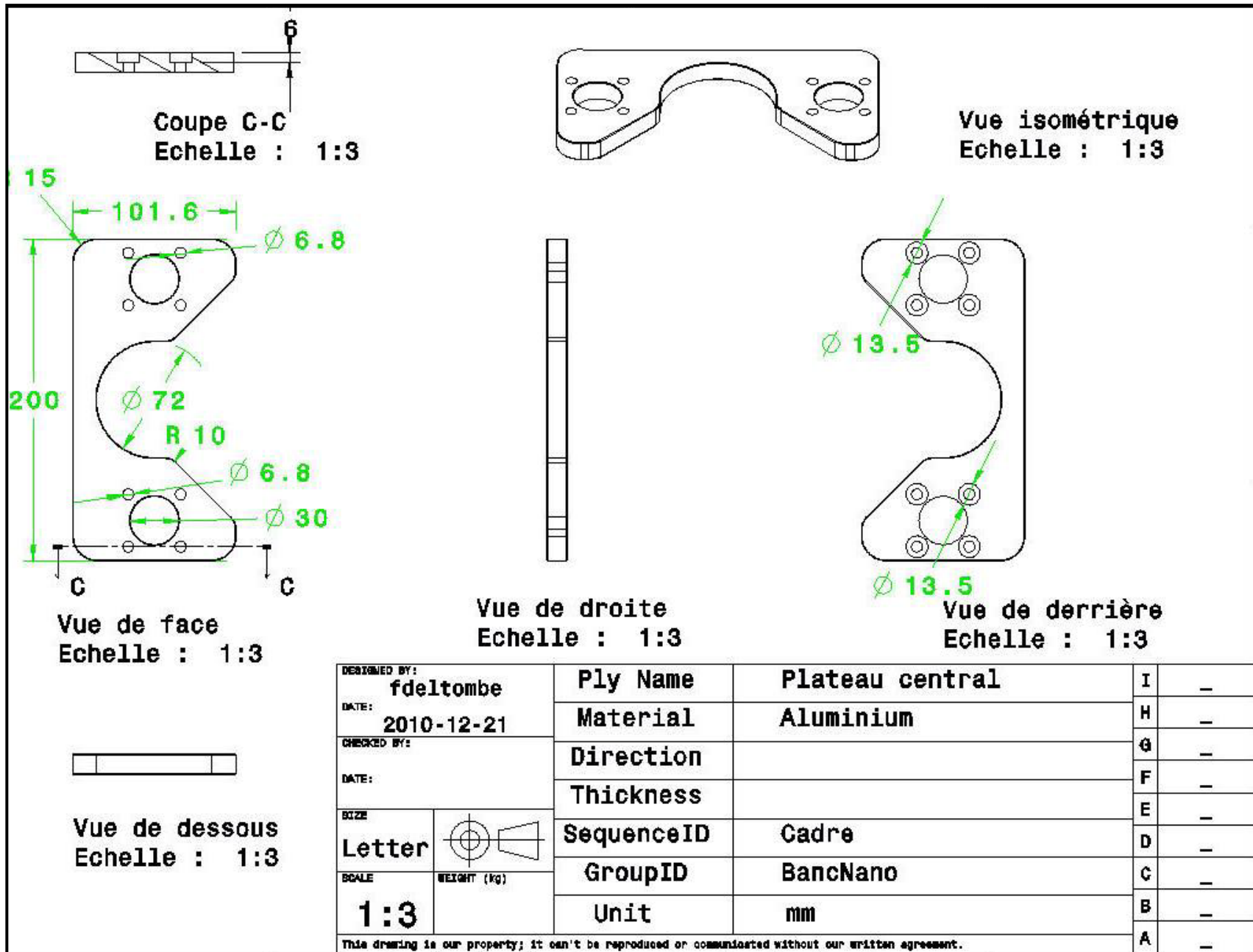
DESIGNED BY: Félicien Deltombe		Ply Name	Vue globale BancNano	I	-
DATE: 2010-09-13		Material	Polyethylene et Aluminium	H	-
CHECKED BY:		Direction		G	-
DATE:		Thickness		F	-
SIZE A4		SequenceID	Cadre, Cellule, Sonde	E	-
SCALE 1:5		GroupID	BancNano	D	-
	WEIGHT (KG)	Unit		C	-
This drawing is our property; it can't be reproduced or communicated without our written agreement.				B	-
				A	-

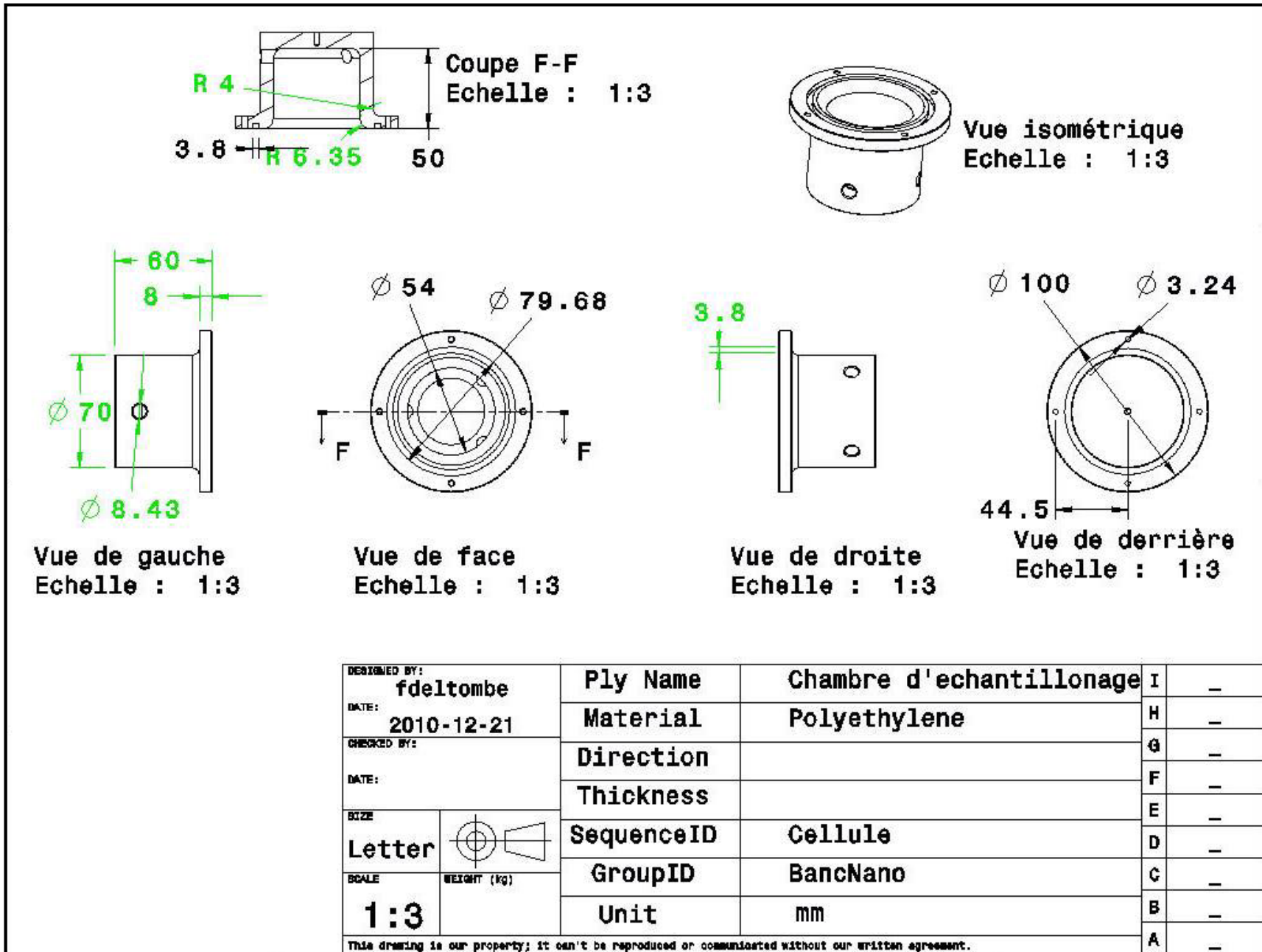


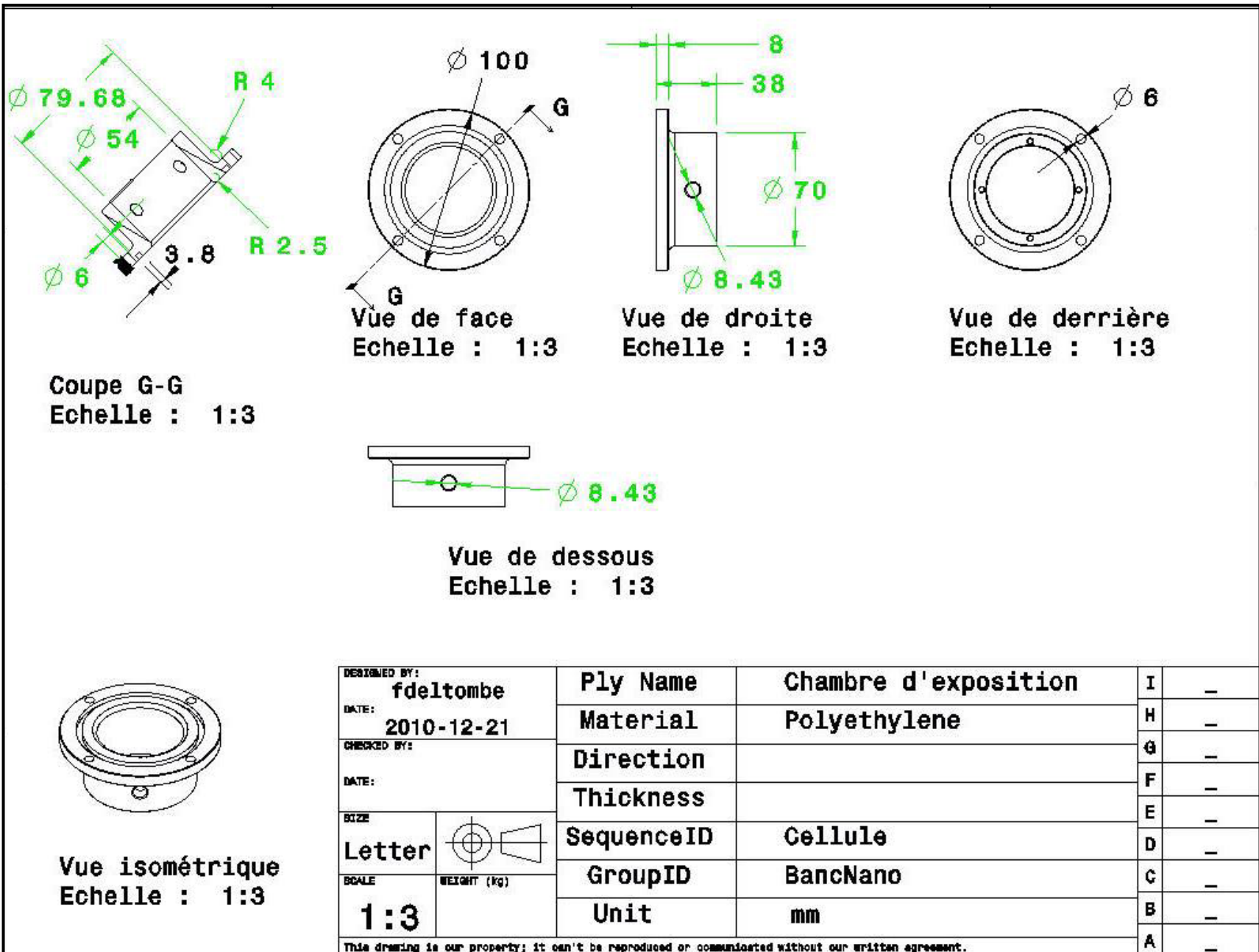
DESIGNED BY: fdeltombe		Ply Name	Plateau inférieur	I	-	
DATE: 2010-12-21		Material	Aluminium	H	-	
CHECKED BY:		Direction		G	-	
DATE:		Thickness		F	-	
SIZE		SequenceID	Cadre	E	-	
Letter		GroupID	BancNano	D	-	
SCALE		Unit	mm	C	-	
1:3		WEIGHT (kg)		B	-	
This drawing is our property; it can't be reproduced or communicated without our written agreement.					A	-

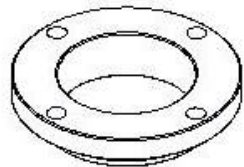
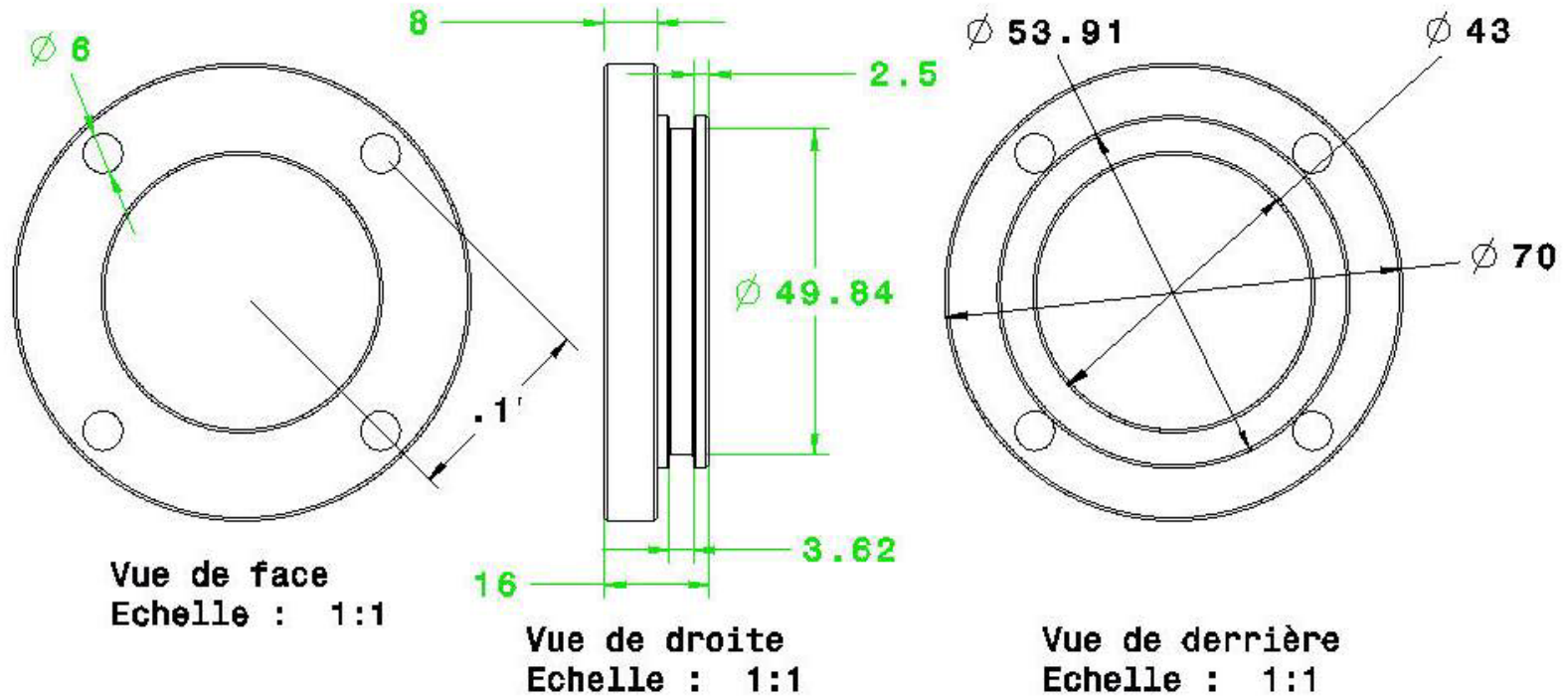








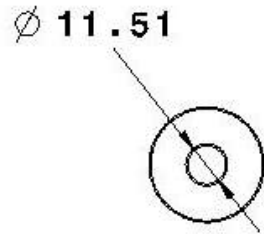
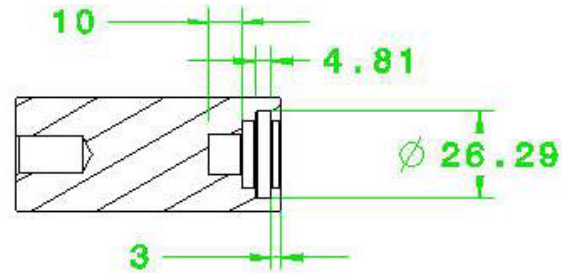




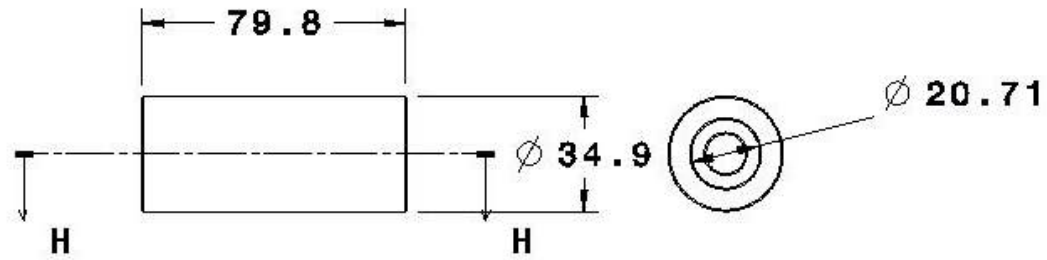
Vue isométrique
Echelle : 1:2

DESIGNED BY: fdeltombe		Ply Name	Bague chambre exposition	I	-	
DATE: 2010-12-21		Material	Polyethylene	H	-	
CHECKED BY:		Direction		G	-	
DATE:		Thickness		F	-	
SIZE		SequenceID	Cellule	E	-	
Letter		GroupID	BancNano	D	-	
SCALE		Unit	mm	C	-	
1:3		WEIGHT (kg)		B	-	
This drawing is our property; it can't be reproduced or communicated without our written agreement.					A	-

Coupe H-H
Echelle : 1:2



Vue de face
Echelle : 1:2



Vue de droite
Echelle : 1:2

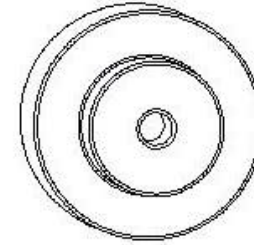
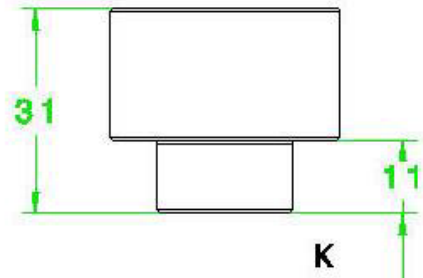
Vue de derrière
Echelle : 1:2



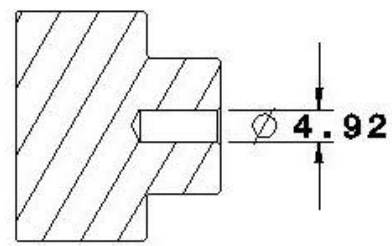
Vue isométrique
Echelle : 1:2

DESIGNED BY: fdeltombe		Ply Name	Tige de la sonde	I	-	
DATE: 2010-12-21		Material	Polyethylene	H	-	
CHECKED BY:		Direction		G	-	
DATE:		Thickness		F	-	
SIZE	Letter	SequenceID	Sonde	E	-	
SCALE		GroupID	BancNano	D	-	
1:3	WEIGHT (kg)	Unit	mm	C	-	
This drawing is our property; it can't be reproduced or communicated without our written agreement.					B	-
					A	-

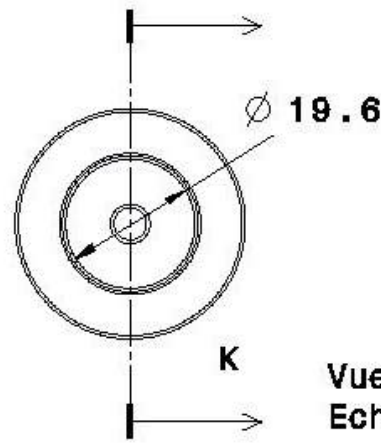
Vue de dessus
Echelle : 1:1



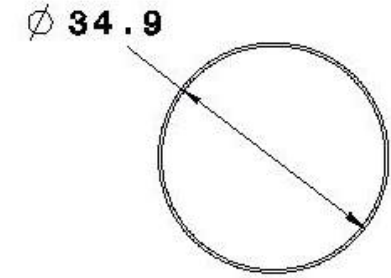
Vue isométrique
Echelle : 1:1



Coupe K-K
Echelle : 1:1

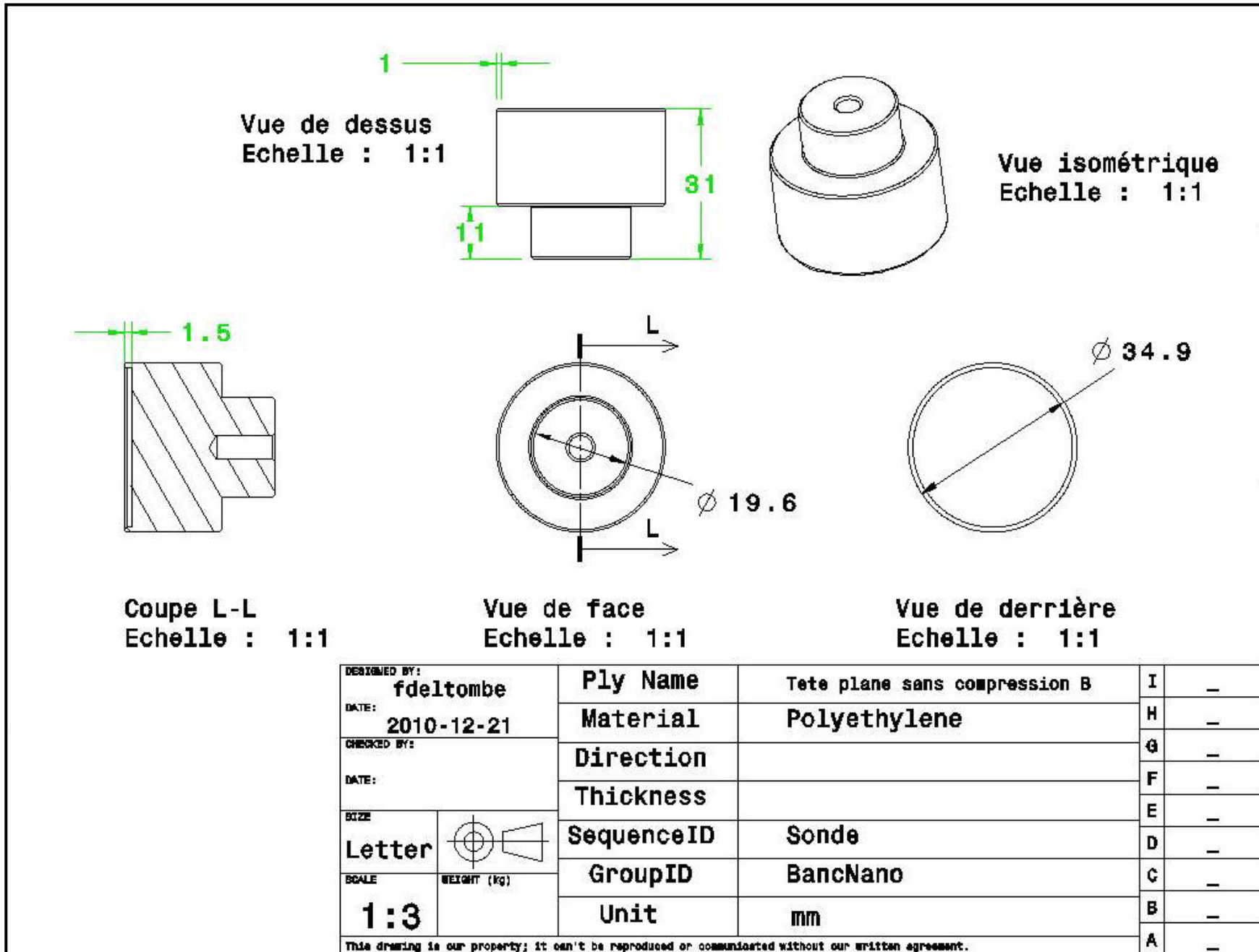


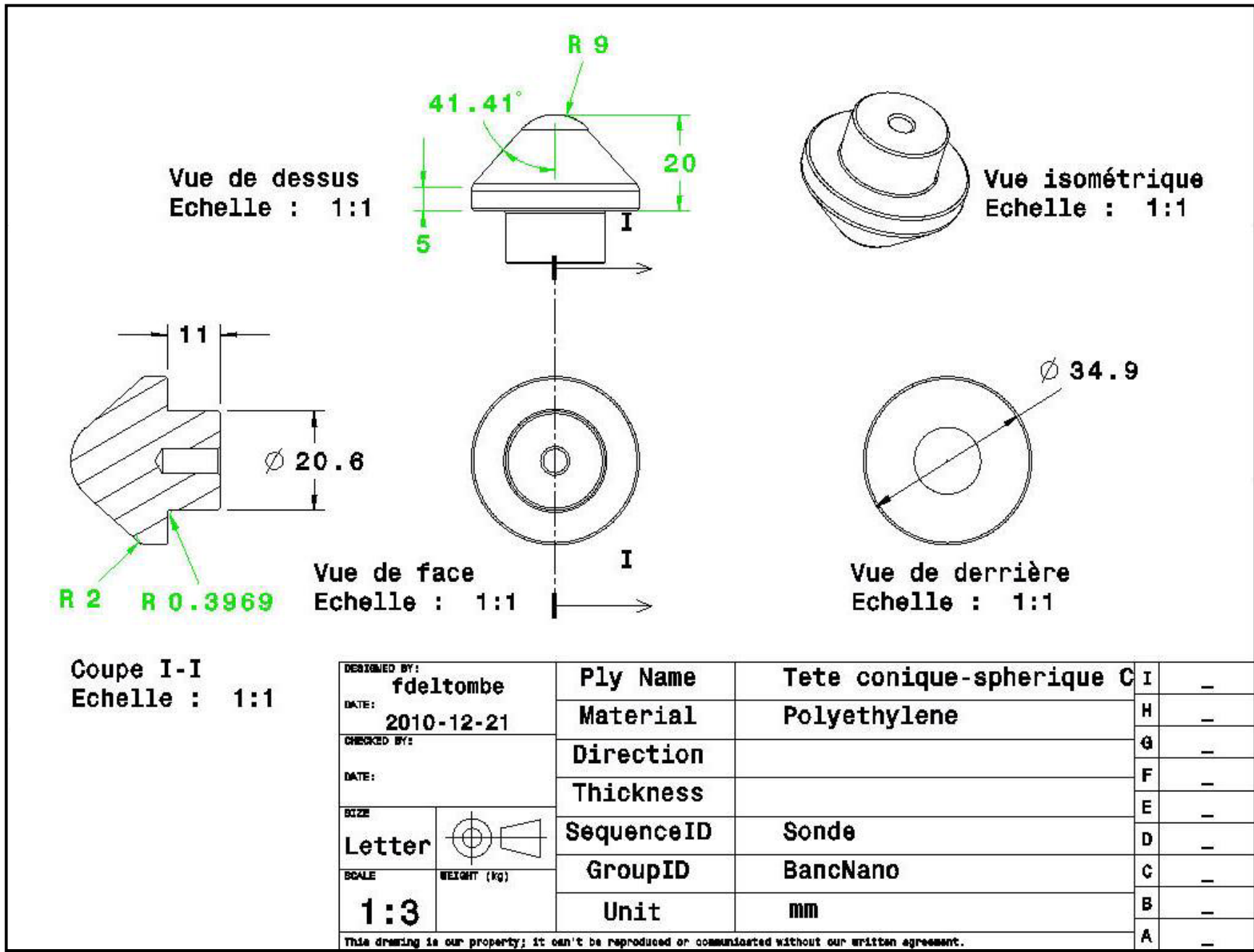
Vue de face
Echelle : 1:1



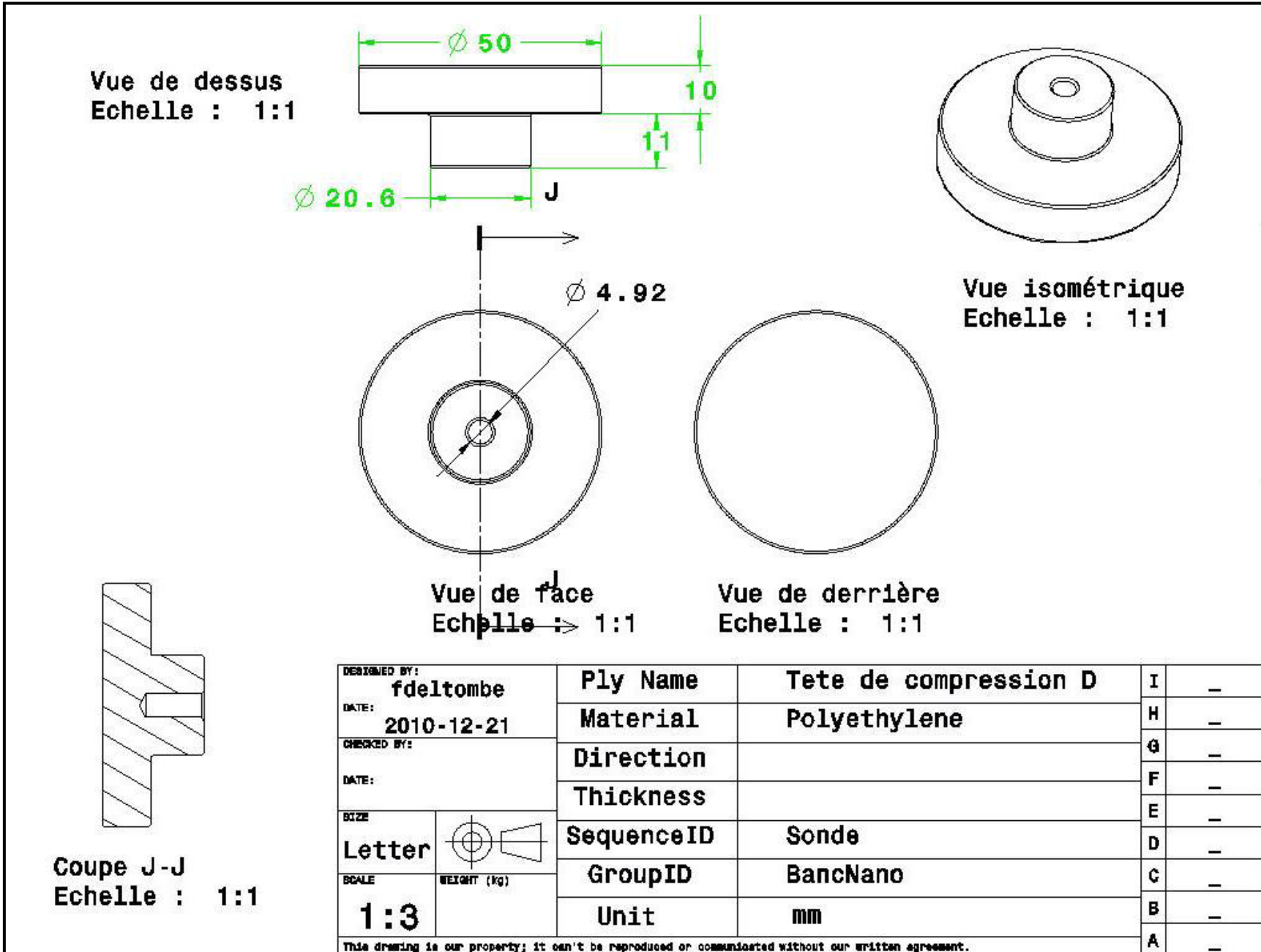
Vue de derrière
Echelle : 1:1

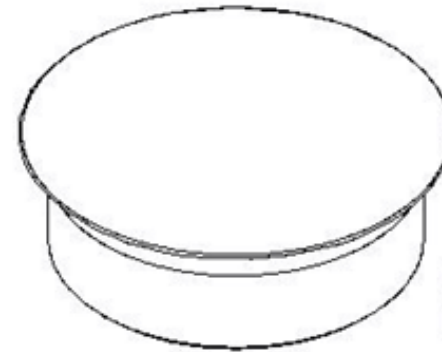
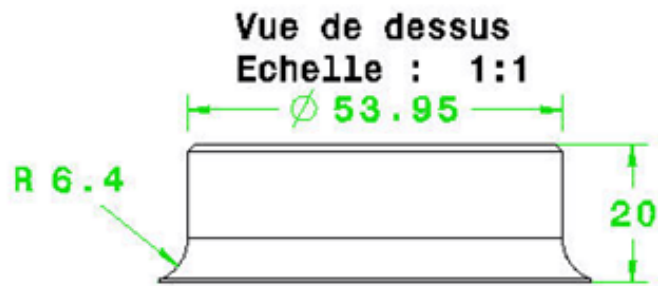
DESIGNED BY: fdeltombe		Ply Name	Tete plane avec compression A	I	—
DATE: 2010-12-21		Material	Polyethylene	H	—
CHECKED BY:		Direction		G	—
DATE:		Thickness		F	—
SIZE		SequenceID	Sonde	E	—
Letter		GroupID	BancNano	D	—
SCALE		Unit	mm	C	—
1:3	WEIGHT (kg)			B	—
This drawing is our property; it can't be reproduced or communicated without our written agreement.				A	—



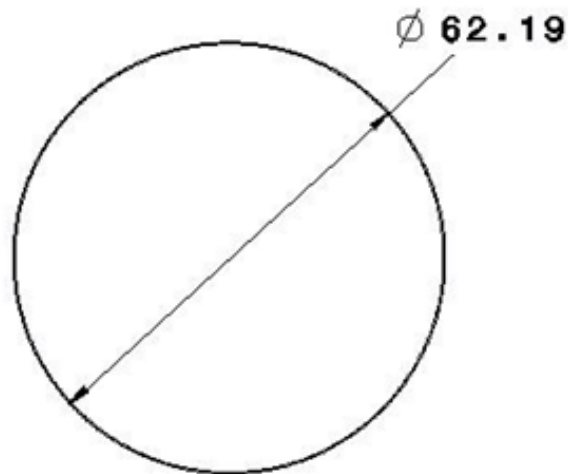


DESIGNED BY: fdeltombe		Ply Name	Tete conique-spherique C	I	-	
DATE: 2010-12-21		Material	Polyethylene	H	-	
CHECKED BY:		Direction		G	-	
DATE:		Thickness		F	-	
SIZE		SequenceID	Sonde	E	-	
Letter		GroupID	BancNano	D	-	
SCALE		Unit	mm	C	-	
1:3	WEIGHT (kg)			B	-	
This drawing is our property; it can't be reproduced or communicated without our written agreement.					A	-

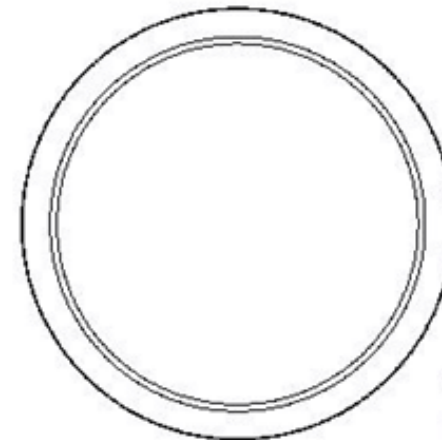




Vue isométrique
Echelle : 1:1



Vue de face
Echelle : 1:1



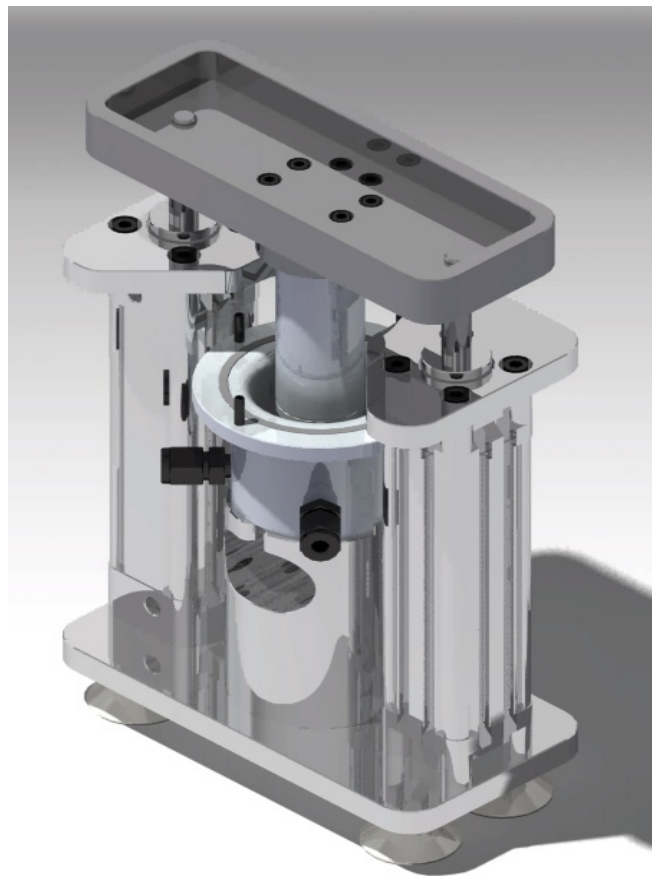
Vue de derrière
Echelle : 1:1

DESIGNED BY: fdeltombe	Ply Name	Support mesure en compression	I	—
DATE: 2010-12-21	Material	Polyethylene	H	—
CHECKED BY:	Direction		G	—
DATE:	Thickness		F	—
SIZE	SequenceID	Sonde	E	—
Letter	GroupID	BancNano	D	—
SCALE	Unit	mm	C	—
1:3			B	—
			A	—

This drawing is our property; it can't be reproduced or communicated without our written agreement.

APPENDIX B: USER MANUAL

User Manual Nano Bench Setup



January 2011



This user manual is based on the *Notice d'utilisation du montage de mesure de la pénétration des nanoparticules à travers les matériaux de gants de protection* [Operating instructions for setup to measure nanoparticle penetration through protective glove materials] (Jambou, 2009).

The various protocols take into account the two types of nanoparticles (NPs) used:

- NPs in dry powder (TiO₂ and NTC)
 - NPs in colloidal solution (TiO₂ in ethylene glycol, propylene glycol or water)
-

Contents

- A. Clean chambers, connectors and overflow
- B. Prepare glove sample and double membrane
- C. Prepare nanoparticle sample
 - 1. Nanoparticles in powder
 - 2. Nanoparticles in colloidal solution
- D. Prepare sampling solution
- E. Assemble setup
 - 1. Nanoparticles in powder
 - 2. Nanoparticles in colloidal solution
- F. Set parameters and run experiment
- G. Wind up experiment

A. Clean chambers, connectors and overflow

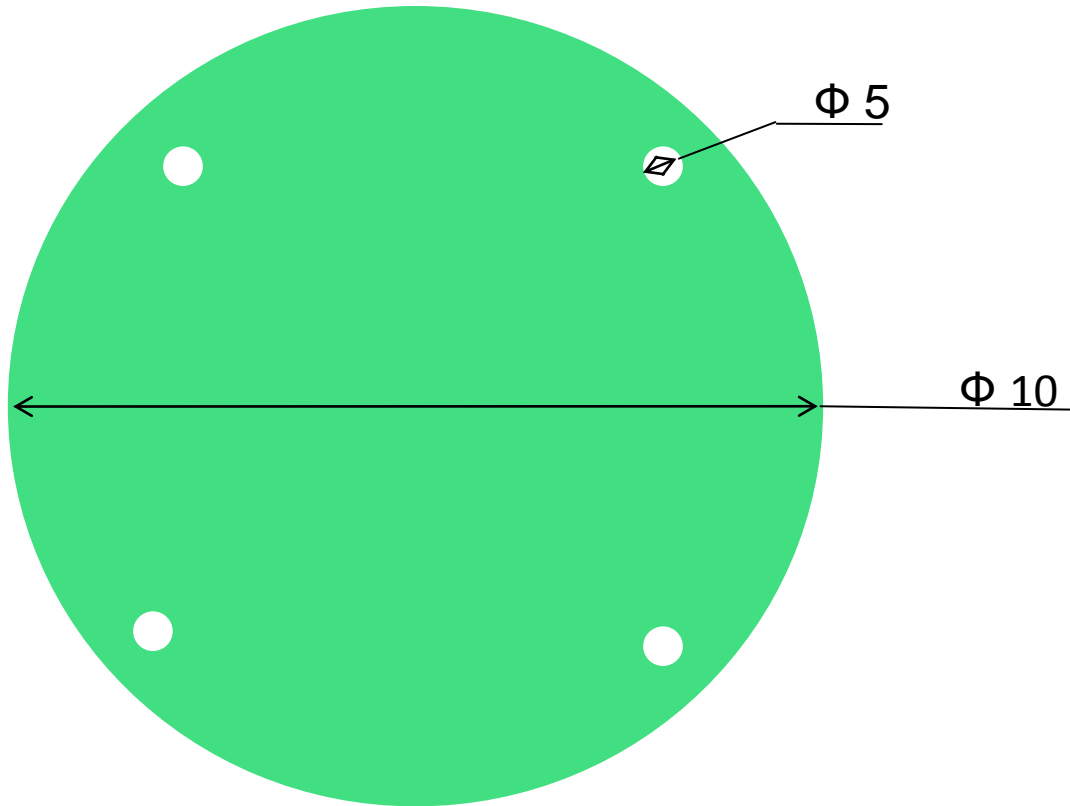
Take all safety precautions throughout this procedure by wearing nitrile lab gloves and safety goggles. Perform all operations under a hood.

In the event of a NP deposit (if the membrane breaks, for instance), pour water into the lower chamber, rinse and transfer the resulting solution into a container for that purpose.

1. Rinse cell and overflow thoroughly with water.
2. Remove stopcocks and stoppers from inlet/outlet ports and from overflow. Also remove seals.
3. Clean inside of sampling and exposure chambers with 25% hydrochloric acid and paper towel.
4. Rinse chambers and stopcocks, stoppers and seals thoroughly with water.
5. Rinse both chambers with acetone. Dry with compressed air.
6. Rinse overflow thoroughly with water, then with acetone. Dry with compressed air.

B. Prepare glove sample and double membrane

1. Take a 10-cm diameter sample of glove material or textile and pierce four holes near outer edge, as shown below. Use plastic template to cut out sample and position holes.



2. Make a mark on one side of sample to indicate surface exposed to nanoparticles, i.e., surface that will be on exposure chamber side.
3. If nanoparticles are in dry powder form, prepare a nitrile double membrane having same dimensions as sample.

C. Prepare nanoparticle samples

1. Nanoparticles in powder

1. Take all appropriate safety precautions throughout this procedure by wearing nitrile gloves, safety goggles and a disposable protective mask.
2. Material required: 1 HDPE flask – 1 oz (container for storing nanoparticles), 1 micro weighing spatula and 1 analytical balance.
3. Turn on balance and place flask on pan. Determine tare. Add desired quantity of NPs (approximately 250 mg) using spatula. Wait for balance to stabilize, then seal flask again.

2. Nanoparticles in colloidal solution

1. Take all appropriate safety precautions throughout this procedure by wearing nitrile gloves.
2. Material required: 1 polypropylene Pasteur pipette.
3. Take 6 mL of colloidal solution and bring it into contact with sample through top of exposure chamber.
4. Dispose of pipette in container for that purpose.

D. Prepare sampling solution

Sampling solutions may be

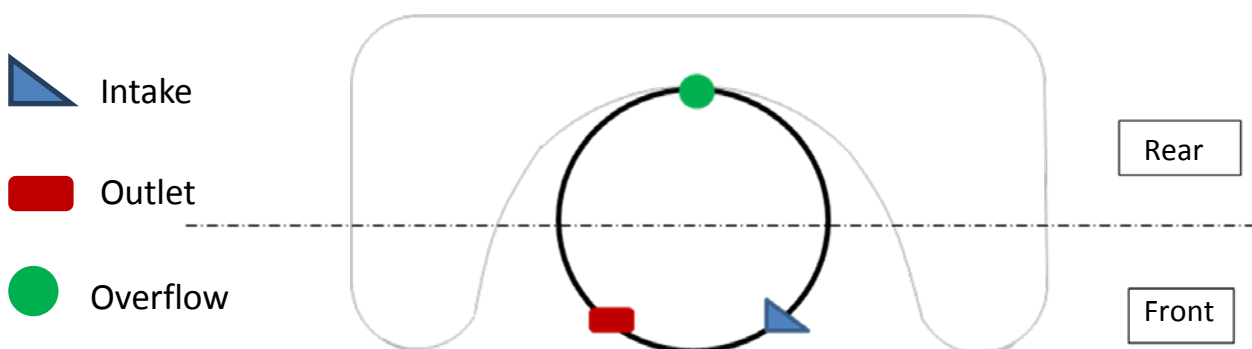
- Ultrapure water
- Ultrapure water with 1% ultrapure nitric acid
- Methanol

Great care must be exercised in using these solutions in order to minimize contamination.

1. Take all appropriate safety precautions throughout this procedure by wearing nitrile gloves and safety goggles.
2. Under hood, wash graduated cylinder with 25% hydrochloric acid and rinse thoroughly with water. Then rinse with methanol and dry with compressed air.
3. Using graduated cylinder, measure out 2 x 20 mL of sampling solution. Set aside.

E. Assemble setup

1. Place all necessary equipment in glove box. Close glove box (handle and fastening) and turn on vacuum pump for 5 minutes.
2. Adjust probe to position 55 (high).
3. Install probe and deformation tip on load cell.
4. Position sampling chamber on assembling stand, with inlet/outlet ports at front and overflow port at rear. Place closed stopcock at inlet port and closed stopcock at outlet port. Close port of overflow using stopcock.



5. Pour 20 mL of sampling solution into lower chamber. Rotate slightly to rinse walls of chamber, then transfer solution to flask ("blank" solution).
6. Pour 20 mL of sampling solution into lower chamber. This solution will be labelled "sample."
7. Position membrane (glove material) on lower chamber and secure by means of the four inserts. Check that seal is properly positioned. Sample must close off lower chamber.
8. Position butyl double seal over membrane in order to secure it, ensuring there are no ripples in it.

1. Nanoparticles in powder

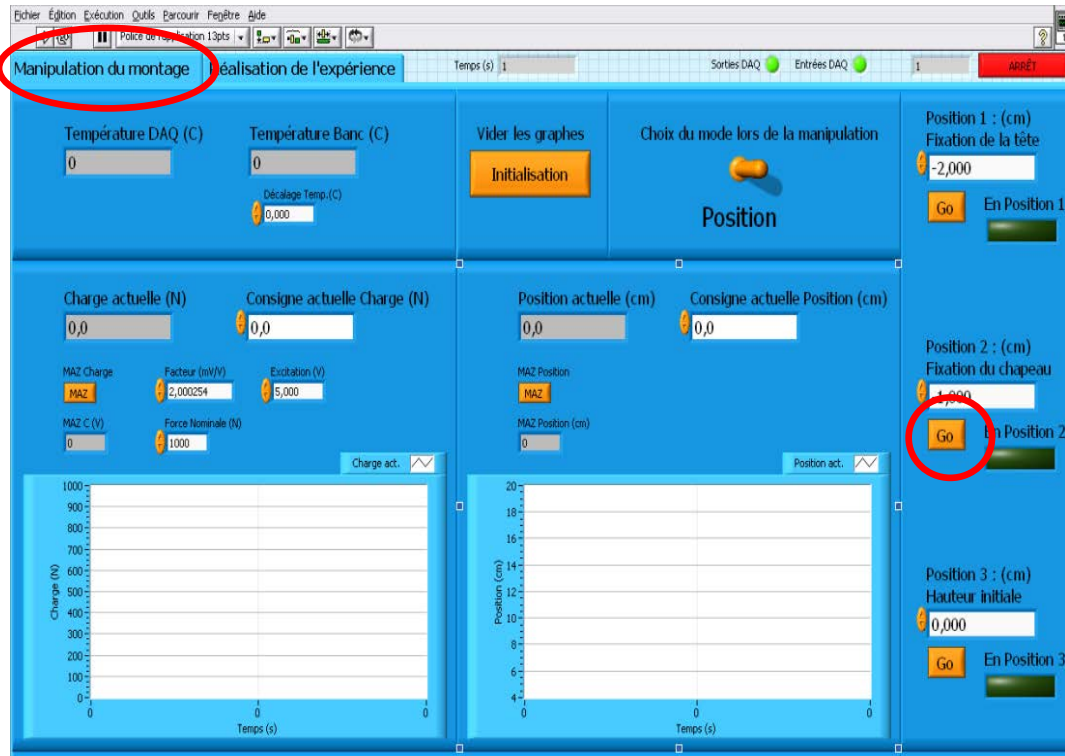
1. Place prepared quantity of nanoparticles in middle of membrane.
2. Position double membrane on top of sample so that it covers nanoparticles.
3. Ensure that second seal of upper chamber is in position.
4. Place upper chamber on top of lower chamber and tighten four bolts. Sample–double seal–double membrane assembly should thereby be secured in position between two chambers.
5. Install cell on support between two actuators.
6. Install overflow and open stopcock connecting it with lower chamber.
7. Set probe to position 0.

2. Nanoparticles in colloidal solution

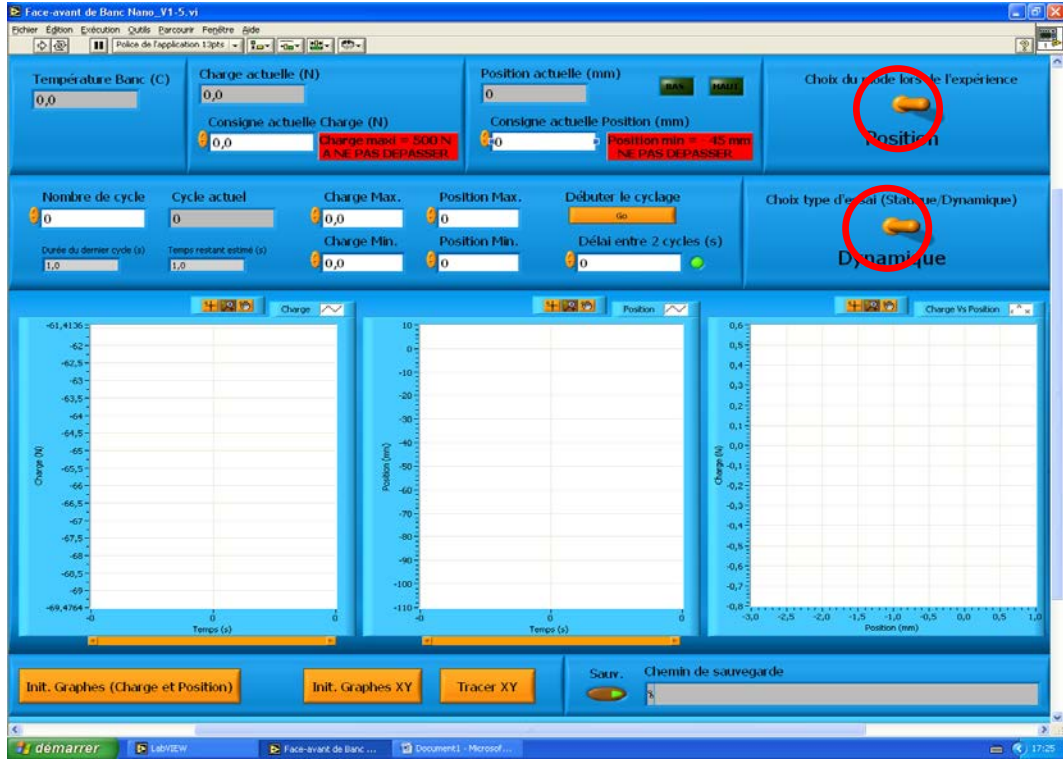
1. Check that second seal of upper chamber is in position.
2. Place upper chamber on top of lower chamber and tighten four bolts. Sample–double seal assembly should thereby be secured in position between two chambers.
3. Install cell on support between two actuators.
4. Transfer desired quantity of nanoparticles onto sample, in upper chamber, using a Pasteur pipette.
5. Install overflow and open stopcock connecting it with lower chamber.
6. Set probe to position 0.

F. Set parameters and run experiment

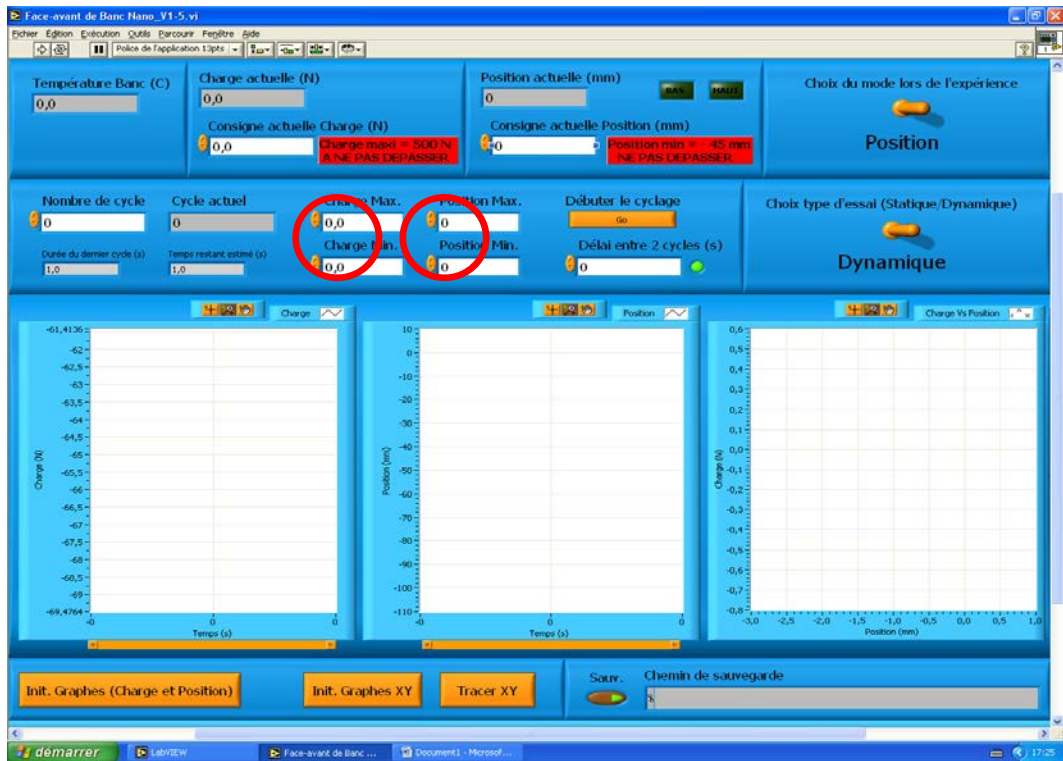
1. Start data acquisition and actuator control software program (Labview).
2. On *Manipulation du montage* [Operate setup] tab, click “Run” and “Automatique TOR” [Automatic All or Nothing]. Probe will automatically move to position 2 (initial height).



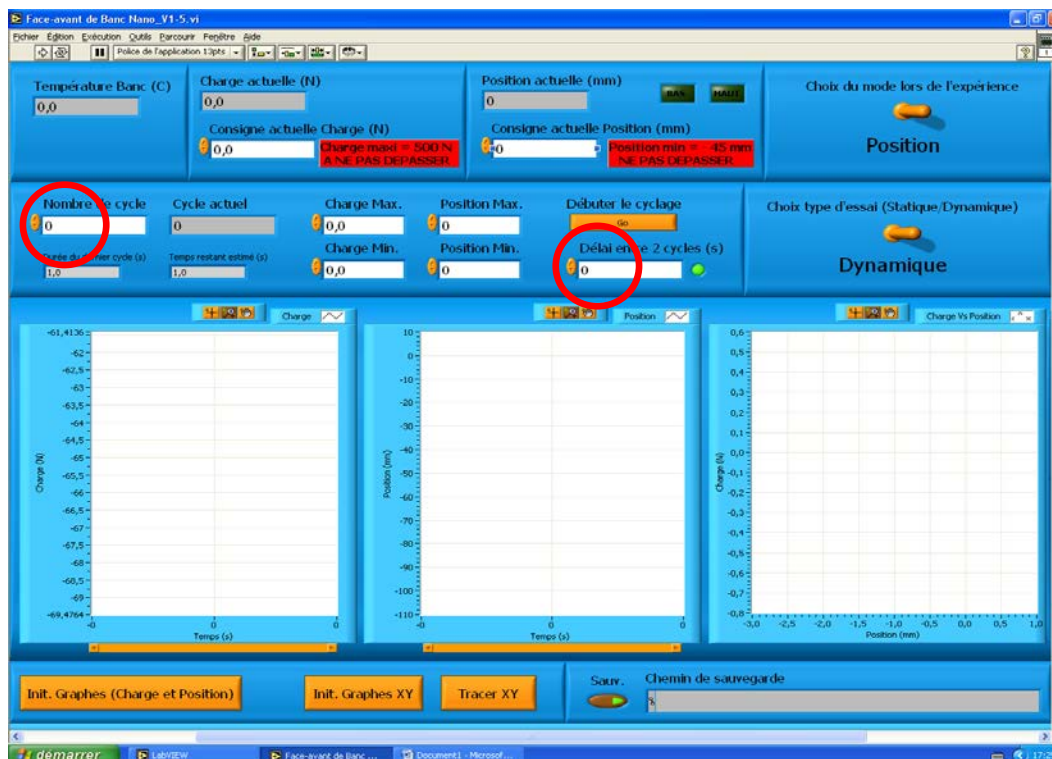
3. On *Réalisation de l'expérience* [Conduct experiment] tab:
 - Select operating mode: static or dynamic.
 - Select means of control: force or position.



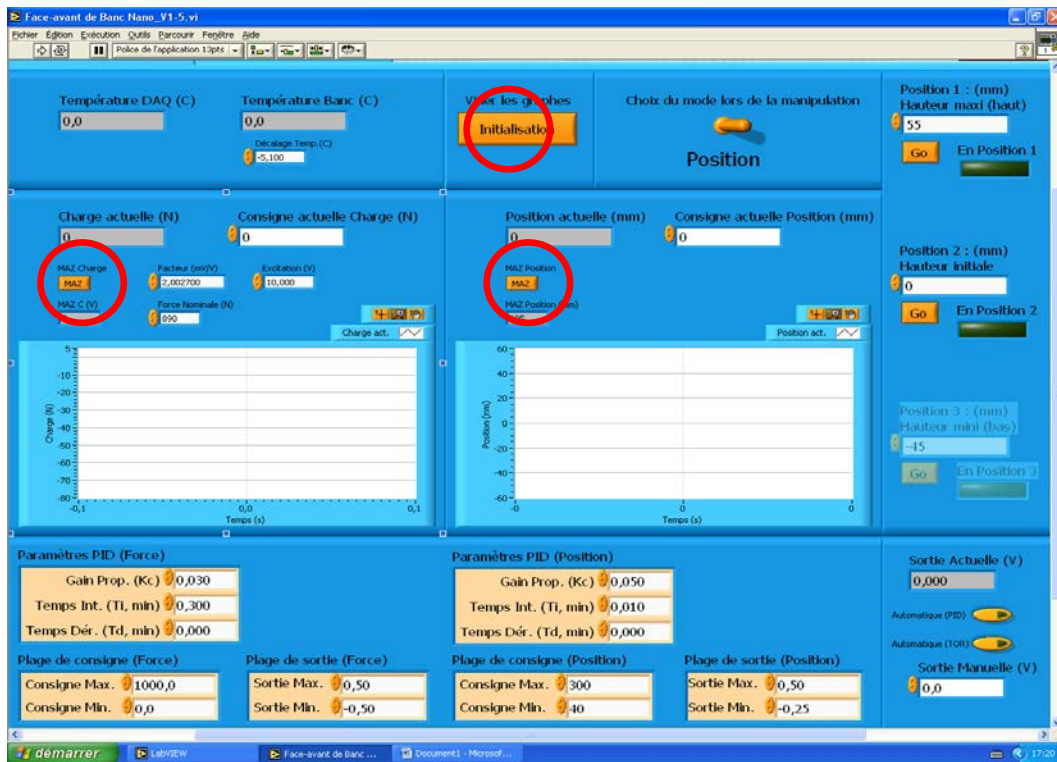
- 4. Enter set point values for actuators: *charge* [load] (N) (min. and max.) or position (mm) (min. and max.), depending on selected means of control (force or position).



- If “Dynamic” option has been chosen, enter number of cycles in “*Nombre de cycles*” box and time between two cycles in “*Délai entre 2 cycles*” box.

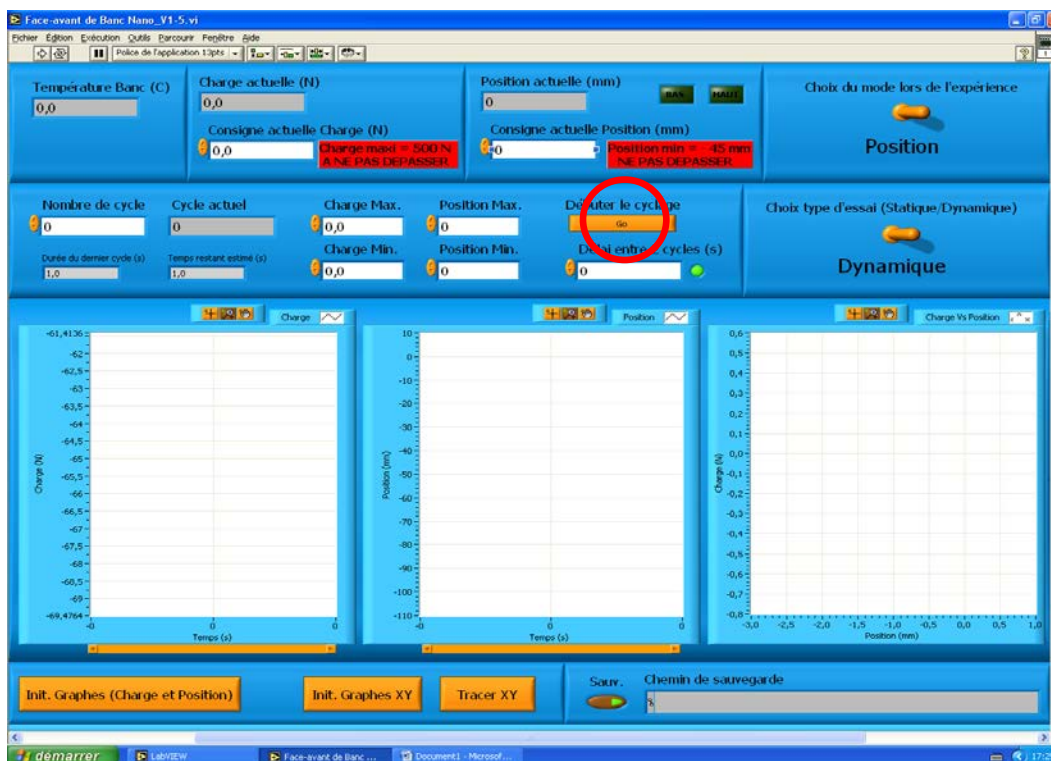


- 6. On *Manipulation du montage* [Operate setup] tab, reset values to zero by clicking on “MAZ” buttons and initialize data acquisition by clicking on “Initialisation.”



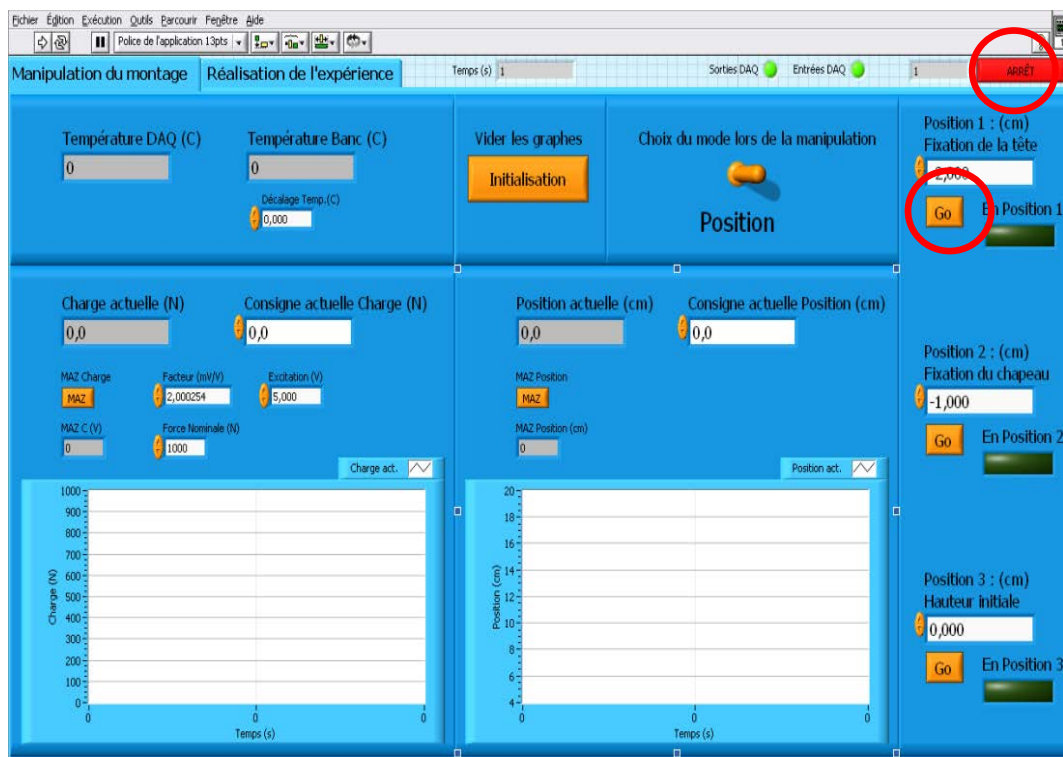
7. On “*Réalisation de l’expérience*” [Conduct experiment] tab:

- In dynamic mode, click “Go” to start cycling.
- In static mode, click “Go” to bring actuators down to maximum set point value, then click “Go” again to bring it back up to minimum set point value.



G. Wind up experiment

- At end of experiment, go to “*Manipulation du montage*” [Operate setup] tab:
 - Place rod in high position (55 mm) by clicking on “Go” in position 1.
 - Stop data acquisition in control software by clicking on “*Arrêt*” [Stop].



- Remove cell from support.
- Rotate slightly to rinse walls of lower chamber, then transfer solution to flask for that purpose (sample solution).
- Place cell on dismantling support and remove exposure chamber.
- Remove double membrane, nanoparticles and membrane. Dispose of everything in waste container for that purpose, inside glove box.
- Turn on vacuum pump for 5 minutes before opening glove box.
- Wash and rinse chambers, seals and equipment, including all small items, as instructed in Part A.